Decellularized Dental Pulp Extracellular Matrix as a Biological Scaffold for Dental Pulp Regenerative Therapy

by

Qahtan Alqahtani

Bachelor of Dental Surgery, King Saud University, 2011

Submitted to the Graduate Faculty of

School of Dental Medicine in partial fulfillment

of the requirements for the degree of

Doctor of Philosophy in Oral Biology

University of Pittsburgh

2018

UNIVERSITY OF PITTSBURGH

School of Dental Medicine

This dissertation was presented

by

Qahtan Alqahtani

It was defended on

Nov 28th, 2018

and approved by

Elia Beniash, Professor, Department of Oral Biology

Bryan N. Brown, Associate Professor, Department of Bioengineering

Herbert L. Ray, Associate Professor, Department of Endodontics

Dissertation Advisor: Dr. Charles Sfeir, Associate Professor, Department of Periodontics

Decellularized Dental Pulp Extracellular Matrix as a Biological Scaffold for Dental Pulp Regenerative Therapy

Qahtan Alqahtani, BDS

University of Pittsburgh, 2018

In the current theme of dental pulp regeneration, biological and synthetic scaffolds are becoming a potential therapy for pulp revitalization. The extracellular matrix has shown success in preclinical models and humans, promoting constructive remodeling and formation of site-appropriate tissue after injury. The use of ECM-based scaffolds has shown an improved tissue remodeling outcome, as it modulates the host response into an anti-inflammatory response that is characterized by the presence of alternatively activated macrophages around the scaffolds. This effect was demonstrated in other studies, yet the underlying mechanism is still largely unknown. There is currently a growing evidence that the source and composition of ECM scaffolds can be responsible for a pro-inflammatory response, while other scaffolds were able to maintain M2 like macrophage response. This phenomenon has led us to the conclusion that host immune cells behavior varies depending on the chemical composition of the matrix. Cathepsin V, K, S, and L have shown collagenolytic ability with cathepsin K being the most potent. We speculate that lysosomal cathepsin K might play a major role in the hydrolysis of collagen in endosomes. In this work, the swine decellularized pulp extracellular matrix (DP-ECM) was used to understand its effect on dental pulp cells and periodontal ligament cells as a candidate for cell-based pulp therapy. The goal is to understand the process of tissue remodeling and cells contribution to this process over the course of 6 and 12 weeks. The generated matrix was analyzed for odontogenic proteins, levels of retained growth factors and bioactive molecules. To simulate the dental model of pulp regeneration, the ECM was placed into the canal space of human tooth root fragment that

were implanted subcutaneously in immune compromised mice. The resulting tissue was analyzed for the expression of βIII-Tubulin, CD31, and DSPP. This was followed up with an investigation of macrophage response toward the DP-ECM. We also, investigated the effect of collagen and matrix components on Cathepsin K activity and macrophages polarization.

TABLE OF CONTENTS

LIST OF TABLES

LIST OF FIGURES

PREFACE

This work is dedicated to my wonderful family and friends. It is their love, support, and encouragement that helped me achieve my ambition and fulfill my dreams. I am forever in debt to Luluah Alkatheeri and Vanessa Hall as they have always pushed me forward and believed in me all the way.

A very special thanks to my mentor Dr. Charles Sfeir for adopting my research and for the wonderful mentorship over the past few years. You truly inspired me to grow and become a scientist and for that I am very grateful. This work would not have been possible without the support of my amazing committee. Special thanks to Dr. Elia Beniash, Dr. Herbert Ray, and Dr. Bryan Brown for their kind help and guidance through this project. A special thanks to the Center of Craniofacial Regeneration members and faculty for creating a scientific research environment that helped me grow as a professional. Thank you to the Department of Oral Biology and Dr. Mark Mooney for creating this great learning opportunity.

1.0 INTRODUCTION

1.1 GENERAL

Dental caries is the second most prevalent infection in the world (Islam et al. 2007). Its initiation and progression lead to a process of continuous loss of minerals along with an invasion of bacteria. At this stage, the dental pulp will provide sensation (pain) and promote the formation of reparative dentin in an attempt to stop the bacterial invasion (Farges et al. 2015). If left untreated, the bacteria will reach the dental pulp causing inflammation (Martin 2003). The current treatment for irreversibly inflamed dental pulp is root canal therapy. The treatment involves the removal of soft tissue followed up with cleaning, shaping, and obturation using bio-inert material. This form of treatment is performed routinely with a success rate (78%-98%) (Kojima et al. 2004). The problems associated with this treatment are a complete loss of pulp functions, loss of significant amount of hard tissue and the technical difficulties that can result in tooth extraction (Reeh et al. 1989; Ruddle 2002).

The regeneration of the dental pulp has the potential to regenerate lost dentin, provide sensation to disease progression and re-establishment of humoral immunity (Cao et al. 2015). In regenerative endodontics, it is evident that growth factors, scaffolds, and stem cells are the main effectors in pulp regeneration and formation of dentin-pulp complex (Mullane et al. 2008). From this perspective, pulp regeneration approaches were categorized into two types, a cell-based

approach and a cell-free approach each offering different advantages (Caton et al. 2011; Galler et al. 2014).

In the proposed work, the cell-based and cell-free approaches were implemented using the generated Decellularized Pulp-ECM (DP-ECM). The goal is to compare the outcome from the two different approaches to determine the importance of using stem cells in the treatment of devitalized pulp (Hoshiba et al. 2016). Cells harvested from dental pulp and periodontal ligaments will be included as these two population can be easily obtained in a clinical environment where intact extracted 3rd molars, represent a source for the two cell populations.

The extracellular matrix (ECM) is a multi-component material secreted into the extracellular space, it maintains the shape and integrity of tissues and organs. It is composed of collagen, GAGs, proteoglycan, glycoproteins, adhesion molecules and growth factors. UBM derived and ECM-based scaffolds were shown to have anti-microbial properties (Brennan et al. 2006), chemoattractant ability (Agrawal et al. 2011), improved tissue remodeling and election of an M2 like response that helps in tissue remodeling and homeostasis (Sicari et al. 2014). It has been used as a biological device that showed regeneration and neo-tissue formation in different areas of the body (Brown et al. 2012a; Wu et al. 2016). The aforementioned properties of ECM-based scaffolds make it a great choice for dental pulp revitalization applications. The use of decellularized dental pulp ECM may provide a readily available source for growth factors needed for regenerative therapy. The scope of the delivery system of ECM devices provides the versatility needed to overcome complicated root anatomy (irregularly shaped spaces and accessory canals) as it is possible to create hydrogels and 3D printed cones (Sackett et al. 2018). It also shows biocompatibility between species, providing a harvesting source for dental pulp scaffold. In this scenario, the use of DP-ECM will provide an environment that mimics the

natural environment of dental pulp system giving cells a better chance for the regeneration of pulp-like tissue.

Macrophages have been recently identified as cells that are capable of polarization into different states which can regulate and guide the process of tissue formation. They have been identified into pro-inflammatory or classically activated M1 macrophages and an anti-inflammatory or alternatively activated M2 macrophages. Other types of macrophages have been further characterized into M2a, M2b, and M2c (Mantovani et al. 2004). Persistence of the M1 response was shown to be responsible for chronic inflammation, fibrosis, and graft rejection (Wynn and Barron 2010). In contrast, the presence of M2 macrophages at different stages of remodeling showed a better treatment outcome. It remains unclear how the transplanted material can elect M1 or M2 response yet a set of factors can help in avoiding the inflammatory response.

Macrophages are considered one of the main factors in ECM breakdown and remodeling using a wide array of proteases (Huang et al. 2012). It was shown that macrophages are capable of collagen degradation in the extracellular matrix using membrane-bound and soluble proteases (Madsen et al. 2013). Once degraded in the extracellular space, collagen is then internalized by the cells surface receptors and then completely degraded in the lysosomes. The internal degradation pathway of collagen remains largely unexplored in macrophages and macrophages polarization state. Collagen uptake was shown to be dependent on Mannose receptors in macrophages (Mrc-1) and independent of β1-integrins and uPARAP/Endo180 (Mrc-2) (Madsen et al. 2011). Interleukin-4 (IL-4) is a cytokine that induces macrophages polarization toward M2, was found to upregulates the expression and function of macrophage mannose receptors (MMR). Recently, one study demonstrated the uptake and degradation of collagen in M2-like macrophages utilizing the mannose receptor pathway (Madsen et al. 2013). We speculate that

collagen uptake and degradation intracellularly is a process that can influence macrophages polarization in tissue regeneration and remodeling. In order to understand this process, we chose Collagen type I as a baseline to build a scaffold with different components to enhance and reduce the degradation rate of collagen.

Collagen is the most abundant protein in ECM and the human body, it represents 25% of the body total protein. There are more than 25 collagen types that serve different functions (van der Rest and Garrone 1991) resulting in different families of collagen having different roles for example collagen type I, II and III are fibril-forming collagens, collagen IV, and VII are network forming collagens and collagen IX and XII are fibril-associated collagens. Collagen type I is an important extracellular component in soft and mineralized tissues, it represents the organic phase of mineralized tissues and it's responsible for providing structure and support to soft tissues. The basic composition of this protein is 3 separate helical alpha chains, two α1 chains, and one α2 chain. Each of the 3 chains is about 1000 amino acids in length and it is mainly made of a repeating Gly-X-Y, as X is frequently proline and Y is often hydroxyproline. The 3 chains form a triple helix, which will form fibrils that eventually form collagen fibers.

So, as one of the main components of ECM, DP-ECM and one of the major proteins encountered by macrophages in health, we decided to use collagen as a model to study the effect of its degradation intracellularly on macrophages. A pathway that could explain macrophages behavior to ECM and collagen-based scaffold. Matrix Metalloproteases (MMPs) and serine proteinases are considered the main agents in ECM degradation due to their stability at neutral pH and localization extracellularly (Werb 1997). On the other hand, cathepsins are localized in the lysosomes where they participate in the intracellular degradation of proteins and turnover. Cysteine cathepsins were found to be secreted by macrophages and have shown the ability to

degrade collagen and ECM given the right conditions (pH, GAGs) (Fonovic and Turk 2014; Li et al. 2002; Turk et al. 2012). Cathepsins with collagenolytic activity (cathepsin V, K, S, and L) have been observed in inflammatory disorders like atherosclerosis, arthritis, COPD, osteoporosis, osteopetrosis, and pycnodysostosis (Kitamoto et al. 2007; Reddy et al. 1995; Zavasnik-Bergant and Turk 2007). Monitoring and understanding the effects of these cathepsins and their presence and expression during different stages of macrophages polarization is important. The goal is to bring insight into cathepsins function in relation to different macrophage phenotype in matrix degradation and remodeling.

Cathepsin K is one of the major cathepsins that possess a potent collagenolytic activity along with its elastolytic properties. It is mainly expressed in osteoclasts and it's responsible for the breakdown of collagen in bones following demineralization in the osteoclast lacuna. Excessive activity of cathepsin K was associated with osteoporosis and arthritis (Costa et al. 2011). In contrast, cathepsin K knockout models have shown increased collagen deposition, delayed wound healing, osteopetrosis, and pycnodysostosis (Gowen et al. 1999; Wen et al. 2016). These findings highlight the important role of cathepsin K in inflammation and collagen turnover. Interestingly, studies have shown that cathepsin K collagenolytic activity can be boosted in the presence of Chondroitin 4-Sulfate (C4-S) and hindered in the presence of Dermatan Sulfate and Heparin (Aguda et al. 2014). On another observation, solubilized brain-ECM was found to elect M1 response and contained no Hyaluronic Acid, when compared to urinary bladder-ECM which showed higher content of HA (Meng et al. 2015). Hyaluronan can bind to the sulfated-Glycosaminoglycans which in turn can affect the collagenolytic intracellular activity of cathepsins. In this work, the effects of the removal and addition of chondroitin sulfate and dermatan sulfate on cathepsin K activity and macrophage phenotype will be investigated.

1.2 BIOLOGY OF THE DENTAL PULP

1.2.1 Development of the Dental Pulp

Developmentally, the thickening of the primary epithelial bands marks the earliest stage of teeth development. This thickening gives rise to the dental lamina that proliferates and interacts with the neural crest cells underneath leading to an accumulation of ectomesenchymal cells that starts tooth development through the bud, cap and bell stages.

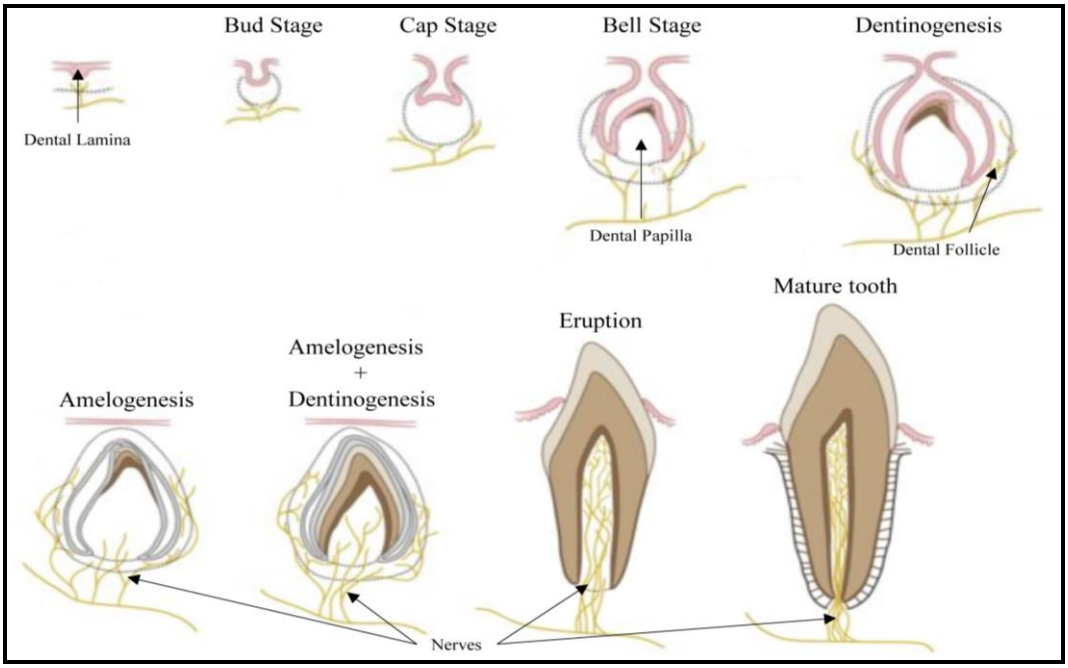

Figure 1. Stages of tooth development from the epithelial thickening to a mature tooth. Following the thickening of the oral epithelium, the tooth develops into bud, cap and bell stages followed by dentinogenesis and amelogenesis

The bud stage is the ingrowth of the epithelial cells into the ectomesenchyme of the jaw and the proliferation of these cells. Followed by the cap stage, which marks the beginning of morphogenesis in teeth, the epithelium develops into the enamel organ while the ectomesenchyme gives rise to the dental papilla which will form the dental pulp and dentin

(Balic and Thesleff 2015). The remaining condensed ectomesenchymal cells will allow for the formation of the dental follicle which will develop into the tooth supporting tissues (Wang and Feng 2017).

Together, the enamel organ, dental papilla, and dental follicle are called the dental organ. As the dental organ continues to grow and the undersurface of the epithelial cap extends deeper, it starts to resemble a bell (hence the name bell stage). At this stage, the tooth crown assumes its shape and cells undergo histo-differentiation to perform their proper functions. At the same time, the dental papilla shows undifferentiated mesenchymal cells and scattered collagen fibrils occupying the extracellular space, its name changes to the dental pulp when mineralization is apparent in the cusps tip during the bell stage. Through cap and bell stage, clusters of blood vessels start to enter and enrich the dental papilla where future roots will form. Nerve fibers start to penetrate the dental papilla during dentinogenesis and are thought to have a relationship with developing blood vessels.

1.2.2 Anatomy of the Dental Pulp

The dental pulp is defined as the soft connective tissue part of the tooth encased within the dentin. In general, it is recognized as a central pulp chamber and root canals that together make the dental pulp. From an embryological and functional point of view, the soft pulp and dentin tissues are closely related and should be considered as a unit. Together, the dental pulp and dentin perform the following functions: 1) Developmental, the dental pulp allows for the formation of dentin during tooth development. 2) Nutritive, as it allows for the delivery of nutrients to the avascular dentin (Rombouts et al. 2017). 3) Sensory, dentin protects the dental pulp from exposure and bacterial invasion by acting as a barrier while the dental pulp provides

the nerves that give dentin its sensitivity (Couve et al. 2014). 4) Protective, the dental pulp has been shown to increase the process of dentin deposition to isolate itself from the noxious stimuli in a process called: reparative dentin formation (Farges et al. 2015).

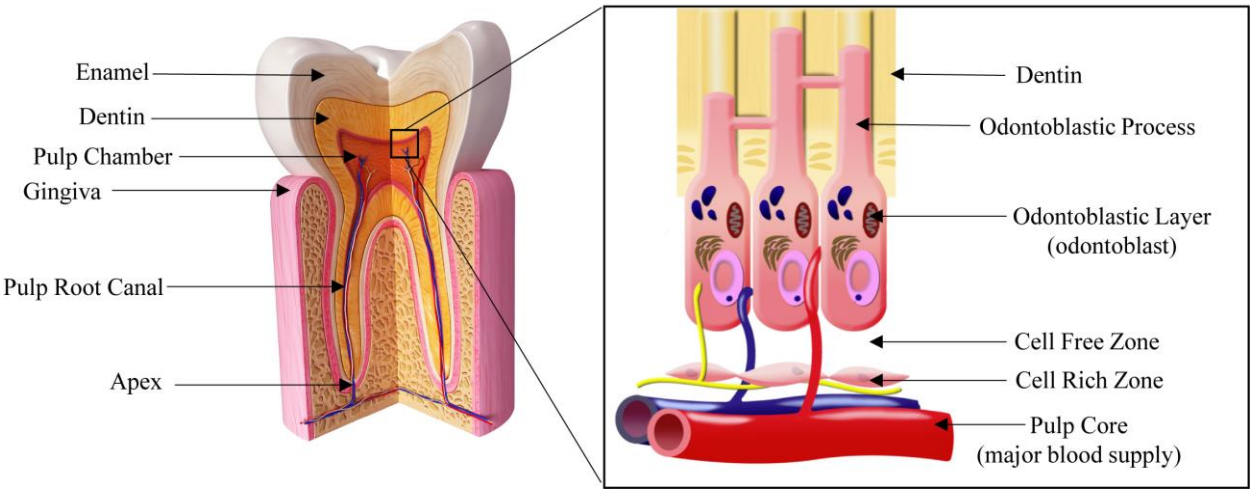

Figure 2. Tooth anatomy and dental pulp zones. Inside the pulp, the tissue organization follows a layering pattern starting from the dentin to the pulp core as dentin, pre-dentin, odontoblastic layer, cell-free zone, cell-rich zone, and the pulp core.

Histologically, four layers can be distinguished in the dental pulp. 1) The Odontoblastic zone, which is the layer of cells adjacent to dentin consisting mainly of odontoblasts with some of its extensions extruding to dentin. 2) The cell-free zone also called the zone of Weil is the area beneath the odontoblastic zone that is most prominent in the coronal part of the dental pulp. 3) Cell-rich zone is the next zone where cells density is shown to be high. 4) Pulp core is the main area of the dental pulp and it's characterized by the presence of major nerves and blood vessels.

In addition to the structural arrangements of the dental pulp, is also known to contain different types of cells. Odontoblasts, a distinctive feature of the dental pulp, are capable of tissue mineralization and dentin production showing flexibility between an active formative phase and a less active quiescent phase (Kawashima and Okiji 2016). Fibroblasts are the main cells in the

dental pulp in terms of number and density in the cell-rich zone. These cells make and maintain the dental pulp matrix, allowing for the formation of collagen and ground substance. Along with these cells, immunocompetent cells like macrophages, T-cells and dendritic cells are also present in the pulp (Gaudin et al. 2015; Hahn and Liewehr 2007). Lastly, the dental pulp was found to be a source for mesenchymal stem cells. These cells are capable of self-renew and show a great ability to differentiate into odontoblasts, chondrocytes, adipocytes, and neurons under the appropriate treatment conditions (Sharpe 2016).

1.3 CURRENT TREATMENT

At the moment, different modalities and methods of treatment are being developed to improve the outcome and reduce the cost of treatment for patients. Mainly, two forms of treatment are currently followed: Root Canal Treatment (Thoden van Velzen 2005) and Regenerative Endodontics (Diogenes and Ruparel 2017).

1.3.1 Root Canal Treatment

Currently, the common treatment for an infected dental pulp is Root Canal Treatment (RCT). The treatments involve the preparation of an access cavity to reach and expose the dental pulp. After that, the dental pulp and the infected tissues are removed by means of barbed broaches and rotary files. Sometimes, canal medicament or antibiotics are placed inside the canals to help the healing process and eliminate contamination. The canal is then filled with gutta-percha (rubber-isomer) and sealant to ensure a three dimensional filling of the void space to avoid future

infection of the canals. The tooth is then filled temporarily or permanently with a filling or a crown to seal the root canal from the oral environment and provide it with the strength to withstand the occlusal forces (Varlan et al. 2009).

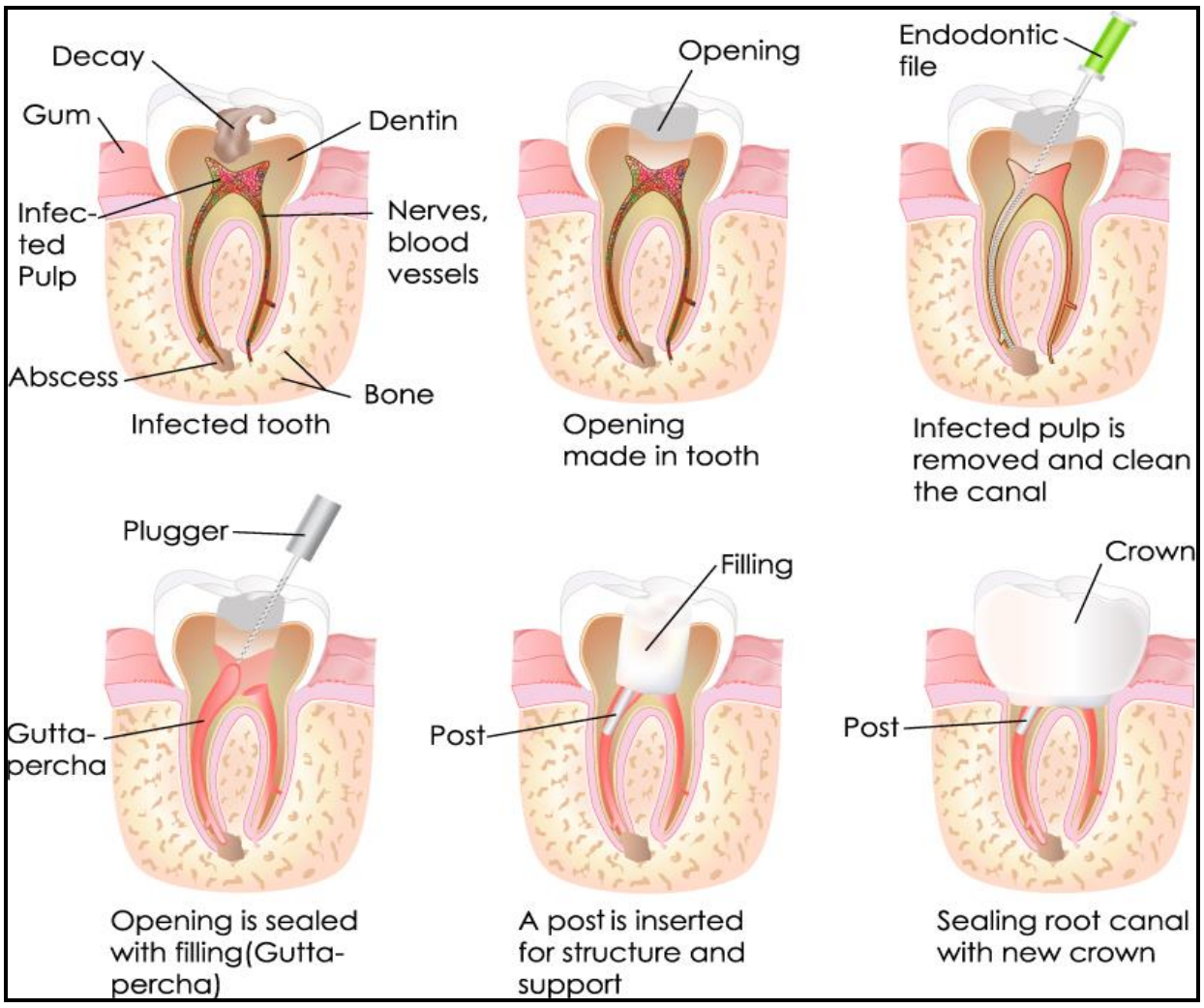

Figure 3. Root Canal Treatment procedure. Removal of the infected pulp and cleaning of the canals is followed by application of Gutta-percha to seal the pulp system.

1.3.2 Regenerative Endodontics

In current and futuristic approaches, the field of regenerative endodontics was invented to overcome some of the problems associated with techniques like apexification, apexogenesis, and RCT. While apexification and apexogenesis would allow for the closure of the apex of immature teeth, it will also dictate the devitalization of the tooth. Once lost, the dental pulp is no longer able to provide sensation, nutrients or development of reparative dentin.

Regenerative endodontics and revitalization techniques were developed to allow for the natural repair and development of the tooth root canal system (Galler 2016). Initially, revascularization techniques were performed on immature teeth by using endodontic files to stimulate bleeding into the apex allowing for the infiltration of cells and the establishment of a biological front. On the other hand, regenerative endodontics techniques aim to regenerate the dental pulp for both mature and immature teeth as an alternative to RCT. The goal is to restore the functions of the dental pulp, allowing teeth to regain sensation to disease progression and attain an immune response against the invading organisms.

In efforts to regenerate the dental pulp, different studies were conducted ectopically and orthotopically aiming to understand the main factors in pulp regeneration. Findings of these studies suggested three main factors to be necessary for the process to occur: 1) Presence of cells capable of repopulating the pulp (Na et al. 2016), 2) biological factors to allow for the recruitments and maintenance of these cells (Yadlapati et al. 2017) and 3) a supporting scaffold to carry the cells and the biological factors (Chen et al. 2015). Collectively, these factors were narrowed down to two main approaches in regenerative endodontics: The cell-free approach which relies on the use of a biocompatible scaffold and extracellular proteins to serve as a vehicle for delivery of growth factors aiming to provide a suitable environment for cells

infiltrating the apical foramen. Studies using growth factors like bFGF, SDF1, VEGF and PDGF that have been delivered by collagen hydrogels have shown recruitment of cells, neovascularization, and formation of dentin-pulp complex (Kim et al. 2010; Suzuki et al. 2011). The second approach is the cell-based approach that involves the use of scaffolds and growth factors in combination with tissue-specific cells, which can be harvested from the same subject at a prior point. De novo regeneration of dental pulp was observed in a mouse model when using human dental pulp stem cells. The cells of the regenerated tissue were positive for human mitochondrial antibodies, showing their human origin, positive for DSPP and alkaline phosphates (Huang et al. 2010). Dental stem cells from dental pulp, periodontal ligaments, and apical papilla were shown to have high proliferation rate, high viability and capability of multilineage differentiation (Mrozik et al. 2017; Tatullo et al. 2015). These findings make it difficult to decide which approach will have a better outcome in terms of tissue remodeling and function. It is apparent that growth factors have a profound effect on cell recruitment and regeneration while stem cells potential for differentiation and tissue maintenance can’t be ignored.

1.4 EXTRACELLULAR MATRIX

1.4.1 Role in Regenerative Medicine

The extracellular matrix (ECM) is considered as one of the main tools used in tissue engineering and regenerative medicine. It is composed of the proteins secreted extracellularly including growth factors, collagens, elastic fibers, mucins and glycosaminoglycans along with other structural and functional molecules. The ECM shows the capability of remodeling and is affected by degradation and synthesis by cells (Hynes and Naba 2012). It gained popularity as an inductive template scaffold for tissue engineering due to its ability to induce constructive remodeling, providing a shift in the healing response away from fibrosis and scar tissue formation. The success of this material for tissue regeneration purposes has been attributed to the degradation products of ECM.

The degradation of the ECM achieved by cathepsins and metalloproteinases result in the degradation of the matrix and exposure of new recognition sites with potential bioactivity (Davis 2010; Maquart et al. 2005). These sites have the ability to influence cellular behavior and can influence a wide array of biological processes, such as migration, angiogenesis, and adhesion (Davis et al. 2000; Ramchandran et al. 1999).

ECM based scaffolds have been tested for a variety of applications because of their ability to promote constructive remodeling and the formation of site appropriate, functional tissue (Badylak 2002; 2004). This was possible because the ECM is highly conserved among

species and is a naturally occurring substrate for cells. Several aspects about the ECM highlights its role as an inductive scaffold, including its ability to transmit mechanical forces, modulation of the host response, bioactive degradation products, and the instructive niches for stem cells.

The ECM is also capable of providing structural support to large defects and injury areas. It allows for the transmission of mechanical forces, promoting matrix degradation and the release of biological cues. Another distinct ECM property to consider is the matrix chemical composition. The chemical composition of the ECM varies greatly from one tissue to another, but it usually contains some common components like collagen, glycoproteins, proteoglycans and growth factors. The composition of any specific ECM is highly influenced by the function and origin of that tissue. The detailed and specific physical and chemical properties of ECM scaffolds, makes it difficult to tissue engineer a synthetic replacement, although attempts are being made through methods such as electrospinning (Barnes et al. 2007; Kumbar et al. 2008). The ECM is also known to have pleiotropic effects upon tissue resident cells, including cell adhesion, proliferation, migration, differentiation, and apoptosis (Lu et al. 2011). This occurs when the ECM is constantly exerting these effects upon cellular behavior and phenotype, and that cells in return can remodel the ECM in a process called dynamic reciprocity (Boudreau et al. 1995; Ingber 1991). The different properties and roles of ECM described above, makes it highly desirable to be used as an inductive scaffold for tissue engineering. However, for the ECM to not elect an inflammatory response, the tissue selected for scaffold sourcing must be decellularized prior to implantation.

Decellularization is the process by which the ECM becomes acellular, it is important to maintain the ultrastructure and ligand landscape during decellularization. This process includes the use of physical, chemical, ionic and enzymatic agents for decellularization. Each method is

customized to the thickness, density and intended clinical application of the scaffold (Crapo et al. 2011; Gilbert 2012; Gilbert et al. 2006). When the ECM is not decellularized properly, due to excessive remaining cellular content or significant disruption of the matrix architecture, they tend to induce a pro-inflammatory response that adversely affects tissue regeneration (Londono et al. 2017). Also, if the decellularization process leads to chemical cross-linking of the tissue, it can disrupt the ligand landscape, preventing the degradation of ECM in-vivo (Brown et al. 2010). The ECM is thought to supports its constructive remodeling through three major mechanisms, although the exact interactions between these mechanisms are not understood. The three mechanisms are mechanical forces, modulation of host responses and through ECM scaffold degradation. All of these mechanisms are important to induce an acellular scaffold to be populated by host cells to start a remodeling response and deposits site-appropriate tissue instead of a pro-inflammatory response.

1.4.2 Host Immune Response

In general, the host will elicit an immune response either to Pathogen Associated Molecular Patterns (PAMPs) or Damage Associated Molecular Patterns (DAMPS) during scaffold placement. After that, neutrophils migrate to the implantation area within the first two days. This is followed by recruitment and activation of macrophages to produce a prominent response within 3 days of implantation. These activated macrophages will generally switch from a predominately M1 (Pro-inflammatory) macrophage response to M2 (Anti-inflammatory) macrophage response between 7 to 14 days post-implantation to promote healing (Badylak et al. 2008; Brown et al. 2012b).

On the other hand, if the macrophages pro-inflammatory response persists, giant cells formation and graft rejection are expected to occur. In recent studies, the SIS-ECM was shown to elect an M2-like response, via the expression of Fizz-1. In-vivo, ECM based studies investigating macrophages response to ECM and implanted meshes were conducted. The ECM showed a better shift in the healing response and improved the outcome of the mesh implants. Other studies focused on the macrophage response to ECM scaffolds showed similar results. While it's still unclear how the ECM elects its response, speculations of microRNAs embedded in the ECM scaffold might be responsible for the influential effect. The degradation of the matrix using different enzymes showed a rich profile of released DNA and RNA content (Huleihel et al. 2016). It has been shown before that if the ECM is cross-linked, the favorable host response it lost too (Daly et al. 2012). This indicates the importance of matrix degradation in order for the process of regeneration and tissue remodeling to take place (Badylak et al. 2008; Brown et al. 2012b). It's well established now that ECM devices show a degradation rate of 60% after 30 days of placement and 90% after 60 days as shown when the degradation of carbon-labeled ECM scaffolds was observed post-implantation in the canine Achilles tendon repair (Gilbert et al. 2007a; Gilbert et al. 2007b). The degradation observed is thought to be responsible for the exposure of new binding sites, increasing the bioactivity of the implantation.

In terms of host response, the ECM has been shown to modulate the host response to promote constructive remodeling and formation of site-appropriate tissue (Brown et al. 2012a). The applications of ECM scaffolds focusing on the host response modulation are many, including but limited to: esophagus, skeletal muscle, heart, brain, bone, and connective tissue replacement (Badylak et al. 2011a; Medberry et al. 2013; Sawkins et al. 2013; Seif-Naraghi et al. 2013; Zantop et al. 2006).

2.0 SPECIFIC AIMS

The overall goal of this dissertation is to assess the decellularized pulp ECM as a biological scaffold for dental pulp regeneration. We hypothesize that DP-ECM can serve as a natural scaffold for pulp therapy by providing a unique combination of proteins and the election of a favorable host response. To test this hypothesis, we will study the DP-ECM effect on cells in-vitro as well as in-vivo through the following specific aims.

2.1. Specific Aim 1: Dental pulp decellularization and matrix characterization. The goal is to obtain a biological dental pulp scaffold that has been minimally disrupted while being completely decellularized. The resulting matrix will be analyzed for odontogenic proteins, growth factors and sulfated-GAGs to be compared to native pulp tissue. The matrix will be used to assess proliferation and migration of dental pulp cells to confirm its bioactivity.

2.2. Specific Aim 2: Effect of decellularized pulp extracellular matrix on dental pulp and periodontal ligaments cells. The DP-ECM will be used to assess wound healing and gene expression of dental pulp and PDL cells in-vitro. The scaffold will be implanted subcutaneously inside tooth root fragments model that will be used to assess the regenerative ability of the ECM with and without tissue-specific cells. The implantations will contain cells from dental pulp and periodontal ligament to determine which cells will be a better candidate for pulp regeneration applications.

2.3. Specific Aim 3: Host immune response to decellularized pulp extracellular matrix: effect of matrix chemical composition on macrophages. The host response characterization will be focused on Macrophages and their polarization state toward different materials. In-vivo, the implanted materials will be assessed for the expression of macrophage markers F4/80, iNOS, and Arg-1. Cathepsins are thought to be involved in the intracellular degradation of collagen yet, their role and regulation remain unknown at different states of macrophage polarization. We aim to investigate the effects of different substrates on the lysosomal activity of cathepsins and the states of polarization that macrophages will attain.

3.0 SPECIFIC AIM 1: DENTAL PULP DECELLULARIZATION AND MATRIX CHARACTERIZATION

3.1 INTRODUCTION

In the frame of the recently coined tissue engineering strategy (Langer and Vacanti 1993), the paradigm of regenerating the dental pulp is paving its way for the revitalization of irreversibly ailing or lost pulp tissue; challenging all preconceptions about the fate of a non-vital tooth and a tooth longevity as a whole. As for the current root canal therapy, more than 90% of 8-year success rate in terms of tooth retention is reached only with post-devitalization full coronal coverage (Salehrabi and Rotstein 2004). Statistically, most root canal failures, and their subsequent tooth extraction, occur during the first 3 years after the initial endodontic treatment and are primarily attributed to secondary intraradicular infection through missed canals, or to tooth/root fractures as a consequence of the alteration in the dentin mechanical properties (Friedman and Mor 2004; Nakashima and Akamine 2005; Siqueira 2001).

With pulpal extirpation, the pulp-dental complex is impacted by the loss of an intact vasculature. This empty space is now void of the ability to mount an immune response and keep the dentinal tubules filled with cellular components and dentinal fluids due to the loss of intra-pulpal pressure. These lost components are paramount in limiting the invasion of bacteria that leads to the development of apical periodontitis and possible tooth loss after root canal therapy.

Physical alterations of the dentin following pulpal extirpation have been argued to leave the root more susceptible to fracture and eventual tooth loss (Winter and Karl 2012). With regenerative endodontic techniques, the possibility of re-establishing an innervated, vascularized pulp-like tissue back into this voided space would provide the tooth with a biological seal of the root canal over a purely mechanical barrier as in current endodontic therapy (Simon and Smith 2014). This newly formed tissue would permit normal physiological functions to be returned to the root canal system.

In regenerative endodontics, two main concepts have emerged, cell-based and cell-free approaches (Galler et al. 2014). The cell-based approach requires cells from dental populations alone (Syed-Picard et al. 2014) or combined with a carrier scaffold (Huang et al. 2010) with or without growth factors (Vo et al. 2012). While the cell-free approach offers minimal manipulation and eliminates the need for cells to be harvested from the host because it depends on the scaffolds ability to support cellular infiltration, proliferation, and differentiation. As scaffolds gained attention in this field, synthetic (Bohl et al. 1998) and biologically inspired scaffolds (Galler et al. 2010) showed the ability to support cell migration into the root canal space.

Currently, there is no gold standard for scaffolds replacing the dental pulp. This is largely due to limits in material sourcing or its ability to have a successfully and functionally remodeled dental pulp. While some aspects are still concerning in the regeneration of the dental pulp, including limited blood supply and liability to infection, new materials in regenerative medicine are shown to be anti-microbial and capable of recruiting and interacting with host cells to create a well-maintained environment (Brennan et al. 2006). Also, the ability to create different shapes

and gel form scaffolds are of value in the regeneration of the root canal system where some areas are difficult to reach and fill (Medberry et al. 2013; Sawkins et al. 2013).

The utilization of tools from regenerative medicine appears to be a viable solution for the treatment of devitalized dental pulp. Although cell-based approach might stand out as the obvious option that guarantees the presence of a biological front that is autologous and host compatible, problems like difficulty of obtaining host cells or maintaining and applying cells along with the financial cost might arise. This makes cell-based approaches to be lengthier and labor intensive than the regular root canal treatment. Those shifting focus to cell-free approach and host compatible scaffolds with the appropriate properties is favorable.

The extracellular matrix (ECM) represents a biological and natural source for the production of scaffolds mimicking the tissue's native chemical and mechanical properties (Reing et al. 2010). The introduction of a pre-knitted decellularized ECM with its spatial distribution of trophic factors was found to trigger local progenitor and stem cells trafficking to re-colonize the construct unlocking the body's innate powers of regeneration. In a similar process to tissue remodeling, the recruited cells from the surrounding tissues migrate to and become enmeshed into the new ECM network. These cells start depositing their own matrix and most importantly maintain its turnover (Badylak et al. 2011b). Lately, ECM-based scaffolds showed promising results in terms of recruiting progenitor cells, promoting constructive remodeling and modulation of host response (Badylak et al. 2011a; Huang et al. 2009; Swinehart and Badylak 2016).

To regenerate the dental pulp tissue, our approach is to introduce the decellularized pulp extracellular matrix (DP-ECM) of swine origin into the debrided pulp space to function as a "home-like" environment with recognized signals for progenitor/stem cells homing from the periapical tissues. In this study, we have adapted decellularization protocols for swine dental

pulp tissue. These DP-ECM were then thoroughly characterized in vitro for cellular compatibility and growth factors content. We have also conducted an in-vivo pilot study in beagle dogs to investigate the potential of the decellularized pulp matrix (DP-ECM) for pulp regenerative therapy.

We believe our approach to regenerate the dental pulp by DP-ECM has the following advantages: i) The employment of growth/cryptic peptides within the debrided pulp space promises the recruitment of host cells to repopulate the dental pulp from the periapical tissues in a process mirroring physiological tissue remodeling (Agrawal et al. 2010). ii) The cells trafficking warrants the re-establishment of the stem-cell niche, hence a lifetime of proper tissue turnover (Sacchetti et al. 2007; Zaky and Cancedda 2009). iii) Less cost and complexity from approaches requiring substantial ex-vivo cell manipulation; and iv) with its minimally invasive procedure, DP-ECM based pulp regeneration would stand as an auspicious approach to pulp regeneration for translation to the dental clinic.

3.2 MATERIALS AND METHODS

3.2.1 Decellularization

3.2.1.1 Dental pulp harvesting, decellularization, and sterilization

Fresh six months old pig heads were obtained from the slaughterhouse. Pulp tissue was extirpated from molar teeth and subjected to a decellularization protocol modified from Carey et al (Carey et al. 2014) with the assistance from Dr. Badylak's group at the McGowan Institute for Regenerative Medicine, University of Pittsburgh.

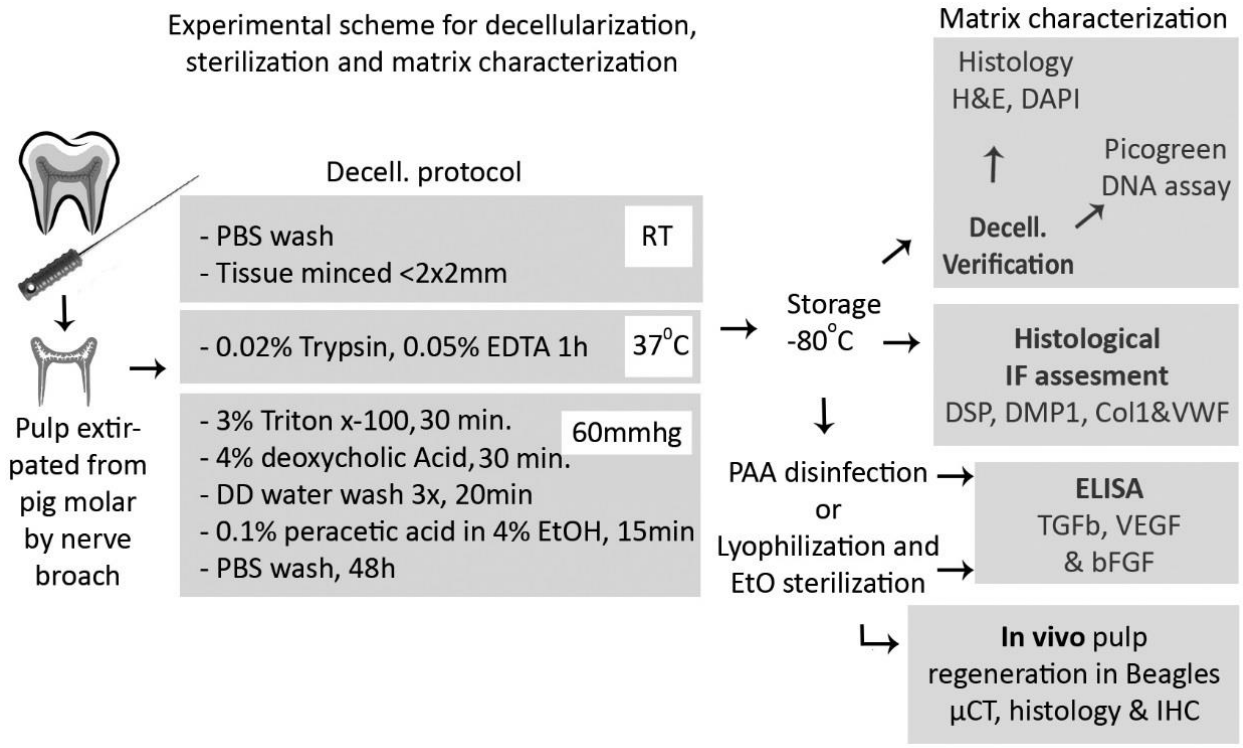

Figure 4. Scheme of the experimental design illustrating the steps for the decellularization protocol and our decellularized matrix characterization.

For decellularization, the pulp tissue was minced by scalpel blades (<2 × 2 mm) and processed according to a decellularization protocol; the ratio of tissue to liquid volume was 1:20 for best tissue wash and penetration. The minced pulp tissue was subjected to treatment with 0.02% Trypsin, 0.05% EDTA at 37°C for 1 h. Then the tissue was placed in a vacuum incubator under 60 to 80 mm Hg. The tissue was treated with 3% Triton X-100 for 30 min and then with 4% deoxycholic acid for 30 min. The tissue was washed 3 times with Deionized water for 20 min/wash. Then it was treated with 0.1% peracetic acid (PAA) in 4% Ethanol (EtOH) for 30 min. A final wash with PBS was performed for 2 d at 4°C, where PBS was changed every 12 h. At that point, the tissue was weighed and stored at −80°C until thawed for characterization and immunohistochemical application.

3.2.1.2 Assessment of decellularization: Histology and PicoGreen® assay

For verification decellularization, DP-ECM samples were checked for the presence of nuclei histologically (formalin-fixed and cryo-embedded) and for the presence of nuclear DNA by PicoGreen® assay. The 5µm-thick sections were stained for H&E and for the nuclear fluorescent label DAPI. Decellularization was considered successful when no intact nuclei were visible in the histological H&E or DAPI stained sections.

For PicoGreen assay, tissue samples were dried by speed vacuum, weighed and mixed with 300µl of cell lysis buffer (50mM Tris pH 7.5; 100mM EDTA; 0.5% SDS in water) and 3µl of proteinase K for water bath overnight digestion at 55°C with agitation. Samples were then mixed and spun for 1 min in 100µl of protein precipitation solution (7.5M NH4 C2H3O2 in water). The supernatants were transferred to a new tube with 300µl of 100% 2-propanol then mixed and spun again for 2 min. Samples were washed with 300µl of 70% ethanol twice and left

to dry overnight then re-suspended in 200µl of nano-pure water for DNA quantification (n=15) by Quant-iT™ PicoGreen® dsDNA assay kit according to manufacturer's instructions. Native pulp tissue was subjected to the same digestion protocol as a control. The DP-ECM was considered successfully decellularized when the total DNA content was less than 50ng/mg of dry tissue weight.

3.2.2 Matrix Characterization

3.2.2.1 Immunolabeling of ECM molecules and SEM

For immunofluorescence, formalin-fixed samples were paraffin-embedded and sectioned at 5µm thickness. Immunolabeling was performed against antibodies specific to a variety of swine dental pulp ECM components: Collagen type I (Col1, Abcam Ab34710), dentin sialoprotein (DSP, Larry Fisher LF153) and dentin matrix protein1 (DMP1, Larry Fisher LF148) and Von Willebrand factor (vWF, Abcam Ab68545). Of note, another group of antibodies is detailed in the in-vivo immunolabeling section below.

Briefly, after sectioning, slides were treated with 1.5% Sudan Black B (Sigma-Aldrich) in 70% Ethanol for 20min to dim auto-fluorescence, followed by thorough PBS washes with 0.2% Tween 20 (TBS). When antigen retrieval step was required (Col1, DSP & DMP1), slides were immersed in the citric acid solution at 95-100ºC (10mM, pH 6.0) followed by TBS rinses. Samples were blocked against non-specific binding using serum from the same species as the secondary antibody in 0.3M glycine to reduce the background for 1h at room temperature (RT). Primary antibodies were diluted in the blocking solution (Col1 1:50; DSP 1:100; DMP1 1:200; vWF 1:50) and applied to the sections overnight at 4ºC. Samples were washed in TBS and appropriate fluorescently labeled secondary antibodies (diluted 1:1000 in the blocking solution)

were applied for 1h at RT. Slides were washed, counter-stained with DAPI and cover-slipped in aqueous mounting medium before observation under a fluorescent microscope. (Nikon Eclipse TE2000-E, NIS Elements software).

For SEM, native and DP-ECM tissue samples were PBS washed and fixed in 2.5% Glutaraldehyde for 4 hours, washed in PBS again, dehydrated and critical point dried using Hexamethyldisilazane. Samples were then mounted on studs, sputter coated and imaged using electron microscopy (JSM6330F; JOEL, CBI imaging facility; University of Pittsburgh).

3.2.2.2 ELISA quantification of GF in DP-ECM and S-GAGs quantification

We assessed the growth factors involved in angiogenesis (VEGF), collagen production (bFGF) and fibroblasts function (TGF-b1). Using ELISA the 4 groups tested were: 1) Native non-decellularized pulp samples as control, 2) DP-ECM non-sterilized, 3) DP-ECM disinfected in Peracetic Acid (PAA) and 4) DP-ECM lyophilized and sterilized with ethylene oxide (EtO). Samples were dried using speed vacuum, weighted, dissected and treated with protein extraction buffer composed of 10ml M-PER extraction reagent (Thermo#7850), one tablet of protease inhibitor (Roche#11836170001) and 1% phosphatase inhibitor (Sigma#P5726). The samples were then homogenized individually, left on a shaker for 2h at 4°C, centrifuged for 20min at 13,000 rpm at 4°C, then the supernatants were collected and frozen at -80°C until assayed. Concentrations of bFGF, VEGF, and TGF-b1 were assayed by ELISA kits according to the manufacturer's instructions (Quantikine Human bFGF Immunoassay; Quantikine Human VEGF Immunoassay; and Quantikine Mouse/Rat/Porcine/Canine TGF-b1 Immunoassay- R&D Systems).

To quantify sulfated GAGs, the following modified dimethylmethylene blue (DMMB) assay from Awad HA (Guilak) et al. 2003 was used. Samples were digested overnight in papain

digestion buffer of pH: 6.5 at 60 °C. Samples were added at a ratio of 80 µl:200 µl (sample: DMMB at pH range: 1-3) increasing ratio increases sensitivity for samples with 0-30 µg S-GAG per ml. Read at 595 nm (signal decreases with increasing gag) and 540 nm (signal increases with increasing gag). Computing gags was based on 540-595. Chondroitin-4-sulfate at 0-30 µg/ml concentrations were used to generate standard curves.

3.2.2.3 Dental pulp cells proliferation and migration with digested DP-ECM

Healthy adult third molars were obtained from the University of Pittsburgh, School of Dental Medicine, after routine extraction. Dental pulp was exposed and removed with a barbed broach. The pulp was minced and then digested in an enzyme cocktail containing 3 mg/ml collagenase and 4 mg/ml dispase for 1 to 1.5 hr at 37°C. The total population of human dental pulp cells (DPCs) was plated and expanded in a maintenance medium (M.M) containing Alpha Minimum Essential Media (αMEM; Gibco, Grand Island, NY, USA), with 10% fetal bovine serum (FBS; Atlanta Biologicals, Flowery Branch, GA, USA), and 1% penicillin/streptomycin (P/S; Gibco). Cells were used at P3 for proliferation and trans-well migration experiments. Similar to a previously published protocol (Freytes et al. 2008) DP-ECM was lyophilized and digested in Pepsin 1 mg/ml, 0.01N HCl at the concentration of 10 mg DP-ECM/ml on a stirrer for 72 hrs, neutralized using 0.1N NaOH and diluted to desired concentration using maintenance medium.

For proliferation, cells were lifted with Trypsin/EDTA, counted using a hemocytometer and 5000 cells were seeded into a 12-well plate to adhere overnight. After overnight incubation, the medium was replaced with conditioned medium containing DP-ECM (1 mg/ml ECM, 0.5 mg/ml ECM and 0.1 mg/ml ECM) and cells were treated for 1 day, 3 days and 7 days. At the end of treatment, cells were lysed and cell numbers were determined using CyQuant GR Dye. A cell pellet of known cell number was used to generate standard curves. n = 3 / group.

For trans-well migration, cells were starved overnight in serum-free medium, lifted with Trypsin/EDTA, counted using a hemocytometer and 50,000 cells were seeded into the top compartment of a transwell insert (8 µm pore size, Corning Transwell Polycarbonate #3421). Bottom chamber had 4 groups: 0% FBS (negative control), 10% FBS (positive control), 1 mg/ml DP-ECM and 0.5 mg/ml DP-ECM. Cells were left to migrate for 16 hours. After that, chambers were placed in a cell detachment solution and cell numbers were determined using GR Dye after the addition of cell lysis buffer. n=4 / group.

3.2.3 In-vivo Pilot Study

Dental pulp regeneration in beagle dogs by decellularized swine dental pulp extracellular matrix: a pilot study. (Appendix figure 2)

Two female beagle dogs age 13m (Marshal Bioresources, USA) were included in this pilot study under approved IACUC protocol at the University of Pittsburgh. The procedure is detailed under Appendix Figure2.

Two teeth received lyophilized EtO-sterilized swine DP-ECM (App. fig. 2e) (in 4 root canals), 3 teeth received collagen scaffold (preparation described under Appendix Figure 2) and 3 teeth were left empty (blood clot alone) as controls. Sacrifice took place at 8 weeks.

Post sacrifice micro-computed tomography (µCT), histology and immunohistochemistry.

Jaw explants (10% formalin-fixed for 3 days) were µCT scanned in PBS media at 30mm resolution, integration time of 299 ms, 55 keV, 142 mA with a cone beam and continuous rotation (VivaCT 40; Scanco) After µCT, teeth were hemi-sectioned into mesial (crown and root) and distal portions by Diamond disc (102x0.3mm) on precision saw (Isomet-Buehler). Each root/bone explant was resin embedded (Osteo-bed bone embedding kit, Polysciences, Inc-USA)

separately for maximum penetration. Resin-embedded samples were sectioned into 5µm sections (Leica RM2255 with tungsten carbide blade C.L. Sturkey Inc.) that were collected on sticky tape (Tesa Film-Germany), de-acrylated and stained for 1) Goldner's trichrome histology and 2) immunostaining for two antibodies that demonstrated reactivity against canine but not swine tissues (Appendix figure 3): CD31 (Labome bs-0468R, rabbit anti-human, conc. 1:50 with citrate antigen retrieval) and DSP (Larry Fisher LF151 rabbit anti-human, conc. 1:100, without antigen retrieval). Immunohistochemistry was performed by the Expose Mouse and Rabbit HRP kit (Abcam) according to manufacturer's instructions.

Statistical analysis

Data were presented as arithmetic means with standard deviation (SD) using GraphPad Prism statistics. For PicoGreen® assay a Student's t-test was used to compare the mean values of DNA amount in each group. For proliferation, migration and ELISA assays, means and SD were compared by one-way ANOVA. Differences were considered significant at $p \leq 0.05$.

3.3 RESULTS

3.3.1 Evaluation of the decellularization procedure

According to established decellularization assessment guidelines (Gilbert et al. 2009), our DP-ECM contained significantly less DNA ($p<0.001$) than the native dental pulp tissue (PicoGreen® dsDNA assay) and less than 50ng/mg of dry tissue weight indicating successful decellularization (Fig. 5 A). DP-ECM showed no visible intact nuclei by H&E or DAPI staining (Fig. 5 B).

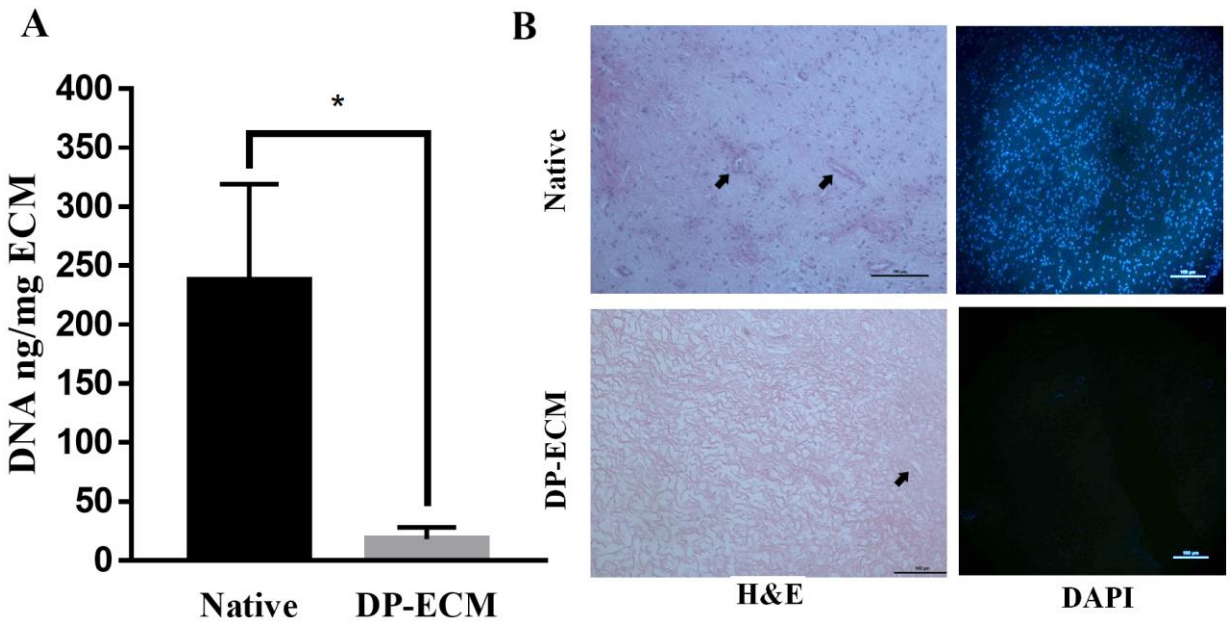

Figure 5. Assessment of the decellularization procedure. A: Quantification of the amount of remaining dsDNA in DP-ECM compared to native pulp tissue. B: Visualization of intact nuclei within native and decellularized tissue by H&E and DAPI stains. Arrows point to intact vasculature before and after decellularization.

Figure 6. Pictures of swine pulp tissue before decellularization (native), after decellularization and after decellularization and lyophilization.

3.3.2 Characterization of DP-ECM

Immunofluorescence and Scanning Electron Microscopy Evaluation of DP-ECM:

ECM components were labeled using immunofluorescence before (native) and after decellularization (DP-ECM). Collagen I was observed throughout the matrix in native and DP-ECM, while DSP and DMP-1 were present in the tissue periphery near the dentinal walls. vWF was found around blood vessels and was conserved and detectable following decellularization (Fig.7). SEM of the native tissue and DP-ECM shows changes in the tissue architecture after decellularization (Fig. 8). These changes could be attributed to the use of vacuum pressure along with the decellularization reagents.

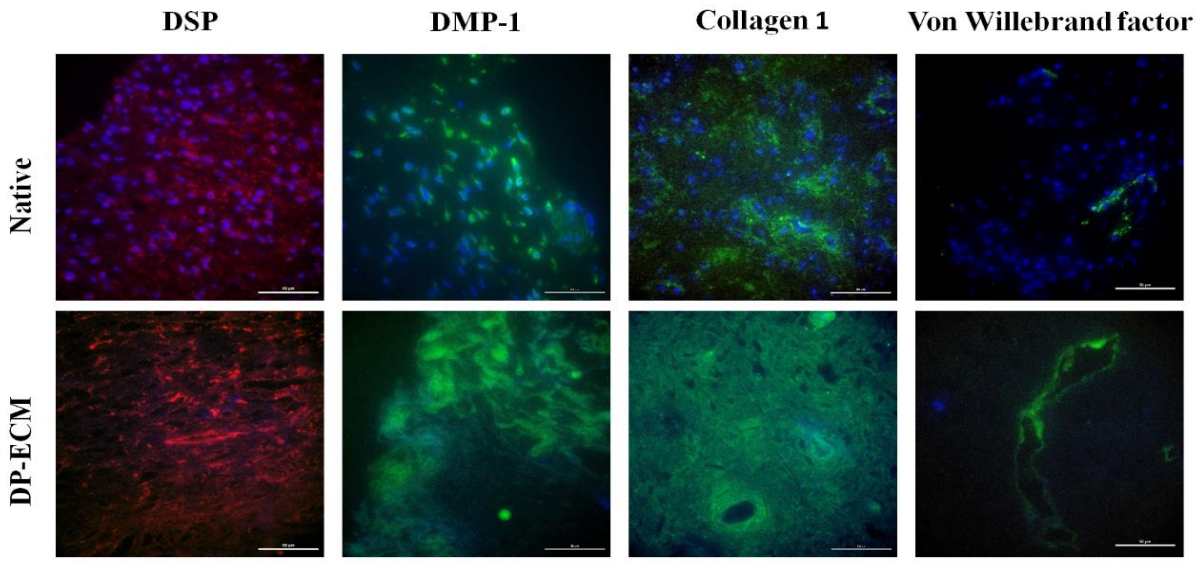

Figure 7. Immunofluorescence labeling of ECM molecules before decellularization (Native) and after decellularization (DP-ECM). DSP and DMP-1 were limited to the periphery of the dental pulp tissue (in proximity to dentin), vWF was localized around blood vessels and collagen throughout the tissue. Scale bars 50µm.

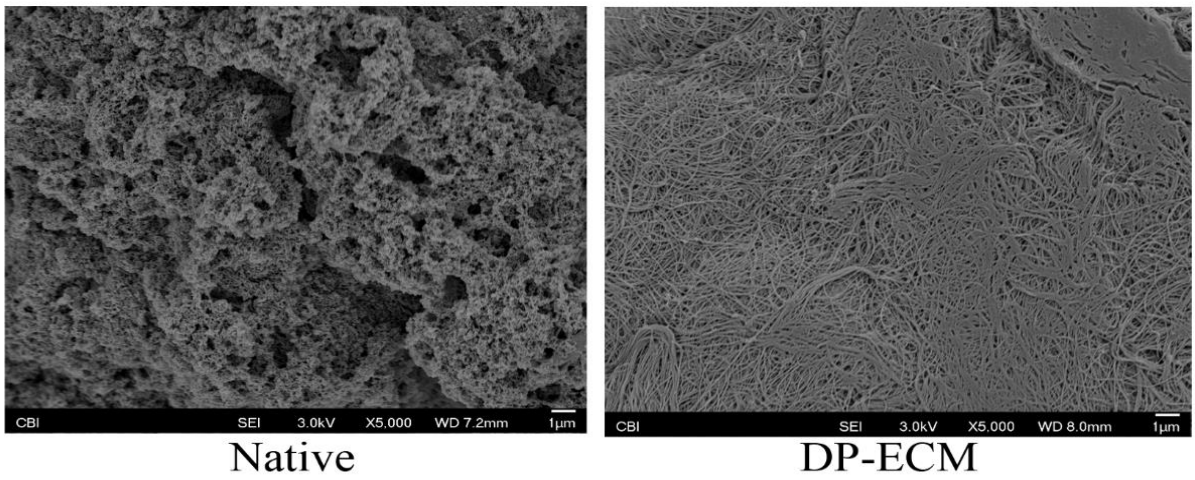

Figure 8. SEM of the native and DP-ECM shows changes in the matrix architecture and filamentous arrangement of DP-ECM. Scale bars 1µm.

ELISA and S-GAGs quantification:

Using ELISA, TGF-β, VEGF, and bFGF were quantified for four groups: native tissue, DP-ECM, PAA, and EtO. Compared to native pulp tissue, TGF-β and VEGF didn't show a significant reduction in the decellularized matrices even after PAA disinfection. Upon EtO sterilization, however, TGF-β and VEGF were significantly reduced (Fig. 9A, B). Basic FGF in native tissue was undetectable after decellularization (Fig. 9C).

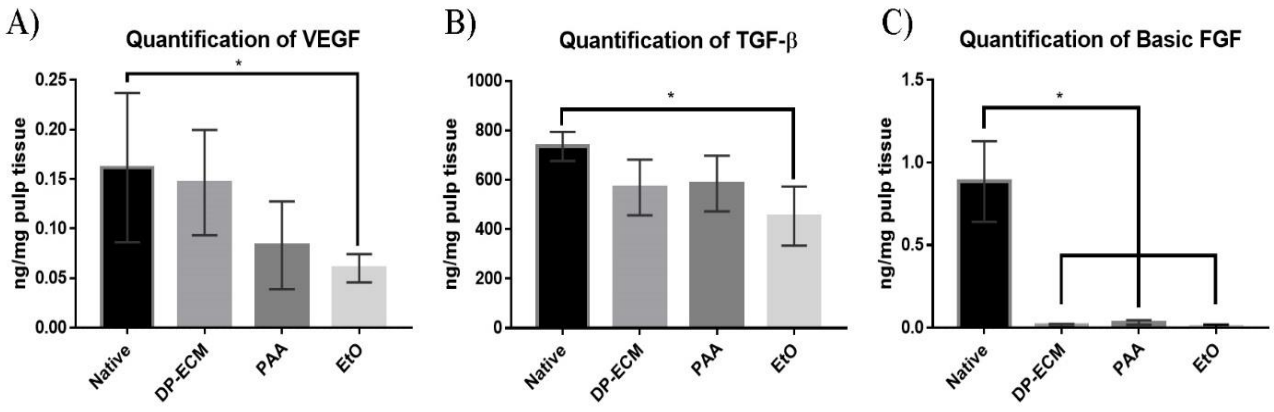

Figure 9. ELISA quantification of (A) VEGF, (B) TGF-β and (C) bFGF from native pulp, DP-ECM, DP-ECM disinfected in PAA and DP-ECM lyophilized and sterilized with EtO. *$p<0.05$.

Upon investigating the individual contribution of the lyophilization and EtO sterilization processes to the reduction of GF, we tested TGF-β reduction from both the native and DP-ECM matrices after lyophilization (Appendix fig.1). Our data indicate that the lyophilization process may have had the greatest contribution to GF reduction rather than EtO sterilization alone.

To further characterize the DP-ECM, dimethyl methylene blue was carried out on Native Pulp, DP-ECM and UBM as an additional control. Overall, the DP-ECM showed a significant reduction when compared to the native pulp. While the amount is reduced, the reduction was only about 1 µg/mg of dry tissue. This validates the presence of S-GAGs in the DP-ECM even after complete decellularization.

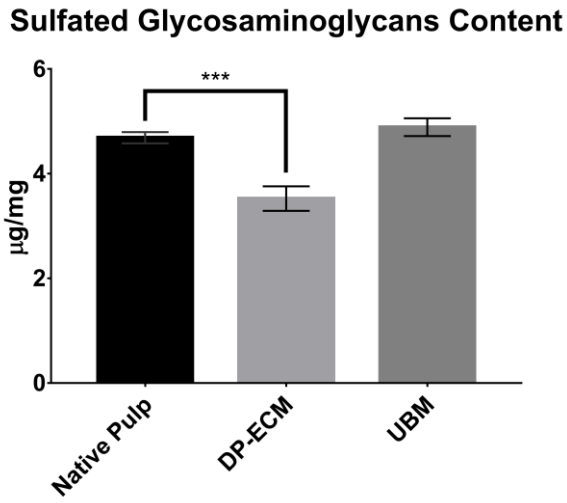

Figure 10. Sulfated Glycosaminoglycans quantification of (Control) UBM, DP-ECM and from the native pulp. *** $p \leq 0.001$.

3.3.3 Proliferation and migration of dental pulp cells.

After 1 day of treatment, all groups showed similar proliferation rate when compared to the M.M group. At 3 days, groups containing 1 mg/ml and 0.5 mg/ml DP-ECM showed an increase in proliferation rate when compared to the M.M group in a dose-dependent manner. 7 days after treatment, the cells are still maintaining a proliferation rate similar to the M.M groups without any statistically significant differences (Fig. 11).

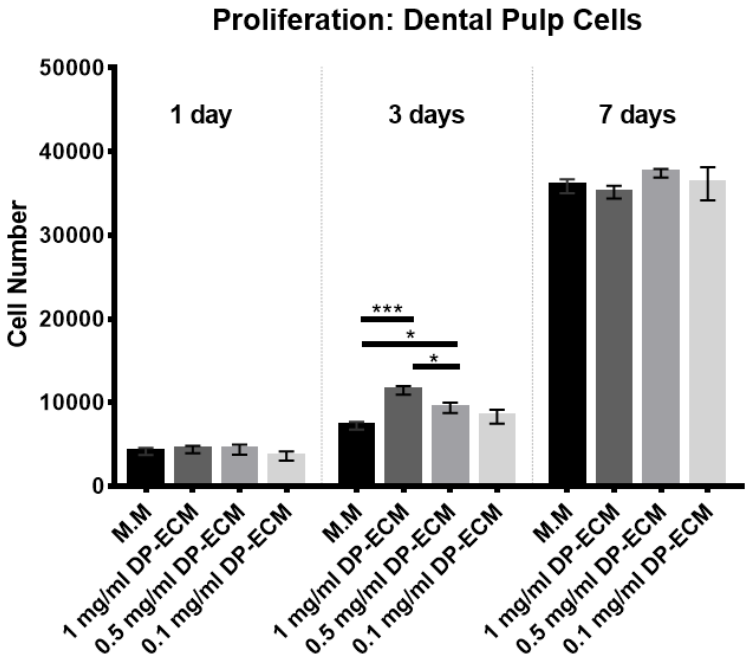

Figure 11. Proliferation of dental pulp cells after 1, 3 and 7 days of treatment with the DP-ECM digest. *p<0.05*** $p \leq 0.001$

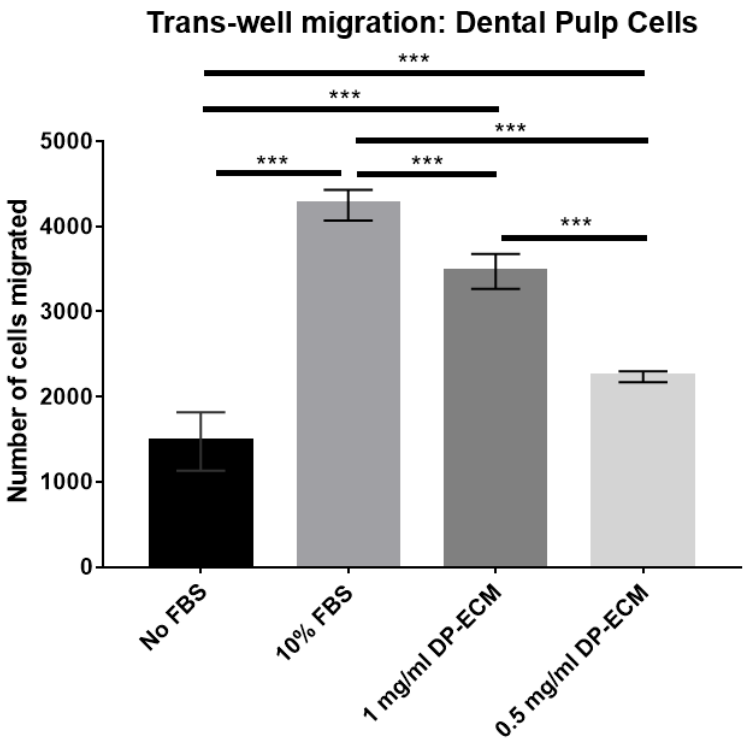

Figure 12. Trans-well migration of dental pulp cells, 16 hours after treatment. ***p<0.001

After 16 hours, the group containing 10% FBS had the greatest effect on the migration of DPCs followed by 1 mg/ml DP-ECM and 0.5 mg/ml DP-ECM. When compared to 0% FBS group, DP-ECM groups showed an increase in the number of migrating cells which was also affected by the dose concentration (Fig. 12).

3.3.4 In-vivo implantation and characterization of DP-ECM

In a pilot study to investigate its regenerative ability, the sterilized DP-ECM was introduced in debrided root canals of beagle dogs' molars and premolars while using collagen sponges and empty canals (filled with a blood clot) as controls. The apical foramen was deliberately prepared

open to 0.5mm to allow periapical cells infiltration. Upon sacrifice at 8 weeks, all 3 groups showed cellular infiltration from the apex through the root canals and up to the pulp chambers (DAPI nuclear stain; Fig.13 F, G, M, N, T& U). All 3 groups showed evidence of intra-canal mineralization visualized by microCT and Goldner's trichrome staining. (Fig.13 A, B, H, I, O & P). These observations indicate that tissue formation was achieved in all three groups. However, immunohistochemical staining for antibodies against canine tissues and not against swine tissue (Appendix. Fig. 3) showed CD31+ cells and DSP+ tissue in the pulp canals that received DP-ECM. This shows that DP-ECM has the ability to recreate the pulp native microenvironment to recruit vascular cells and differentiate the homing cells from the periapical tissues to form a DSP-expressing dental pulp-like matrix (Fig.13 D & E).

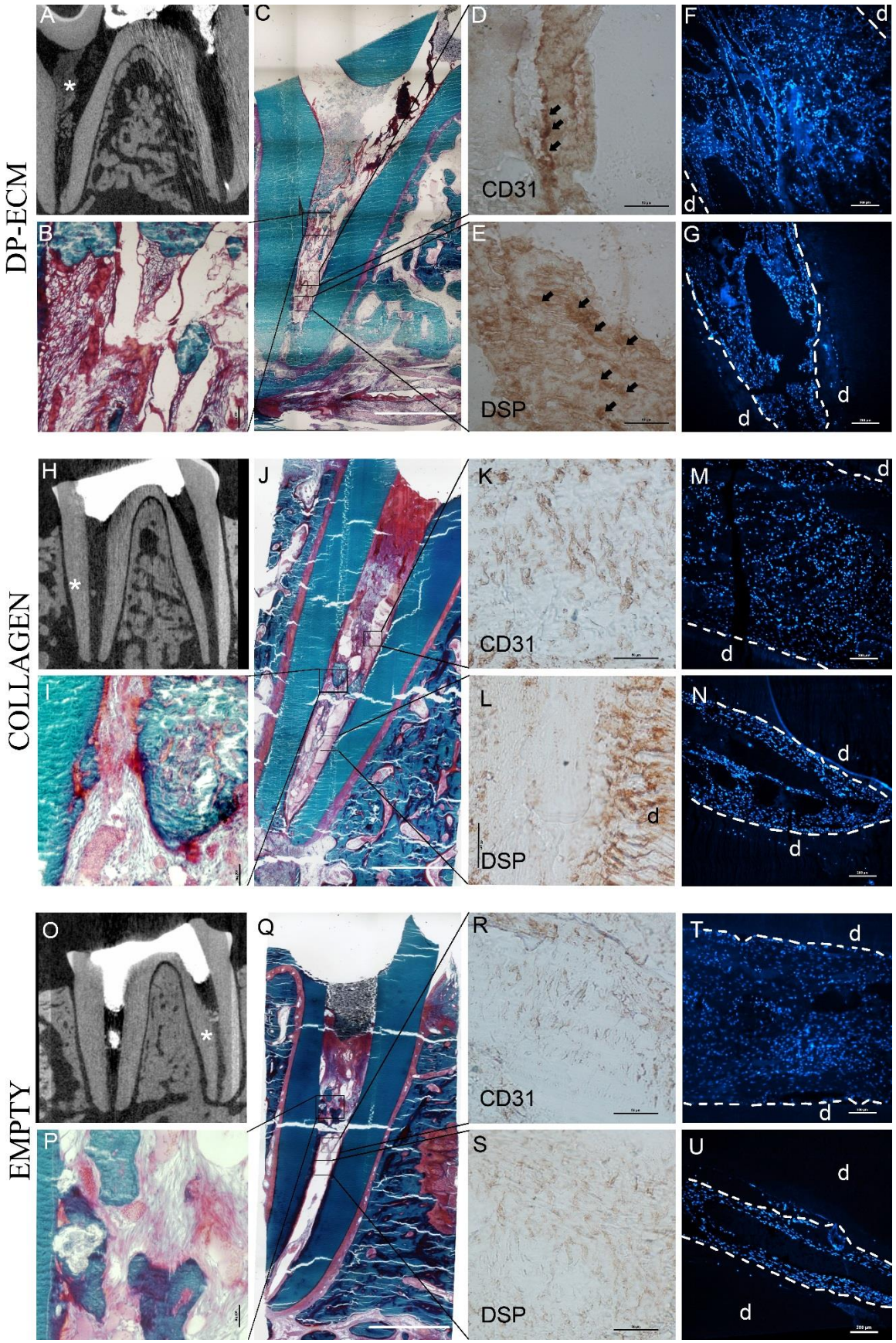
DP-ECM
COLLAGEN
EMPTY
A
B
C
D
E
F
G
CD31
DSP
d
H
I
J
K
L
M
N
O
P
Q
R
S
T
U

Figure 13. µCt (A, H & O) and histology (B-G, I-N & P-U) at 8 weeks for the 3 groups investigated in beagles' dental pulp regeneration: Decellularized swine ECM (DP-ECM; A-G), Collagen sponge control (H-N) and root canals left empty (O-U) The µCt sections show the open apices directly connected to the periapical tissues. The asterisk on µCt sections indicate the roots featured in the gross histology images (Goldner's trichrome) C, J & Q. B, I and P are enlargement of framed area in C, J & Q respectively. D, K & R show the IHC for CD31 from the framed area in C, J & Q respectively. Arrows in D point to positivity around a blood vessel. E, L & S show the IHC for DSP from the framed area in C, J & Q respectively. Arrows in E point to DSP-positive tissue. F, M & T show nuclei (DAPI) of cells infiltrated in proximity to the pulp chamber. G, N & U show nuclei (DAPI) of cells infiltrated at the root apex. d: dentin. Scale bars: B, I & P, 100µm; C, J & Q, 250µm; D, E, K, L, R & S, 50µm; F, G, M, N, T & U, 200µm.

3.4 DISCUSSION

In the present study, we report the successful decellularization of swine pulp tissue from young pigs. We characterized the decellularized pulp matrix (DP-ECM) as a homologous site-specific ECM targeting dental pulp regeneration for regenerative endodontics applications. Although we did not compare young to old ECM, our selection of the 6-month old swine matrix was based on the notion that young ECM performs better in rescuing old cells potential of proliferation and differentiation (Sun et al. 2011; Zhu et al. 2009). As a strategy for regenerative pulp therapy, ECM-based materials are a viable option for scaffold sourcing as they represent a readily available carrier with unique combinations of bioactive molecules from native tissue while not relying on designing a delivery system for a single GF (Hoganson et al. 2010; Ravindran and George 2015).

Investigating the efficiency of our decellularization process, DAPI and H&E histology showed no visible nuclei. Quant-iT PicoGreen results confirmed that DP-ECM had significantly less residual double-stranded DNA compared to native pulp tissue. To reach the standard requirement of less than 50ng of residual DNA per mg of dry tissue (Brown et al. 2011), a marker for the effectiveness of decellularization, we performed several modifications in the original protocol: mincing of pulp tissue while applying vacuum pressure allowed better tissue penetration compared to treatment with acids and detergents alone. (Gilbert et al. 2006).

To understand the effect of DP-ECM on cells of dental populations, we selected human DPCs as a candidate for proliferation and migration assays. The digested DP-ECM showed a statistically significant increase in proliferation at day 3 followed by normal proliferation rate at day 7. On the level of migration, DP-ECM shows a chemotactic effect on DPCs when compared to 0% FBS, the increase in the number of migrating cells was dose-dependent. This observation highlights the role of the ECM degradation products, as demonstrated in previous studies investigating the cell-matrix interaction (Reing et al. 2009).

To determine the effect of the decellularization process on the resulting matrix proteins, Col1, DSP, DMP1, and vWF were fluorescently labeled before and after decellularization. Col1 consists of the matrix body; DSP and DMP-1 are members of the SIBLING protein family and play a role in mineralization and formation dentin-pulp complex (Beniash et al. 2011; Lee et al. 2012); and vWF as a protein involved in blood vessels formation. Immunofluorescence labeling showed the conservation of these original matrix proteins after decellularization.

For further characterization, we selected ELISA to quantify VEGF, bFGF and TGF-β GF shown to be present in other ECM-based materials (Keane et al. 2013; Reing et al. 2010; Wolf et al. 2012) and crucial for dental pulp development and regeneration namely in angiogenesis, collagen production and fibroblasts function (Boyle et al. 2014; Lee et al. 2015). Envisioning clinical application as our ultimate goal for DP-ECM application and to understand the effect of disinfection and sterilization on the produced matrix, we compared the DP-ECM to a group of lyophilized and Ethylene-Oxide sterilized DP-ECM and to another that was only disinfected by peracetic acid; while having the native non-decellularized tissue as a control. EtO sterilization was selected according to its induction to the least physical and chemical changes in the decellularized matrix (Matuska and McFetridge 2015). ELISA analysis showed that the decellularization alone did not affect the amount of VEGF and TGF-β within the tissue while it significantly dropped the amount of bFGF to an undetectable level. This indicates that bFGF may be bound to the cell membrane (Tassone et al. 2015) but also could be easily lost during the wash steps being loosely bound to the matrix (Witte et al. 1989). The additional treatment of DP-ECM with peracetic acid for disinfection did not have a significant reduction on the amount of VEGF and TGF-β; while lyophilization and EtO sterilization did. To rule out the effect of either the lyophilization or the sterilization processes, TGF-β was quantified before and after lyophilization for both native tissue and DP-ECM (Appendix Figure1). After lyophilization, TGF-β was significantly reduced for both groups, while adding EtO sterilization did not reduce further the amount of TGF-β in the matrix (Fig. 9). This suggests that the reduction in GF seen after lyophilization and EtO sterilization is mainly attributed to lyophilization prior to sterilization. On the level of retained glycosaminoglycans, the DP-ECM showed a reduction of about 1 µg/mg of dry tissue weight after complete decellularization with retention of the rest of

the S-GAGs Collectively, our results indicate DP-ECM retained VEGF, TGF-β and S-GAGs, highlighting its biological activity as an implantable scaffold, which was also confirmed by the in-vivo implantation in beagles' root canals.

To investigate the regenerative ability of DP-ECM, we implanted lyophilized and sterilized DP-ECM into fully debrided root canals in beagle dogs for 8 weeks. The canals instrumentation targeted opening the root apex to 0.5mm to recruit and investigate the influx of the periapical cells toward the implanted material (Wang et al. 2015; Zhu et al. 2008). Experimental controls were collagen matrix and empty canals filled only with the blood clot. After 8 weeks, all experimental groups showed cellular infiltration, however, only the DP-ECM group showed CD31 positive and DSP positive tissue within the pulp canals indicating neovascularization and formation of dental pulp-like tissues respectively. The CD31 and DSP were scrutinized to be from canine and not from swine origin by employing antibodies reacting toward canine tissue only (Appendix Figure 3). All three groups showed the formation of mineralized structures within the dental pulp. This tissue is usually considered to be cementum differentiation and attributed to the invasion of mesenchymal cells from the periodontal ligament differentiating into cementoblasts; a common observation in pulp regeneration literature. It is of consensus, however, the necessity to include cementogenesis inhibitor molecules to prevent the development of intracanal mineralization while attempting pulp regeneration (Zizka and Sedy 2017). Our observations and results point to an ECM-based scaffold able to promote constructive remodeling and formation of site-appropriate tissue (Wolf et al. 2012).

In this study, we show that the use of a readily available decellularized pulp ECM provides a structural and functional native scaffold that can recreate the original

microenvironment for dental pulp regeneration. We believe our approach to regenerate the dental pulp by DP-ECM has the following advantages: i) The employment of growth/cryptic peptides within the debrided pulp space promises the recruitment of host cells to repopulate the dental pulp from the periapical tissues in a process mirroring physiological tissue remodeling (Agrawal et al. 2010). ii) This cellular trafficking warrants the re-establishment of the stem-cell niche, hence a lifetime of proper tissue turnover (Sacchetti et al. 2007; Zaky and Cancedda 2009). iii) Less cost and complexity from approaches requiring substantial ex-vivo cell manipulation; and iv) with its minimally invasive procedure, DP-ECM based pulp regeneration would stand as an auspicious approach to pulp regeneration for translation to the dental clinic. Further investigation, however, is needed to fully understand the remodeling process and to gain insight into the host response to DP-ECM.

Acknowledgment

We would like to thank Drs. Stephen Badylak and Scott Johnson for their assistance in developing our decellularization protocol. This work was supported by grants from The American Association of Endodontists (AAE) #26849.

4.0 SPECIFIC AIM 2: EFFECT OF DECELLULARIZED PULP EXTRACELLULAR MATRIX ON DENTAL PULP AND PERIODONTAL LIGAMENTS CELLS

4.1 INTRODUCTION

Currently, the gold standard to treat a patient suffering from irreversible pulpitis is to perform root canal treatment, resulting in the removal of the infected pulp and filling of the empty space. There are no current autografts or xenografts that serve as a potential clinical replacement. This is due to the lake of an appropriate scaffold capable of dental pulp regeneration. This is also true for clinical techniques, as most of the current knowledge is based on the use of root canal treatment related products and procedures.

The shift toward the use of ECM based scaffolds is growing larger in the field of regenerative medicine. The application of these scaffolds in dental pulp cases might carry the potential for the field of regenerative endodontics. Previous attempts to develop synthetic and biological materials for implantation have shown promising results, emphasizing the possibility of pulpal regeneration (Huang et al. 2018; Paduano et al. 2017). Matrices mimicking the dental pulp chemical and physical properties were developed using methods like decellularization and electrospinning (Alqahtani et al. 2018; Kim et al. 2015a; Song et al. 2017).

Along these attempts, different types of cells were harvested and used for this purpose. It is of note that most tissues and organs within the adult human body have multipotent stem and

progenitor cell populations that are specific for the tissue or organ within which they reside. In the 2000s, the dental pulp cells were sorted for stem cell markers and characterized to have myogenic, adipogenic and neurogenic potential, highlighting their role as stem cells (Gronthos et al. 2002; Gronthos et al. 2000). Similarly, cells isolated from the periodontal ligaments and apical papilla were positive for stem cells marker and show potential for tissue regeneration (Ruparel et al. 2013; Seo et al. 2004). Because ECM produced by the resident cells of each tissue is well suited with regard to composition and structure for that particular tissue, the composition of ECM harvested from different tissues will also vary (Sellaro et al. 2007). It is expected that ECM derived from a particular tissue may generate degradation products that recruit progenitor cells that are lineage-directed for that same tissue. Based on this approach it is important to characterize and understand the interplay between the cells and their respected matrix.

The interactions between cells and the extracellular matrix have been shown to influence the behavior of the cells and can result in a diverse array of biological processes such as migration, adhesion, and angiogenesis (Davis 2010; Maquart et al. 2005; Vlodavsky et al. 2002). This is due to ECM constant release of these effects upon cellular behavior and phenotype, and in return, the cells remodel the ECM in a process called dynamic reciprocity (Bissell and Aggeler 1987; Boudreau et al. 1995; Ingber 1991). This dynamic homeostasis is a result of highly regulated cell signaling and patterning processes and is dependent upon the secretion of matrix metalloproteinases (MMPs), tissue inhibitors of MMPs, fibronectin, and collagen.

The dynamic reciprocity of ECM is a distinct feature that has not been replicated in other tissue engineered biomaterials, as synthetic materials can only be adjusted to degrade at specific rates and under specific conditions. The dynamic reciprocal nature of the ECM requires the ECM to release its bioactive products that are also biodegradable. As a result, all the components of the

ECM are subjected to degradation and change. The main components responsible for the degradation of the ECM extracellularly are MMPs, metalloproteinases with thrombospondin motif families (Cawston and Young 2010).

Degradation caused by these proteinases can result in the exposure and recognition of new sites with potent bioactivity on the surface of the ECM. These byproducts include cryptic sites, which can influence cells behavior and bioprocesses including angiogenesis, anti-angiogenesis, chemotaxis, adhesion, and antimicrobial effects (Ramchandran et al. 1999). One of the most common cryptic site peptides is the Arg-Gly-Asp peptide found within fibronectin, collagen, vitronectin, and osteopontin, which have been used for cell adhesion (Hern and Hubbell 1998; Hsiong et al. 2008; LeBaron and Athanasiou 2000; Vidal et al. 2013).

ECM based scaffolds also serve as a niche for stem cells and growth factors. The ECM cell niche contributes to the establishment and maintenance of stem cell differentiation through soluble factors and ECM macromolecules (Brizzi et al. 2012; Kazanis and ffrench-Constant 2011; Votteler et al. 2010). Within the ECM, the degradation and remodeling in the stem cell niche are thought to mediate cell activation and release. The composition, topography, and biomechanics of the ECM can regulate stem cell migration and differentiation (Engler et al. 2006; Reilly and Engler 2010).

The goal of this aim is to understand the effects produced by the DP- ECM on cells from dental pulp and periodontal ligaments. The UBM, a well-characterized scaffold will be used as a control and to also allow us to understand the difference between site-specific matrix and ectopically derived matrix. The use of an appropriate cell population is another important factor since the source of the cells invading the root through the apex remains questionable. So, the two cell populations included in this work are both readily available and can be easily harvested from

the adult's third molar. This chapter focuses on the ability of these cells to promote wound healing and understanding the effect of matrix degradation products on cells gene expression profile. In-vivo, the matrices will be implanted subcutaneously with different cells to characterize the regenerated tissues for vascular, dental and neuronal proteins expression and the tissues resemblance to the natural dental pulp anatomy.

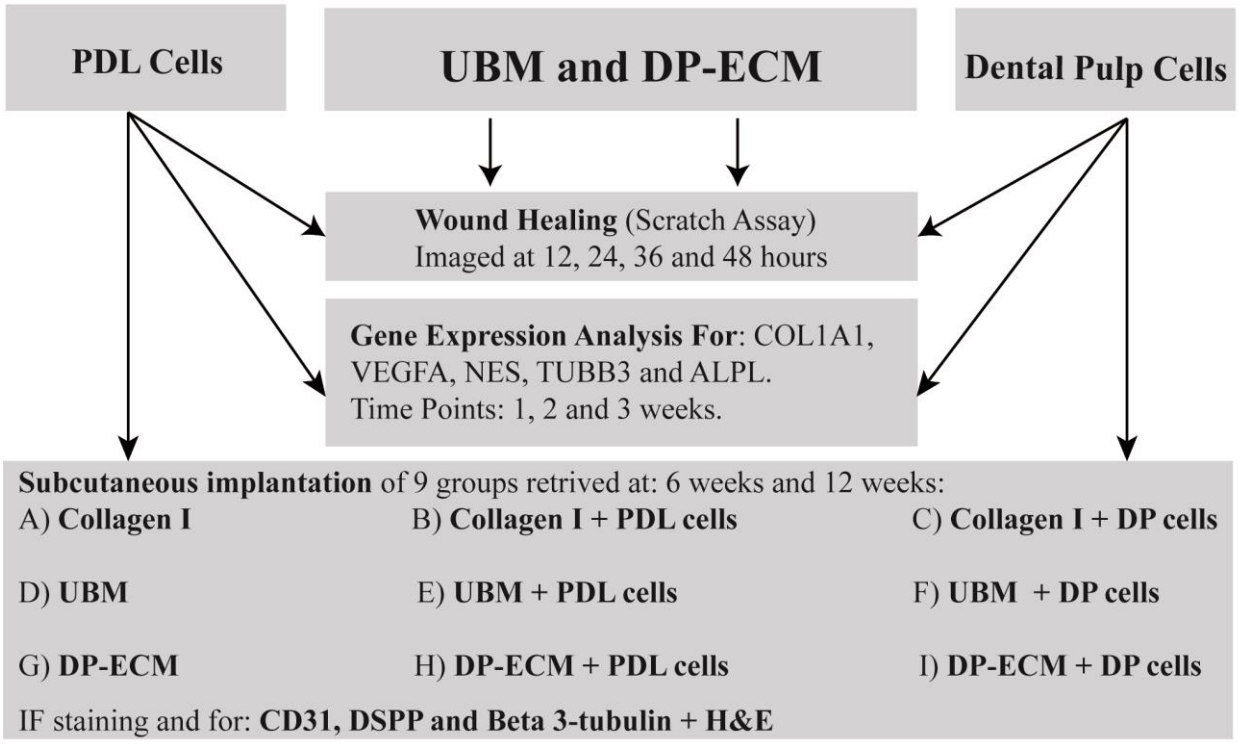

Figure 14. Scheme of experimental design for Aim 2.

4.2 MATERIALS AND METHODS

4.2.1 Wound Healing Assay

To determine the cells ability to heal the extirpated pulp canal and repair the injury area, wound healing assay was performed on dental pulp and periodontal ligaments cells. Cells were cultured to P3, seeded into a 12-well plate at 200,000 cells/well and were cultured to ~90% confluency. Wounds were created horizontally using 200 µl pipette tip across all the wells. After that, cells were washed with PBS to remove the dead cells and stained with Hoechst 33342 for 10 mins, washed twice with PBS to remove the dye and treated with maintenance medium (M.M) as a control, M.M with DP-ECM at 1 mg/ml and M.M + UBM at 1 mg/ml. Wells were imaged at 12 hours interval over the course of 48 hours. Image analysis and counting of cells were performed using ImageJ.

4.2.2 Gene Expression Analysis

To understand the effect of the ECM degradation products on dental pulp and periodontal ligaments cells. The cells at P3 were seeded into 6-wells plate at $4x10^5$ cells/well, cultured to sub-confluency and treated with the following: (control) maintenance medium, M.M with DP-ECM 1 mg/ml and UBM 1 mg/ml for 7, 14 and 21 days. At the end of each time point, total RNA was extracted from the cells using the Trizol technique. The quantity and quality of RNA were measured using a nanophotometer. Complementary DNA was synthesized using Applied Biosystems™ TaqMan™ High-Capacity RNA-to-cDNA kit (Fisher #43-874-06). For quantitative RT-PCR, TaqMan® Fast Advanced Master Mix (Fisher #44-445-57) was used

to analyze the mRNA expression of ALPL, COL1A1, VEGFA, TUBB3, NES, and human 18S as a housekeeping gene to allow for relative quantification of the signal.

Table 1. Genes used to characterize the dental pulp and periodontal ligaments cells response.

Gene Symbol and name	Taqman™ gene expression assay Catalog Number
ALPL (Alkaline Phosphatase)	(Hs01029144_m1)
COL1A1 (Collagen I alpha I chain)	(Hs00164004_m1)
VEGFA (vascular endothelial growth factor A)	(Hs00900055_m1)
TUBB3 (beta 3-tubulin)	(Hs06637750_g1)
NES (Nestin)	(Hs04187831_g1)
18S (human 18S Ribosomal RNA)	(Hs99999901_s1)

4.2.3 Constructs Preparation

To mimic the orthotopic model of the tooth root canal: subcutaneous implants consisting of human tooth root segments were used in this study. The segments contain a combination of different cells and different scaffolds. The goal is to determine the suitability of these scaffolds while understanding the ECM influence on cells in dental pulp regeneration scenario (For all groups sample size n=8, four samples were retrieved at 6 weeks and another four samples at 12 weeks to be used for histology processing and immunofluorescent staining).

4.2.3.1 Tooth Root Segments

Adult human teeth were collected after extraction at the University of Pittsburgh, School of Dental Medicine. The teeth crowns were removed, and the roots were scraped to remove

cementum and cut into radicular segments of 5-6 mm in length using an IsoMet low-speed saw (Buehler, Lake Bluff, IL, USA) with IsoMet diamond blade (Buehler). The root canal space was opened to a diameter of 1-1.5 mm. Root segments were then conditioned in a series of washes with NaOCl and EDTA which has been previously shown to enhance cells differentiation and adhesion to the dentin wall (Galler et al. 2011). The roots were first treated with 0.5 M ethylenediaminetetraacetic acid (EDTA) for 1 min, then rinsed in PBS for 5 min and washed in 6.15% NaOCl for 10 min. The roots were then washed 3 times in sterile PBS and then treated again with 0.5 M EDTA for 10 min. The roots were rinsed again 3 times in PBS. To ensure the sterilization of the segments. The roots were incubated in Growth Medium at 37°C for 4 days and monitored for microbial growth. One side of the canal openings was plugged by Mineral Trioxide Aggregate as an actual presentation of a root canal in-vivo.

4.2.3.2 Scaffolds Preparation and Delivery in Root Segments.

After the preparation of the root segments, cells from dental pulp and PDL were cultured to 80% confluency then it was treated with trypsin, collected and centrifuged to obtain a cell pellet. The pellet was re-suspended in Rat Tail Collagen I (Advanced BioMatrix) at the concentration of $1x10^7$ cells per 1 ml of collagen. To allow the attachment of cells to the scaffolds, the cells suspension was mixed with 3 different scaffolds (Rat Tail Collagen I, DP-ECM and UBM) that have been lyophilized and sterilized with ethylene oxide. Afterward, the cells and scaffolds were placed in the root segments using a plugger and a plastic instrument. The constructs were then incubated at 37°C until surgery takes place on the same day.

The groups included in this study are featured below in **Table 2**.

Table 2. Groups included in the constructs for subcutaneous implantation.

Groups	Matrix	Seeded cells
1	**Collagen**	No cells
2		Periodontal Ligaments Cells
3		Dental Pulp Cells
4	**UBM**	No cells
5		Periodontal Ligaments Cells
6		Dental Pulp Cells
7	**DP-ECM**	No cells
8		Periodontal Ligaments Cells
9		Dental Pulp Cells

4.2.3.3 Surgery and Animal Implantation

All animal studies were approved by the University of Pittsburgh Institutional Animal Care and Use Committee (IACUC). The prepared constructs in (Table 2) were implanted subcutaneously into 8 weeks old immunocompromised NU/NU nude male mice (Jackson Lab); in total, 4 samples from each group were implanted per time point. Mice were exposed to isoflurane and an incision approximately 1 cm in length was made in the dorsum of the mouse, air pockets were created by blunt dissection, samples were implanted and the wounds were closed with interrupted sutures. Four samples were implanted into each mouse, and samples were retrieved after 6 and 12 weeks.

4.2.4 Histology and Immunofluorescence

Upon retrieval of samples, the constructs were placed in a cold 10% Formalin for 24 hours. After that, samples were treated with 0.32 M of EDTA for 3 to 4 weeks. Radiographs were taken to determine decalcification of dentin. Following processing and embedding of samples, 7-µm sections were taken and were used for H&E staining.

To detect and compare the presence of vascular, odontogenic and neurologic markers in the regenerated samples, sections of 7-µm thickness were stained for: CD 31 (Abcam, ab28364), DSPP (Kerafast, LF-151, and LF-153) and β-III Tubulin (Abcam, ab52623) according to the following protocol: Sections were deparaffinized in 3 changes of Xylene and rehydrated in a series of alcohol changes. Once hydrated, samples were inspected for auto-fluorescence and treated with Sudan Black B 1.5% in 70% ethanol or Cupric Sulfate and Ammonium acetate 50mM if needed. After that, heat-induced epitope retrieval was performed using 0.1 mM Sodium Citrate buffer pH: 6 at 98°C for 20 mins or in 10 mM Tris-EDTA buffer pH: 8 at 98°C for 20 mins. Primary antibodies were applied in the following concentrations (DSPP at 1:200, CD31 at 1:100 and β-III tubulin at 1:400) and incubated overnight at 4°C followed by washes and application of fluorophore-conjugated secondary antibody, Goat anti-Rabbit Alexa Fluor 555 for (CD31 at 1:300), (β-III Tubulin at 1:1000) and (DSPP at 1:1000).

4.3 RESULTS

4.3.1 Wound Healing Assay

In order to understand the effect of ECM degradation products on cells isolated from different dental populations, wound healing assay was selected. The periodontal ligaments cells showed an increase in the number of cells migrating to the wound area after 12 hours and 24 hours when compared to the untreated control. It shows that the treatments with UBM and DP-ECM can potentially enhance wound healing when used with PDL cells. After 36 hours of wound induction, it appears that there are no differences in the number of cells and even at 48 hours.

Another cell line, dental pulp cells, was scratched and treated in a similar way. Interestingly, the cells isolated from dental pulp showed a better wound healing response when treated with the DP-ECM digest. At 12 hours the number of cells recruited to the wound area has exceeded the control and also the UBM at 24 hours post-treatment. The wounds created with dental pulp cells also show no differences at time points: 36 hours and 48 hours.

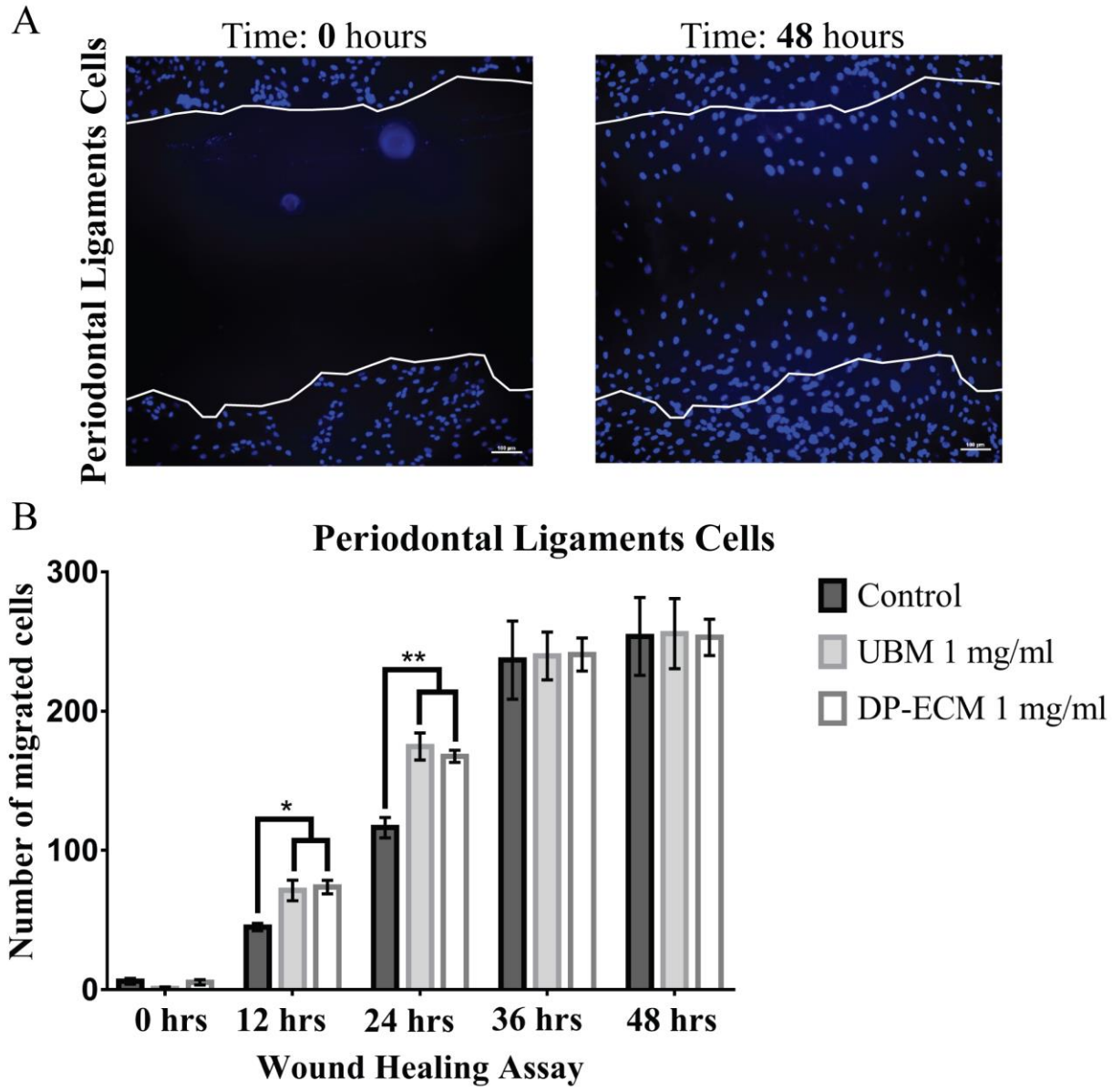

Figure 15. Wound healing assay for PDL cells. A) After the scratch, cells were stained with Hoechst 33342 and left to migrate for 48 hours. B) The numbers of cells migrating to the wound area from 0 hours to 48 hours. Scale bars=100µm (n=4) Error bars are mean ± SEM * $p \leq 0.05$ ** $p \leq 0.01$

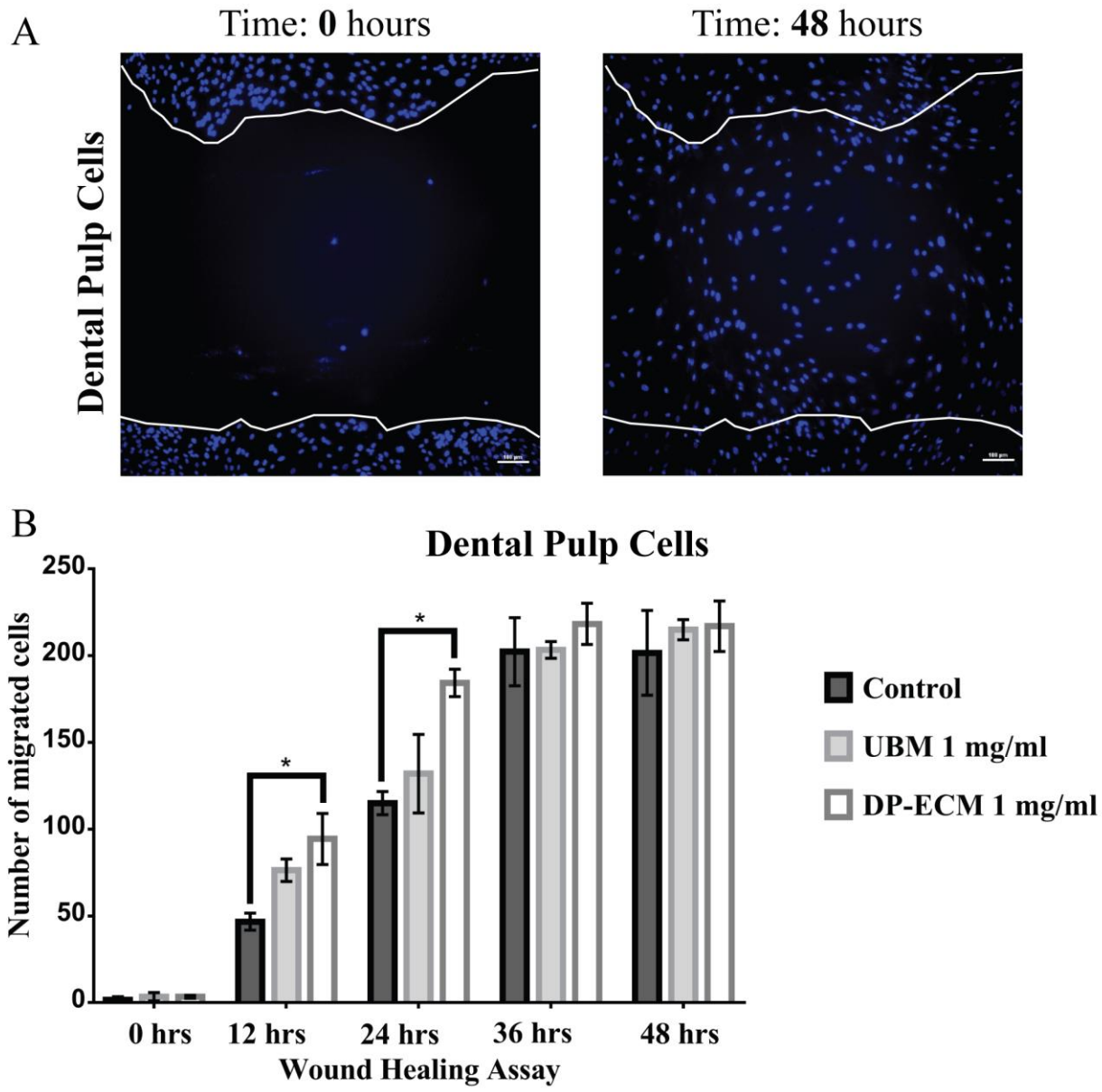

Figure 16. Wound healing assay for Dental Pulp cells. A) After the scratch, cells were stained with Hoechst 33342 and left to migrate for 48 hours. B) The number of cells migrating to the wound area from 0 hours to 48 hours. Scale bars=100μm (n=4) Error bars are mean ± SEM * $p \leq 0.05$ ** $p \leq 0.01$

4.3.2 Gene Expression Analysis

To determine the effects of DP-ECM and UBM on the gene expression of PDL cells and dental pulp cells, both matrices were digested and add to the cells medium at 1mg/ml for 1, 2 and 3 weeks. Gene analysis for VEGFA, Nestin, TUBB3, ALP, and COL1A1 as markers for angiogenesis, neurogenesis, and mineralization. After one week of treatment, the PDL cells showed an up-regulation of ALPL with UBM and down-regulation of VEGFA, Nestin, and COL1A1 when treated with UBM and DP-ECM. For dental pulp cells, the DP-ECM induced a decrease in the expression of VEGFA, Nestin, TUBB3, and COL1A1. Similarly, the UBM group showed a decrease in the expression of VEGFA and COL1A1 but not Nestin or TUBB3.

After two weeks of treatment, the PDL cells still show a downregulation of the genes mentioned above along with the UBM creating the same effect on these cells. Dental pulp cells gene expression of VEGFA, Nestin, and COL1A1 appears to be still down-regulated with UBM and DP-ECM. TUBB3 shows an upregulation for dental pulp and periodontal ligaments cells when treated with UBM compared to control.

At three weeks, PDL cells treated with DP-ECM shows an increase in the expression of VEGFA and down-regulation of collagen I and Nestin. The UBM maintained a similar response to the two weeks group with TUBB3 and ALPL being up-regulated. The cells isolated from dental pulp showed an increase in VEGFA and ALPL while collagen I and Nestin were down-regulated when treated with DP-ECM. The UBM, on the other hand, appears to increase the expression of TUBB3 with Nestin still down-regulated.

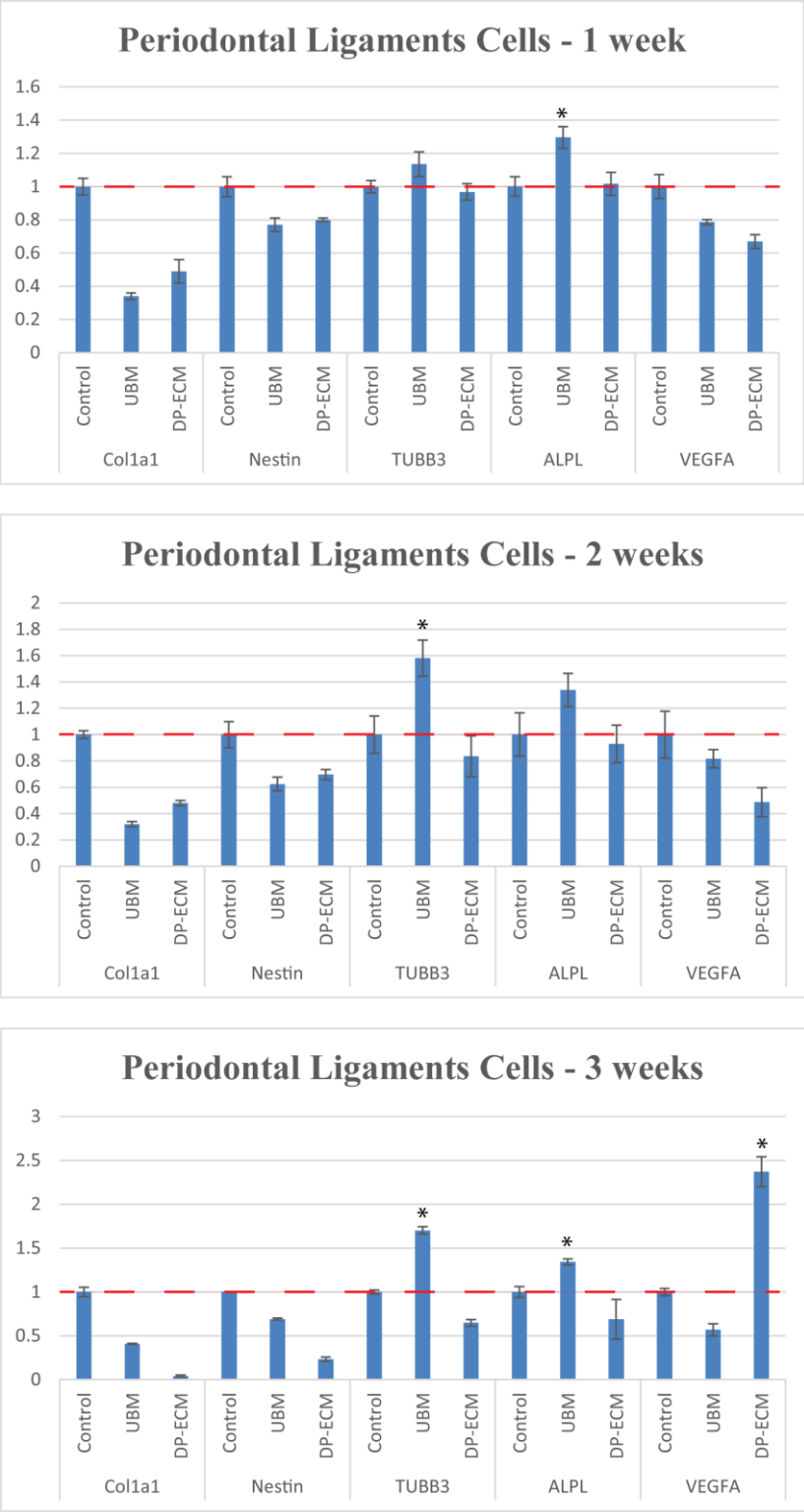

Figure 17. Gene expression analysis of PDL cells at 1, 2 and 3 weeks post-treatment. Genes included: Col1a1, Nestin, TUBB3, ALPL, and VEGFA.

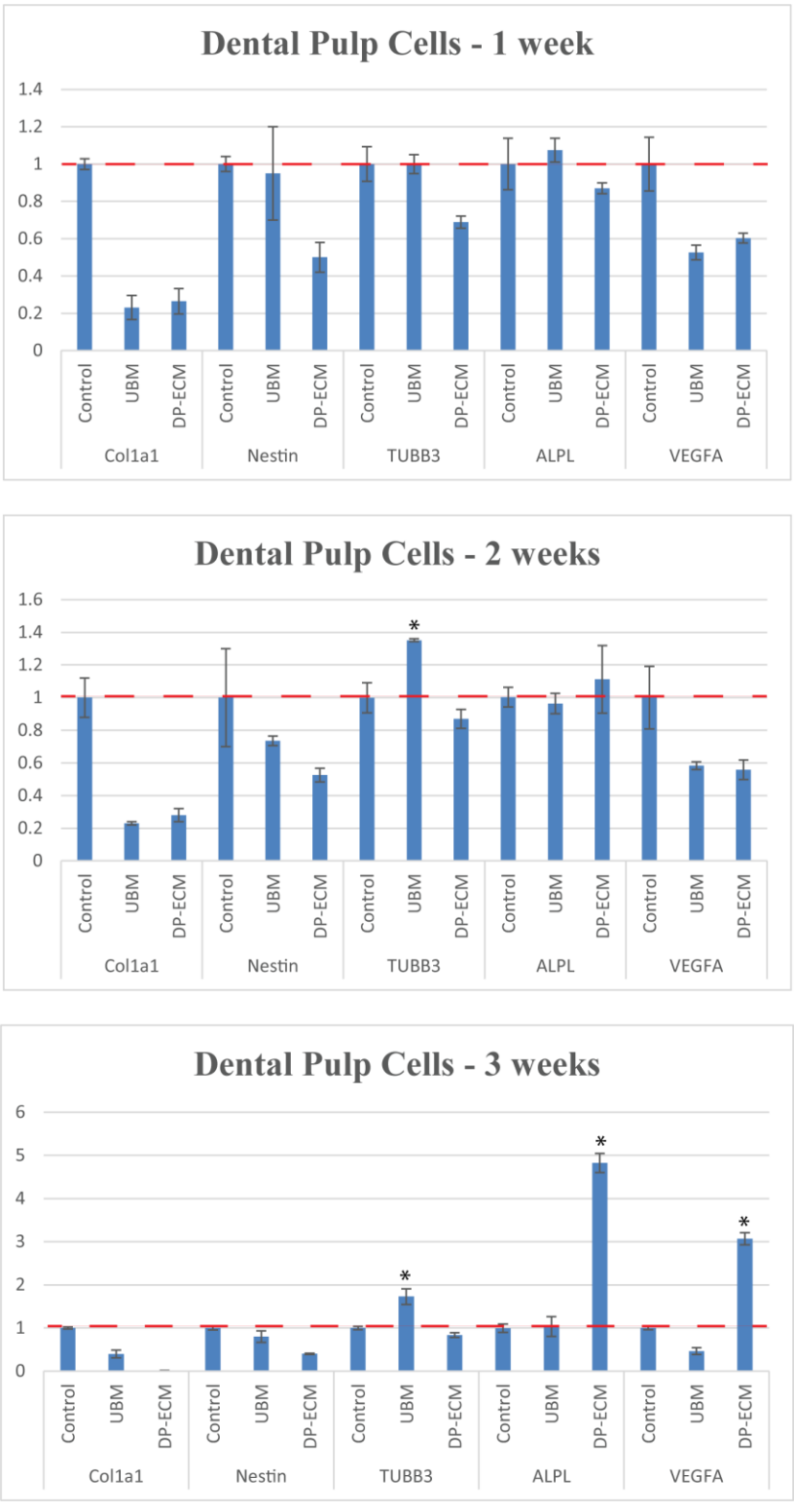

Figure 18. Gene expression analysis of Dental Pulp cells at 1, 2 and 3 weeks post-treatment.

Genes included: Col1a1, Nestin, TUBB3, ALPL, and VEGFA.

4.3.3 Histology and Immunofluorescent Labeling

In this study, constructs made from root segments plugged with MTA on one side were filled with Collagen, UBM, and DP-ECM with and without cells from the dental pulp and periodontal ligaments. Eight samples per group were placed in mice subcutaneously, four samples were retrieved at 6 weeks and four samples were retrieved at 12 weeks. The samples were fixed, demineralized and processed for H&E staining, DSPP, CD31 and β-III tubulin immunofluorescent staining.

At 6 weeks, collagen showed no changes, without any signs of remodeling or cellular infiltration. When seeded with PDL cells, the resulting tissue demonstrates cellularity, organization, and formation of nerves and new blood vessels along with the maintenance of the canal system. When the dental pulp cells were used, similar to PDL, there were signs of neovascularization and moderate expression of β-III tubulin within the canal and DSPP within the cells. Samples filled with UBM powder didn't display any marked infiltration of cells with minimal numbers of cells seen near the UBM/host interface with no expression of either CD31 or β-III tubulin or DSPP. Samples with PDL cells incorporated with the UBM showed a presence of some cells within the canals but no signs of remodeling and regeneration. Similarly, when dental pulp cells were added to UBM it showed no support for these cells and remained negative to vascularity or neurogenesis. The DP-ECM was also included in this study and it was added in a minced tissue form. At 6 weeks, it showed infiltration of host cells mostly around and between the spaces of the DP-ECM. It also shows blood vessels, expression of CD31 and cells expressing DSPP but remained negative to β-III tubulin. When PDL cells were added to the DP-ECM, the ECM showed support for the incorporated cells and shows remodeling of the ECM with positivity for CD31, DSPP and β-III tubulin. Of an interesting note, samples with DP-ECM and

dental pulp cells showed the best remodeling of the matrix and enmeshment of cells into the matrix with areas of the regenerated tissue expressing CD31, DSPP, and β-III tubulin.

Samples retrieved at 12 weeks included the same groups as the ones mentioned above. Collagen remains unchanged in the canal without remodeling or infiltration of the host cells. When PDL cells were added to collagen, it showed cellularity and maintenance of the canal system with markers for CD31 and β-III tubulin still being expressed. The dental pulp cells have also shown similar results when it comes to markers expression and maintenance of cellularity. When using the UBM alone, it shows an outcome similar to the one seen in the 6 weeks group without any signs of tissue remodeling. Dental pulp and PDL cells were also included in the 12 weeks assessment and included in the canal with the UBM. Both groups showed no expression of CD31, DSPP and beta 3-tubulin, with areas of minimal cellularity existing in the canal space. The DP-ECM displayed infiltration of host cells and continues signs of remodeling and expression of vascular, mineral and neuronal markers. The DP-ECM included with PDL cells shows maintenance of cellularity, vascularity, neurogenesis, and expression of DSPP. Last, samples with the dental pulp cells added to the DP-ECM in the canal space appears to be the best in terms of matrix remodeling and neo-tissue formation across the canal, expression of CD 31, DSPP and β-III tubulin are still present.

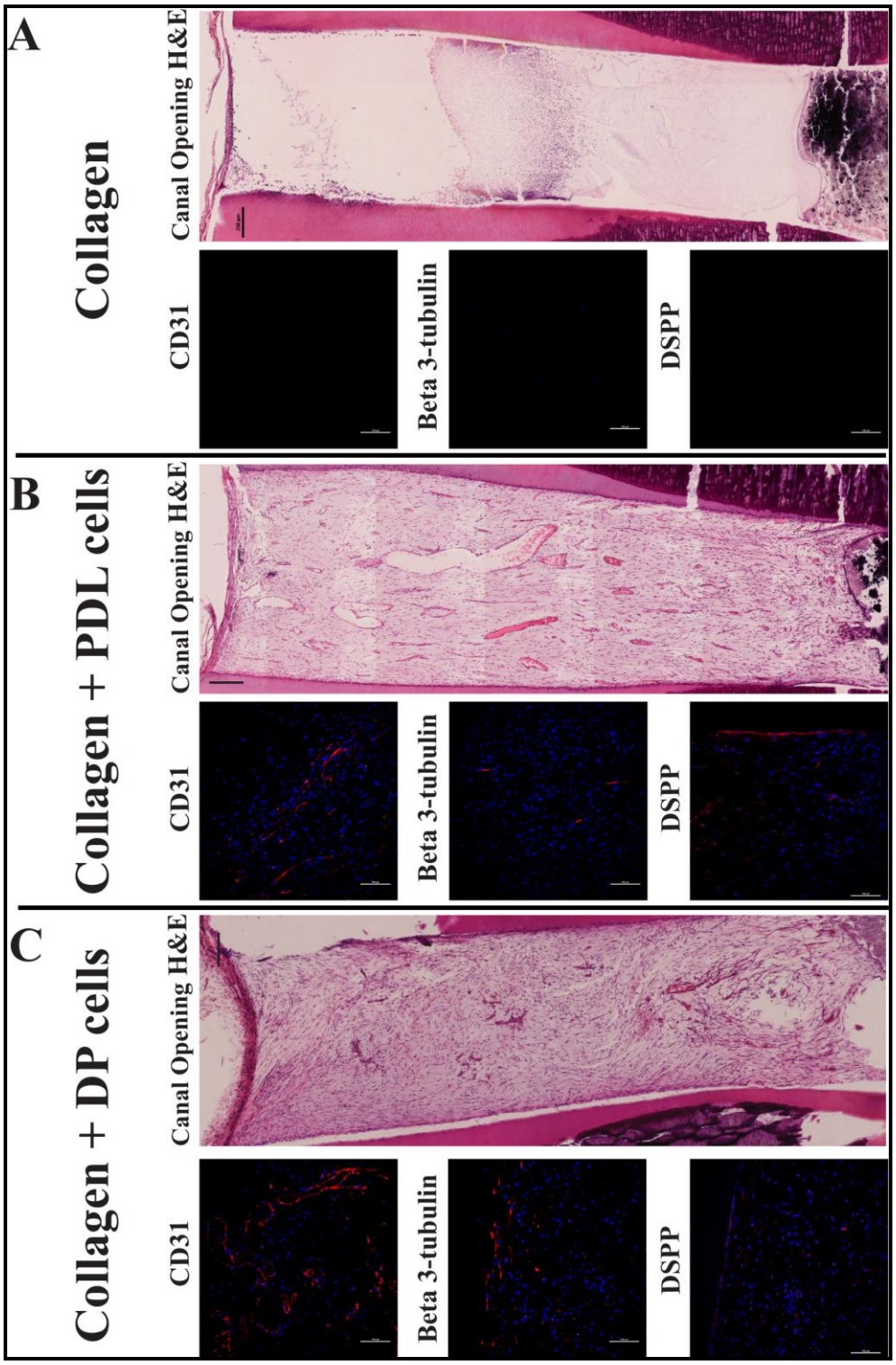

Figure 19. Six weeks after implantation of Collagen alone, Collagen + PDL cells and Collagen + Dental Pulp cells. H&E staining (Scale bar = 250μm) and IF (Scale bar = 100 μm) was done for CD31, β-III tubulin and DSPP.

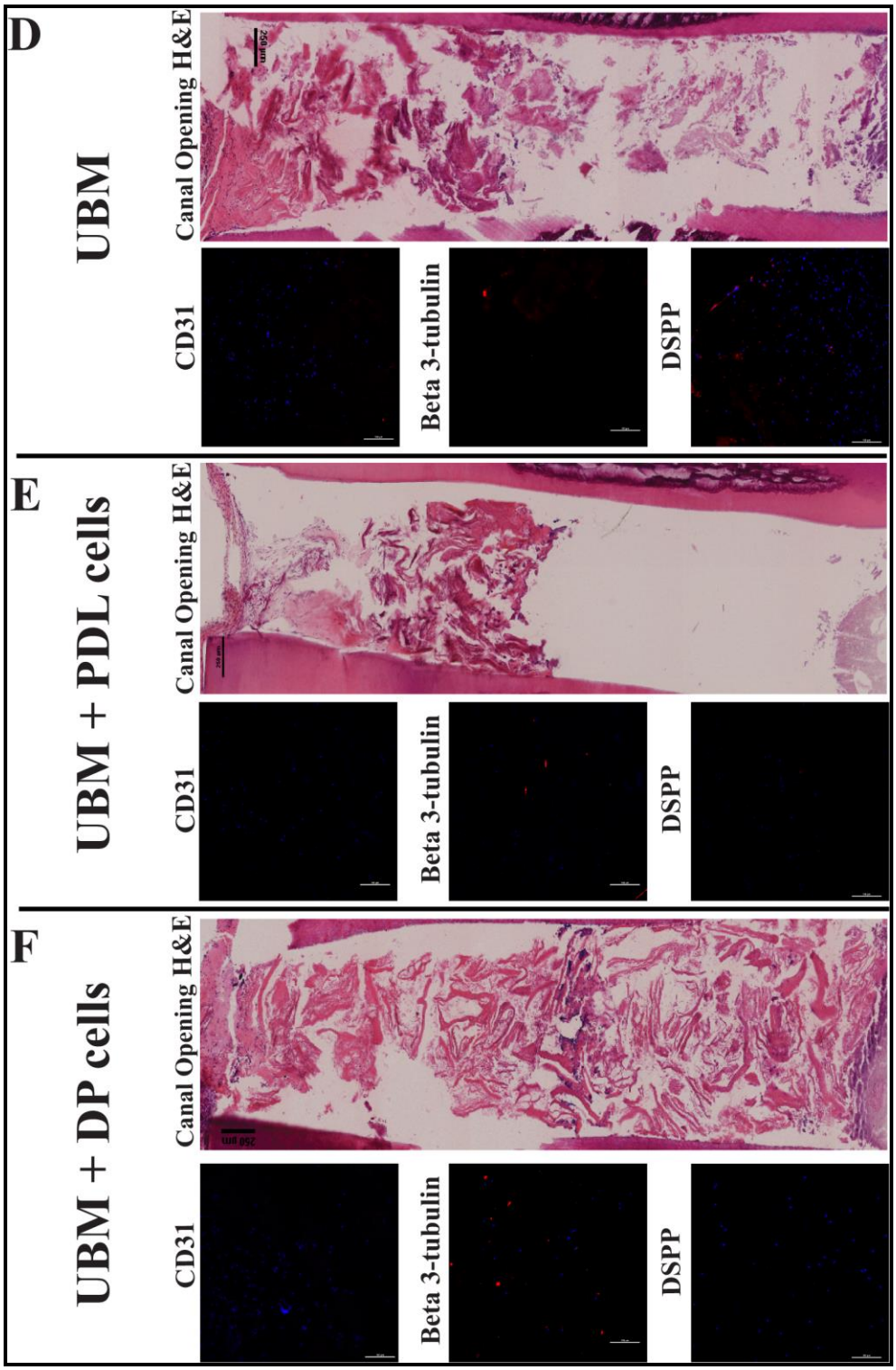

Figure 20. Six weeks after implantation of UBM alone, UBM + PDL cells and UBM + Dental Pulp cells. H&E staining (Scale bar = 250μm) and IF (Scale bar = 100 μm) was done for CD31, β-III tubulin and DSPP.

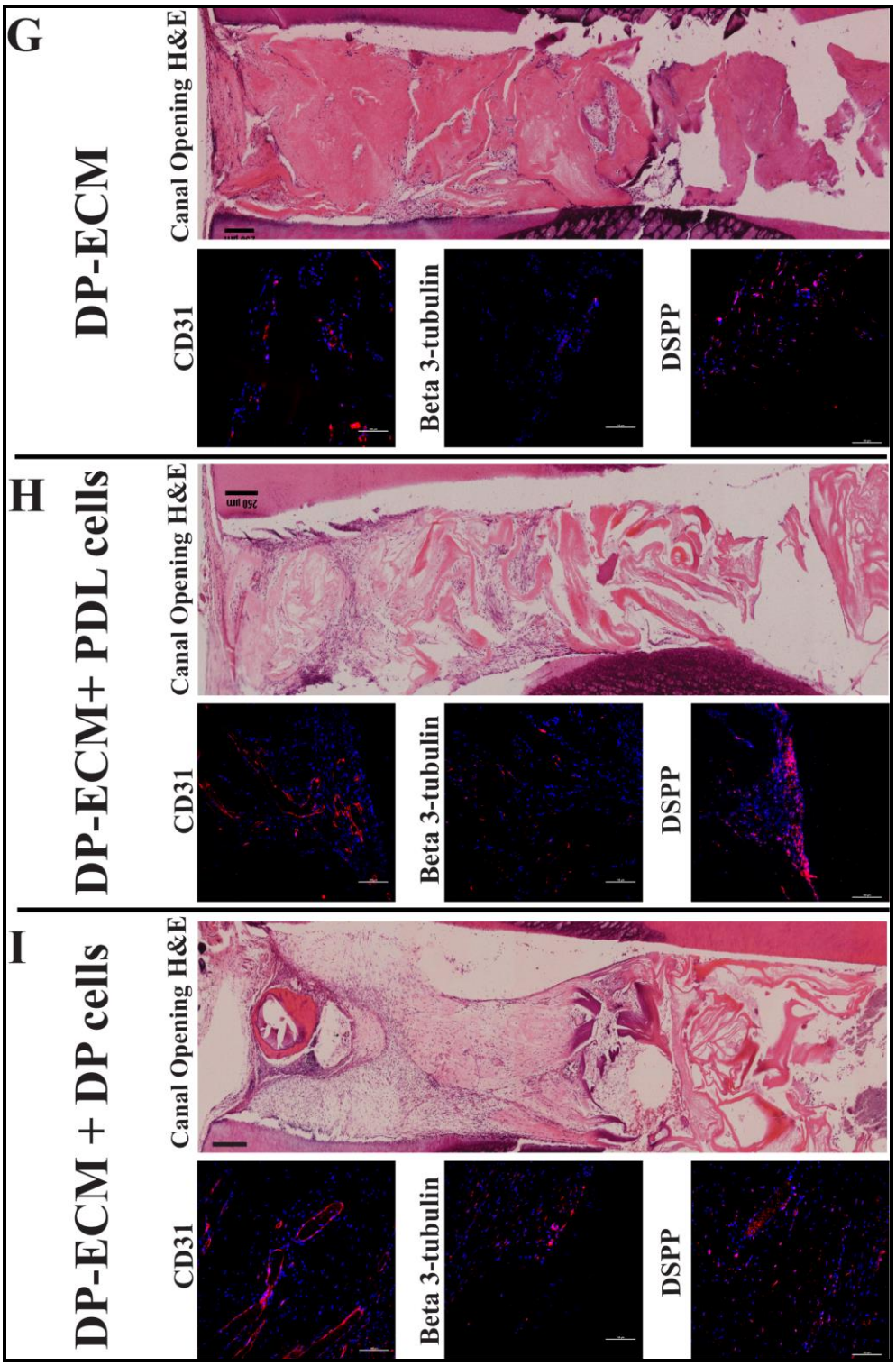

Figure 21. Six weeks after implantation of DP-ECM alone, DP-ECM + PDL cells and DP-ECM + Dental Pulp cells. H&E staining (Scale bar = 250µm) and IF (Scale bar = 100µm) was done for CD31, β-III tubulin and DSPP.

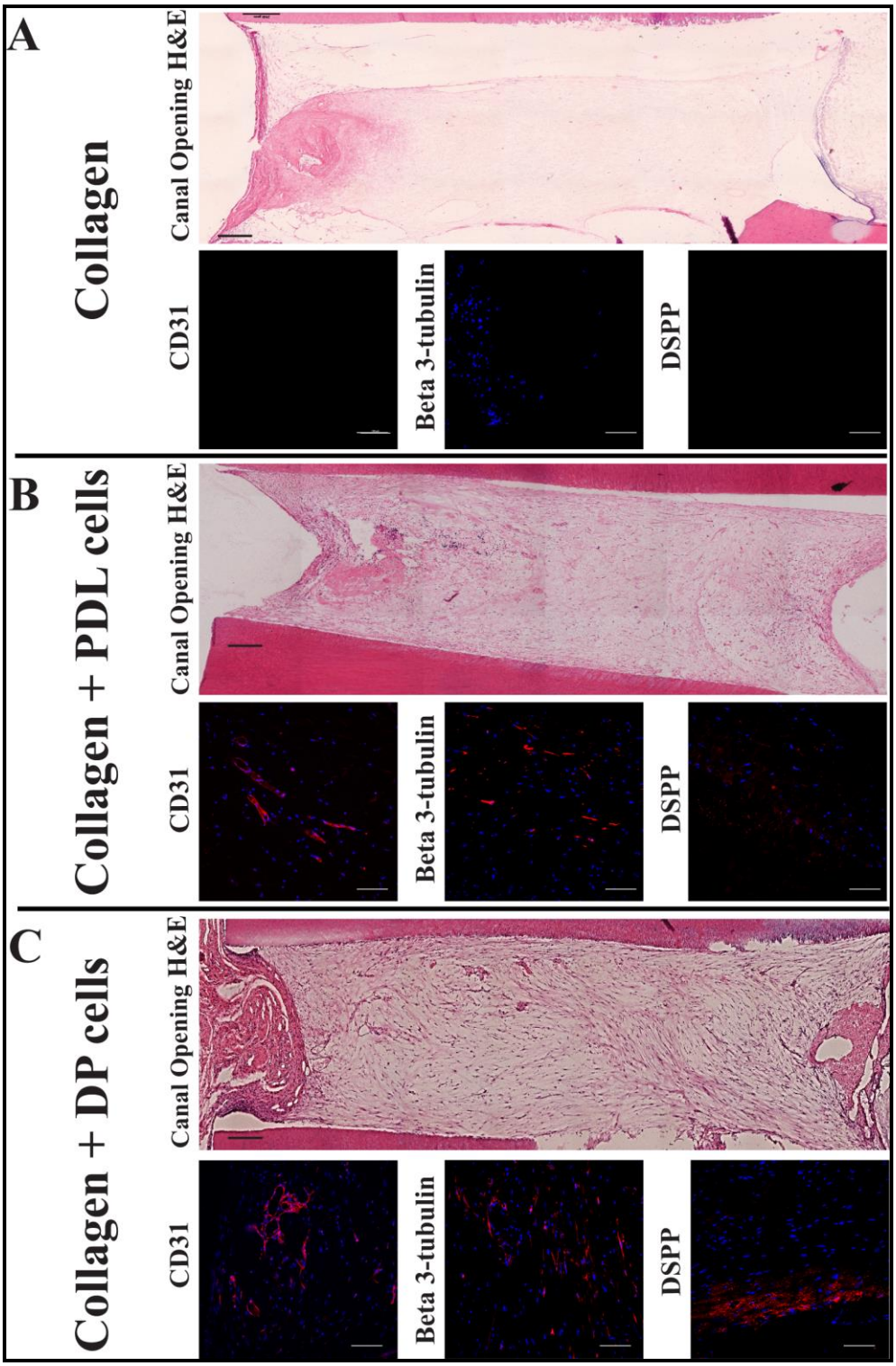

Figure 22. Twelve weeks after implantation of Collagen alone, Collagen + PDL cells and Collagen + Dental Pulp cells. H&E staining (Scale bar = 250μm) and IF (Scale bar = 100μm) was done for CD31, β-III tubulin and DSPP.

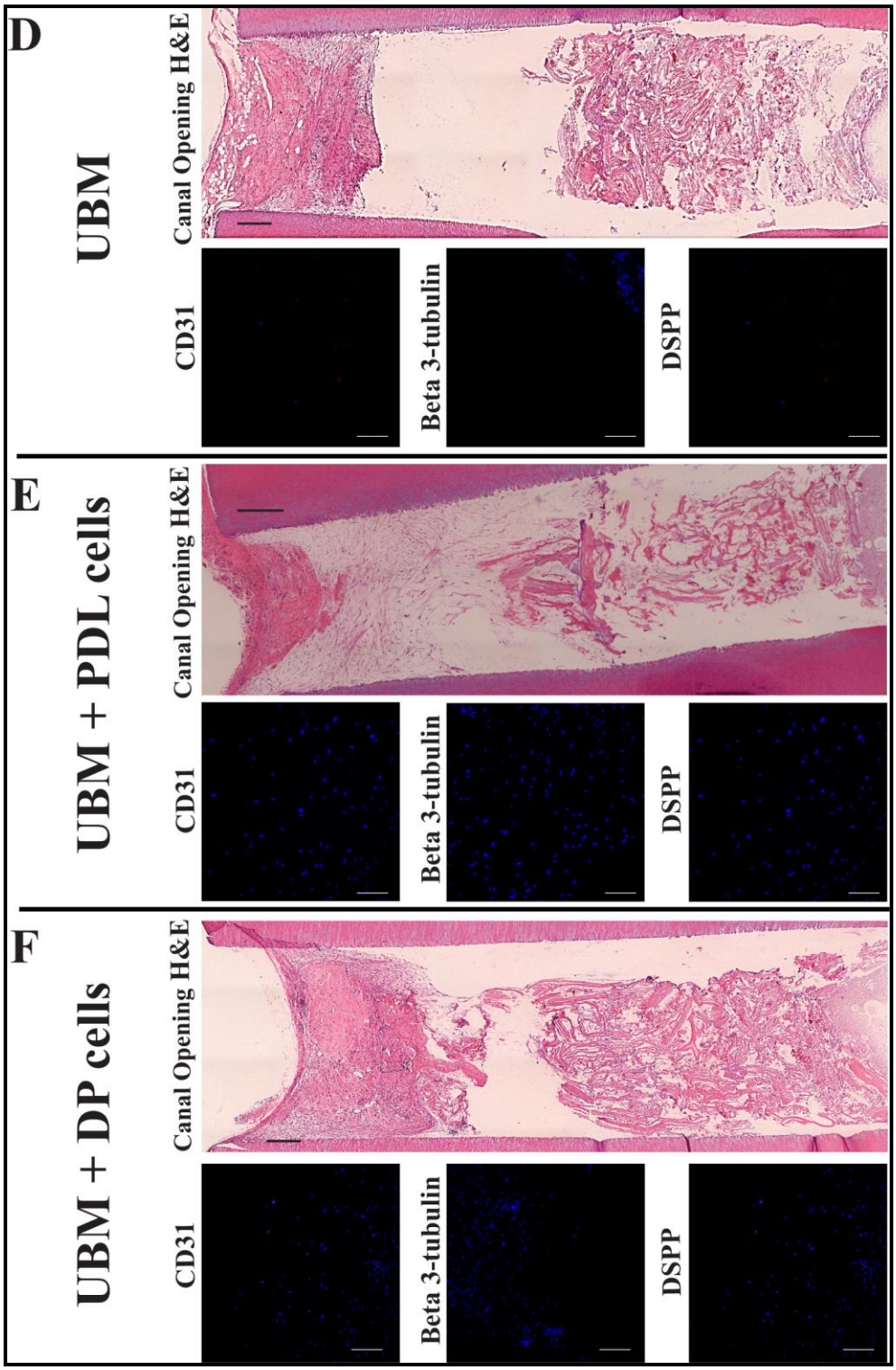

Figure 23. Twelve weeks after implantation of UBM alone, UBM + PDL cells and UBM + Dental Pulp cells. H&E staining (Scale bar = 250µm) and IF (Scale bar = 100µm) was done for CD31, β-III tubulin and DSPP.

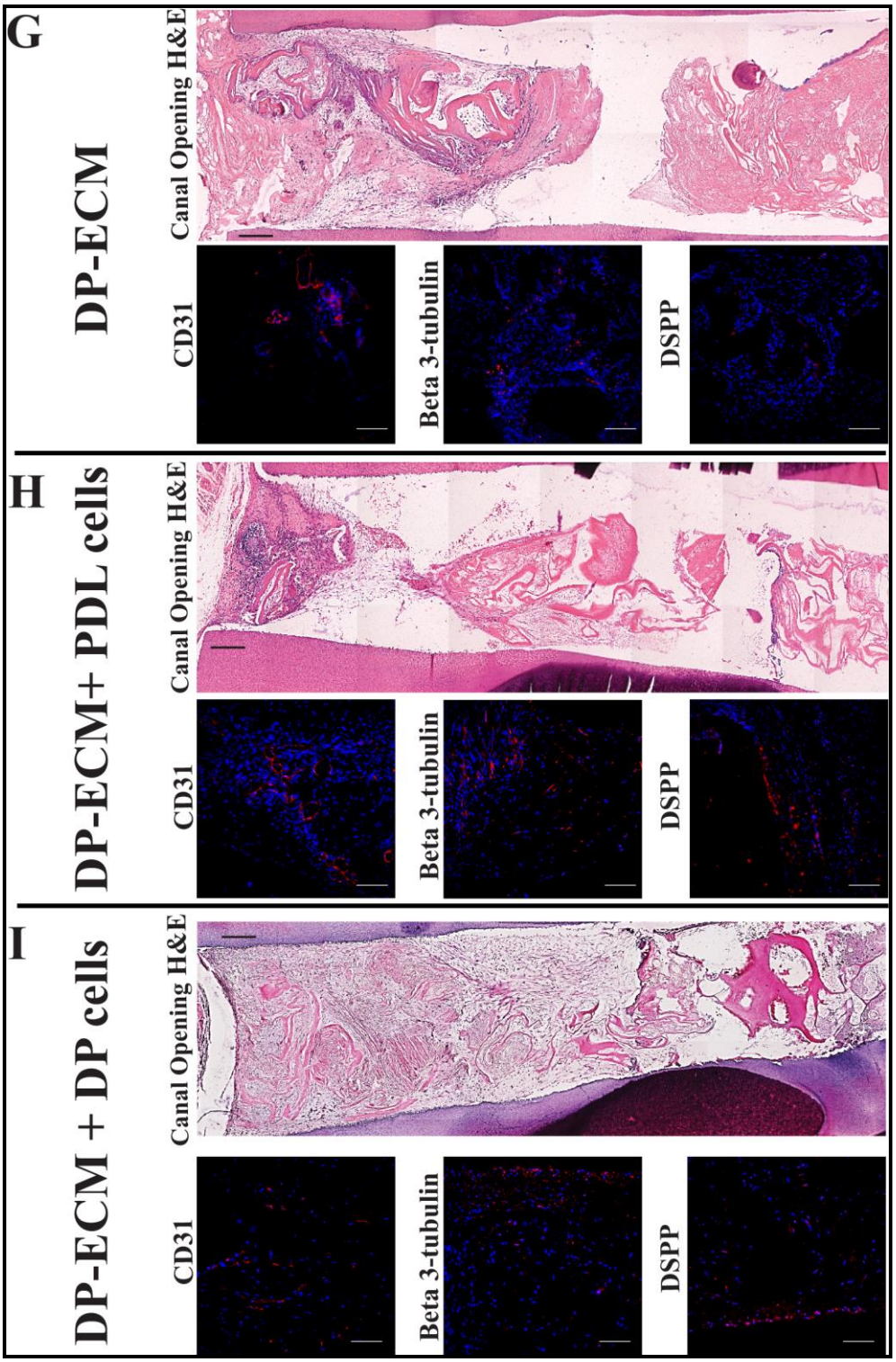

Figure 24. Twelve weeks after implantation of DP-ECM alone, DP-ECM + PDL cells and DP-ECM + Dental Pulp cells. H&E staining (Scale bar = 250μm) and IF (Scale bar = 100μm) was done for CD31, β-III tubulin and DSPP.

4.4 DISCUSSION

In this work, the DP-ECM and the UBM were selected as candidates to study the effect of ECM based scaffolds on cells isolated from the dental pulp and the periodontal ligaments. The goal is to understand the effects of matrix degradation products in-vitro and gain an insight into the remodeling potential of these matrices with and without the cellular component in-vivo ectopically. The choice for an ectopic subcutaneous model over an orthotopic application stems from the need of a bacteria-free environment and an immunocompromised host to allow for the study of the cellular effect on the matrix (Kim et al. 2015b). It was shown before that ECM scaffolds can carry beneficial effects on different cells including chemotaxis, differentiation, and proliferation (Hu et al. 2017; Takewaki et al. 2017). It is of importance to understand the suitability of the cell selected and the proposed ECM scaffold as studies have suggested the benefits of using site-specific ECM (Boruch et al. 2010; Shi et al. 2017).

While the origin of cells expected to fill the canal space in regeneration scenario is unknown, we chose to study dental pulp and PDL cells as these cells are available in adult patients and it would be logical to expect the apical infiltration to be of PDL related cells (Gao et al. 1996). One important aspect of the cells infiltrating the canal is the ability of the recruited cells to heal the wound area and the void pulp space. For this purpose, wound healing assay was carried using the dental pulp and PDL cells utilizing two matrices: DP-ECM and UBM in the form of an acid digest. Cells isolated from the PDL showed an increase in the number of cells migrating to the wound area when stimulated with DP-ECM and UBM, the effect was notable at 12 and 24 hours post-treatment. All of the groups showed similar numbers of migrating cells to heal the wound area 36-48 hours after wound induction. When compared to dental pulp cells, the

DP-ECM group had the highest number of migrating cells between 12-24 hours and the UBM showed no statistically significant difference from control.

Collectively, the results of this experiments come in support of previously reported and established work where ECM degradation products induced chemotaxis and migration of different cells (Brennan et al. 2008; Crapo et al. 2014; Reing et al. 2009). The DP-ECM with its collection of proteins and growth factors show an influence in the ability to recruit both PDL and dental pulp-derived cells in wound healing scenario. These results highlight the ability of DP-ECM in the recruitment of two cellular population with clinical and anatomical relevance. On an interesting note, the UBM showed better support for PDL cells over dental pulp cells, indicating the suitability of the UBM scaffold for periodontal applications (Camacho-Alonso et al. 2018; Wang et al. 2018).

On the level of gene expression, previous reports have shown the influence that ECM based scaffolds can have on cells in-vitro including the changes in secreted MMPs and growth factors (Agrawal et al. 2011; Crapo et al. 2012). The dental pulp cells and PDL cells, in this case, were treated with 1 mg/ml for 1, 2 and 3 weeks. At the 1^{st} 2^{nd} and 3^{rd} week, COL1A1 a gene involved in ECM production was markedly down-regulated for in dental pulp and PDL cells treated with UBM and DP-ECM when compared to the untreated control. This is possibly due to the presence of collagen extracellularly and the upregulation of a different type of collagen (Hu et al. 2017). After the treatment of PDL cells with the UBM for one week, it showed a significant increase in the expression of ALPL. At 1 and 2 weeks of treatment, VEGFA and Nestin were both down-regulated with no increase in folds of the expression of these genes. The UBM was able to upregulate TUBB3 after 2 weeks of treatment for the two cell type. Three weeks after treatment with ECM scaffolds, the DP-ECM shows an increase in the expression of ALPL for

dental pulp cells and an increase in VEGFA for dental pulp and PDL cells. On the other hand, the UBM digest appears to upregulate the expression of TUBB3, a marker for newly formed nerves, for dental pulp and PDL cells while ALPL was only upregulated with PDL cells. These results are not surprising when we consider the UBM effect on Neuroblastoma cells and its ability to induce the formation of neurite extensions along with its use in spinal injuries (Huleihel et al. 2016). The DP-ECM effect on the expression of VEGFA was favorable as one of the important aspects of a functional dental pulp is an intact vascular system. It was shown before that the DP-ECM retained its proteins including VEGFA which is potentially one of the factors contributing to the upregulation of VEGFA (Alqahtani et al. 2018). Overall, the UBM and DP-ECM digests are bioactive and show an influence on dental pulp and PDL cellular behavior as early as 1 week after treatment and as late as 3 weeks after treatment in-vitro.

Upon retrieval of the subcutaneously implanted constructs. Samples filled with collagen type I alone didn't show any signs of remodeling or cellular infiltration. It is possible that the lack of complexity and active degradation products rendered collagen's ability to remodel. When PDL cells were added, the canal was filled with cells where blood vessels were clearly visible, the same trend continued at 12 weeks post-implantation showing persistence of CD31 and β-III tubulin expression. On a similar note, the addition of dental pulp cells permitted the formation of new vessels with a noted expression of DSPP and β-III tubulin around cells and near dentinal walls. At 12 weeks, dental pulp cells maintained the canal vitality showing contentious expression of CD31, DSPP and β-III tubulin. Groups that have received UBM powder show slight infiltration of cells at the UBM/host interface. The UBM didn't remodel in the root canal segments, although shown in other areas to be capable of remodeling and allowing for the formation of functional tissue. When cells from PDL and dental pulp were added, the resulting

tissue appears to follow the behavior of the UBM group where minimal numbers of cells were sparsely present in the canal with no expression of CD31, DSPP and β-III tubulin even at 12 weeks after implantation. Collectively, these results suggest the UBM as a material not suitable for dental pulp regenerative purposes, at least in the powder form. This could be attributed to the dire need for UBM to receive mechanical forces, which will allow for remodeling and release of factors embedded within the UBM. A heavy body of the ECM literature emphasizes the role of mechanical forces in the degradation and functional remodeling of UBM scaffolds (Boruch et al. 2010; Dziki et al. 2018; Turner et al. 2012). Although the outcome might be different for the UBM in the orthotopic application, where occlusal forces are present, the ectopic model shows that mechanical interaction is more important than the presence of vital cellular components. Lastly, the DP-ECM placed inside the canals showed an interaction with the host marked with cellular infiltration and formation of blood vessels within and around the matrix but remains without detectable expression of β-III tubulin. When PDL cells were added, the DP-ECM supported neovascularization mineralization and neurogenesis at 6 weeks and 12 weeks post-implantation. Similarly, when dental pulp cells were added it showed a better interaction and presence of cells through the canal and around the remaining DP-ECM. The introduction of the dental pulp cells showed presence and expression of CD31, DSPP, and β-III tubulin at both time points. These findings highlight the DP-ECM ability to support regeneration in root canal model along with the use of cell-based approach as it shows a better remodeling outcome and expression of factors (Dissanayaka et al. 2014; Syed-Picard et al. 2014; Wang et al. 2013). Although most of the studies conducted on ECM scaffolds displayed remodeling and degradation of the ECM within 4 to 8 weeks (Gilbert et al. 2007a; Gilbert et al. 2007b), in the current model the DP-ECM didn’t remodel completely but it showed a slower progress toward complete

remodeling. Again, this could be attributed to the lack of occlusal mechanical forces transmitted to the apical area in the orthotopic model. Along with the lack of mechanical factors, the root canal system is of limited blood supply and the interaction area between the scaffold and the material is also limited. These challenging factors shift the attention to the use of ECM based hydrogel for this purpose (Ghuman et al. 2016; Massensini et al. 2015). The hydrogels will facilitate the release of the biological factors embedded in the matrix and ensure the complete filling of the root canal space without any voids (Ghuman et al. 2017). To sum up, the DP-ECM alone showed better remodeling results when compared to collagen and UBM alone. The use of dental pulp cells in conjunction with the DP-ECM highlights the importance of a cell-based approach and the role of the DP-ECM in supporting cells of dental origins.

5.0 SPECIFIC AIM 3: HOST IMMUNE RESPONSE TO DECELLULARIZED PULP EXTRACELLULAR MATRIX: EFFECT OF MATRIX CHEMICAL COMPOSITION ON MACROPHAGES

5.1 INTRODUCTION

The use of the extracellular matrix (ECM) as a biological scaffold material for in-vivo regenerative medicine and repair has been studied for different outcomes, ranging from unsatisfactory to satisfactory outcomes (Aurora et al. 2015; Turner et al. 2010; Wolf et al. 2015). It has been suggested that the successful remodeling of the extracellular matrix scaffolds could be attributed to macrophage byproducts released upon digesting the ECM scaffold (Gordon and Taylor 2005; Mantovani et al. 2004; Valentin et al. 2009). Macrophages are a type of white blood cells that exist in all tissues and can attain polarization in response to their surroundings. Two main types of polarizations are M1 macrophages which upregulate inflammation, and M2, which decreases inflammation and induce tissue repair. Correlation between macrophage polarization and tissue remodeling outcome has been reported in several tissues and organs and provides a potential area of investigation for wound healing and tissue repair. The macrophage response is highly regulated, with uncontrolled inflammation proving to be a detrimental process, whereas a controlled and regulated inflammatory response can be a key factor in tissue remodeling following injury. In skeletal muscle wound repair, the macrophage response has been

highly characterized. The capacity for tissue regeneration is highly dependent on the interaction between satellite and inflammatory cells in the wound area (Mauro 1961; Muir et al. 1965). Initially, neutrophils infiltrate the wound area as soon as few hours post injury. The neutrophils reach their maximum numbers between 6 and 24 hours (Bondesen et al. 2006; Tidball and Villalta 2010). After that, the recruited neutrophils will start releasing Reactive Oxygen Species (ROS) and T-helper 1 associated cytokines to recruit the circulating monocytes and macrophages. Three to four days after injury, the neutrophil response subsides and macrophages become the dominant tissue remodeling cells in the wound (Tidball and Villalta 2010). The monocytes recruited by the neutrophils originating from the bone marrow will migrate to the injury area where they will differentiate into macrophages (Swirski et al. 2009). Once recruited and differentiated, the macrophages generally attain M1 polarization, a pro-inflammatory phenotype due to the exposure to the recruiting pro-inflammatory cytokines such as IFN-γ (St Pierre and Tidball 1994; Tidball 2005). M1 macrophages reach their maximum numbers after two days, where they begin showing a transition to the M2 immuno-regulatory and anti-inflammatory phenotype. This paradigm shift is not fully understood yet it has been related to the increased IL-10 concentrations 48 hours post-injury. Classically activated M1 macrophages mediate phagocytosis of bacteria, removal of dead cells and the initial exposure to the ECM degradation products (Sicari et al. 2014). Once polarized to the M2 phenotype, macrophages release anti-inflammatory cytokines that signal tissue remodeling and repair (Gordon 2003; Gordon and Martinez 2010). The pro-inflammatory products from the M1 population are needed for the recruitment and activation of local cells within the injury site (Collins and Grounds 2001; Villalta et al. 2009). After recruitment, these cells are differentiated in the wound site by paracrine signals from the M2 macrophage population that is the results of the paradigm shift

from M1 to M2. It has been shown that the delay or elongation of the timeline of neutrophil and macrophage infiltration, polarization, or transition has a significant effect on a tissue's ability to functionally remodel. For example, when macrophages are depleted prior to a toxin-induced injury, regeneration and the removal of cellular debris was impaired (Arnold et al. 2007). Depletion of macrophages at the site of injury using liposomes was shown to restrict tissue regeneration by preventing the M1 response, which in turn prevents recruitment of local cells (Teixeira et al. 2003; Valentin et al. 2009). Furthermore, TNF-α knockout animals, a product of M1 macrophages, produce significantly less tissue-specific transcription factors, which suggests that TNF-α is necessary for the promotion of tissue repair (Chen et al. 2007). When macrophages were removed from the injury site at 2 days, the time period when they would transition to the M2 phenotype, tissue regeneration was impaired (Tidball and Wehling-Henricks 2007).

Collectively, macrophages play a major and crucial role in the success of implanted ECM scaffolds. These cells are responsible for the early recognition and degradation of the implanted materials along with the recruitment of sub-populations of cells to aid in the process of remodeling (Valentin et al. 2009). The secreted matrix metalloproteases (MMP) are thought to be responsible for the degradation of ECM products extracellularly (Jablonska-Trypuc et al. 2016). Studies looking into the secretion profiles of MMPs of macrophages under pro-inflammatory and anti-inflammatory stimulations showed similar results without major differences in the secreted MMPs (Newby 2008). Although the extracellular degradation pathway appears to be unaffected by the host inflammatory status, intracellular cathepsins were shown to be present in macrophages involved in inflammatory diseases e.g. atherosclerosis and pycnodysostosis (Lutgens et al. 2006). The intracellular digestive pathway of cathepsins shows differences in potency when sulfated glycosaminoglycans were added to collagen (Aguda et al.

2014). In a recent work involving macrophage response, the macrophages were treated with UBM alone or UBM digested with Hyaluronidase. When digested with Hyaluronidase, the UBM showed an increase in nitric oxide production, signifying the role that hyaluronic acid and the attached S-GAGs played in reducing NO production (Meng et al. 2015). Glycosaminoglycan, are long unbranched polysaccharides consisting of a repeating disaccharide unit, they have a negative charge which makes it capable of water retention. Different classes of sulfated-glycosaminoglycans were shown to differentially affect the intracellular digestive pathway (Li et al. 2002).

Cathepsin K, a highly potent collagenase and the predominant papain-like cysteine protease, was shown to increase its collagenolytic activity when chondroitin sulfate and keratan sulfate were present (Li et al. 2004). Another class of sulfated-gags, dermatan sulfate was shown to have an opposite effect on the collagenolytic activity of cathepsin K along with heparin and heparan sulfate (Wilson et al. 2009). So, to investigate the effect of the matrix chemical composition on macrophages behavior we decided to use chondroitin sulfate and dermatan sulfate added to type I collagen. The goal is to enhance and dampen the activity of cathepsin K to gain an insight into its role in the inflammatory process utilizing functional assays and flow cytometry.

5.2 MATERIALS AND METHODS

5.2.1 Isolation of Bone Marrow-Derived Macrophages

Mice were euthanized by asphyxia and rapid cervical dislocation. Using aseptic technique, the skin was removed off the lower limbs along with the feet. Hind legs were cut at the hip joint with scissors and excess muscle tissue was removed from legs by holding the end of bone with forceps and using scissors to push muscle downward away from forceps. The tibia and femur were washed with PBS for 5 mins and placed into 70% EtOH for 1 min and rinsed again in PBS. The ends of the long bones were removed using scissors, placed into 0.5 ml Eppendorf tube which was perforated with a needle at the bottom and placed into 1.5 ml Eppendorf tube and centrifuged at ≥10,000 x g in a microcentrifuge for 30 sec. The total number of bone marrow progenitor cells were counted using a hemocytometer and cells concentration was adjusted to a ~2×10^6 cells/ml in a 10% L929 supplemented macrophage complete medium.

On day 1, cells were seeded at half of the wells required volume (e.g. 5 ml in a 10 cm dish, total of 1 x 10^7 cells) and incubated in 37 °C, 5% CO_2 incubator. On day 2, half the amount of the medium was added to the cells. The medium was replaced at day 3 and day 5. At day 7, cells were switched to maintenance medium or treatment medium (Fig. 25) below depicts cells morphology over 7 days of treatment with 10% L929 medium. After that, the untreated attached cells were detached using ice-cold Accumax, applied twice on ice, counted and stained for F4/80 as a pan-macrophage marker and monocytes marker CD11b (Mac-1 beta chain).

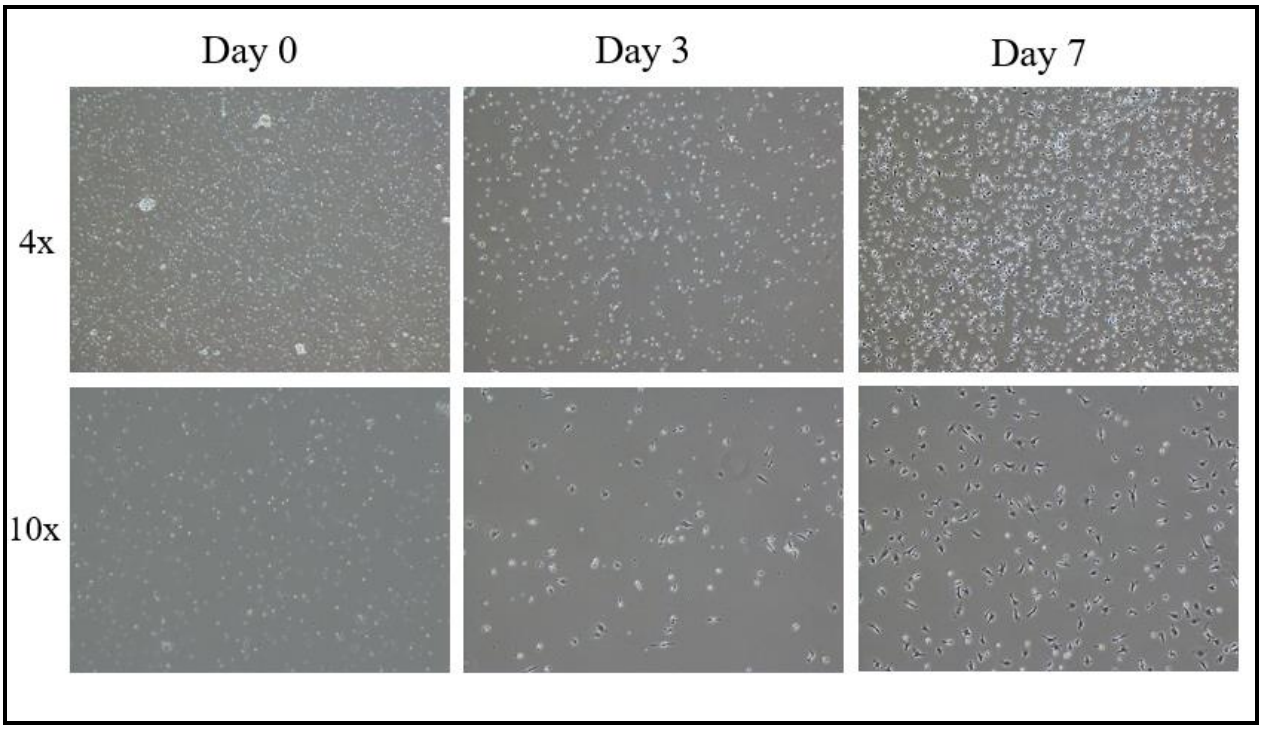

Figure 25. Phase contrast images were taken at 0, 3 and 7 days. After 7 days, mature macrophages showed spreading of cell bodies and attachment to the culture plates.

5.2.2 Preparation of Treatment Groups

In order for us to understand the effect of different matrices on macrophages behavior, the following treatment groups were prepared and included in the in-vitro experiments:

Mϕ: Untreated naïve macrophages.

M1: Classically activated macrophages, treated with IFN-γ at 20 ng/ml and LPS at 100 ng/ml.

M2: Alternatively activated macrophages, treated with IL-4 at 20 ng/ml.

UBM: solubilized UBM was added to the medium at 1 mg/ml.

DP-ECM: solubilized DP-ECM was added to the medium at 1 mg/ml.

Pepsin: as a control for the digestion buffer.

For the study of Cathepsin K and its effect on macrophages, the groups of treatment are detailed under **Cathepsin K Activity** section.

5.2.3 Nitric Oxide Quantification

After 48 hours of treatment, cell culture supernatants were collected to measure the Nitric Oxide concentration was using Griess reagent (Molecular Probes, G-7921). 150 µl of the cell culture supernatants were mixed with 10 µl of 1% sulfanilamide, 10 µl of 0.1% N-(1-naphthyl) ethylenediamine dihydrochloride (NED) solution and incubated for 30 min at room temperature. The absorbance was measured at 540 nm with a microplate reader. Known concentrations of nitrite solutions were used to generate a standard curve. Photometric reference samples were generated using the cell culture medium.

5.2.4 Arginase Activity Assay

Arginase activity was measured using macrophage cell lysate according to the following QuantiChrom Arginase Assay Kit (DARG-100). Briefly, macrophages were lysed with 200 µl of 0.001% Triton-x 100 with 1 × protease inhibitor cocktail on a rocker at 150 rpm for 15 min at room temperature. The cell lysate was centrifuged at 14,000x g for 10 min at 4 °C. Then 40 µl of cell lysate was added to 10 µl of 5x activation buffer including MnCl2. Arginine hydrolysis was conducted by incubating the cell lysate at 37 °C for 2 hours. The reaction was then stopped with the addition of 200 µl of acid mixture. The urea concentration was measured at 540 nm with a microplate reader. One unit of arginase activity is defined as the amount of enzyme that catalyzes the formation of 1 mM of urea/min.

5.2.1 F4/80, iNOS and Fizz-1 Immunolabeling of BMDMs

Bone marrow-derived macrophages were seeded into Lab-Tek II 8-well chambers at the density of $2x10^6$ cells/ml and were allowed to differentiate for 7 days. After that cells were switched to M.M or Treatment medium for 48 hours. At the end of treatment, cells were washed with PBS, fixed with chilled 4% PFA for 15 mins at RT and washed again with PBS to remove the fixative. The primary antibodies used in this immunofluorescent staining were: (1) monoclonal anti-F4/80 (BioRad: MCA497GA) at 1:200 dilution as a pan-macrophage marker, (2) polyclonal anti-iNOS (Abcam, Ab3523) at 1:100 dilution as an M1 marker, and (3) polyclonal anti-Fizz1 (Peprotech, Rocky Hill, NJ) as an M2 marker at 1:200. Samples were inspected for auto-fluorescence and treated with Sudan Black B 1.5% in 70% ethanol or Cupric Sulfate and Ammonium acetate 50mM. Heat Induced epitope retrieval was performed using Sodium Citrate, pH: 6. After that, cells were incubated in a blocking solution consisting of PBS, 0.1% Tween-20, 5% goat serum, 0.3M glycine and 1% bovine serum albumin to prevent nonspecific binding for 1 hour at room temperature. Blocking solution was removed and cells were incubated in primary antibodies overnight at 4 C, primary antibody was omitted for staining control samples. After 3 washes in PBS, cells were incubated in fluorophore-conjugated secondary antibodies (Alexa Fluor goat anti-rat 488 or goat anti-rabbit 488, Invitrogen, Carlsbad, CA) for 1 hour at room temperature. After washing again with PBS, nuclei were counterstained with 50 nM 6-diamidino-2-phenylindole (DAPI) prior to imaging. Light exposure times for ECM treated macrophages were adjusted based on the same settings set for cytokine-treated macrophages, serving as a positive control.

5.2.2 Chemotaxis Assay

The effect of ECM digests upon macrophages chemotaxis was investigated using Boyden chamber cell migration assay. BMDM cells were cultured in 6–well plate (Nunc, UpCell) and treated with starvation media (DMEM, 0.5% Heat Inactivated FBS, 1% Penn/strep) for 18 hours prior to migration. Cells were then removed from the incubator and treated with 2 ml of chilled Accutase and left for 15 mins at RT to facilitate detachment. Cells were then re-suspended in FBS-reduced DMEM, cell density was adjusted to 100,000 cell / 300 µl and seeded in the top chamber on top of the polycarbonate chemotaxis membranes with a pore size of 5 µm. ECM digest (UBM, DP-ECM) or positive (10% FBS, 50 ng CCL2) or negative (0% FBS and 10% Pepsin) controls were added to the lower chamber. Cells were allowed to migrate across the chamber for 8 hours at 37 °C, 5% CO2. Following the migration period, membranes were washed with PBS, cells were detached and the cell's DNA was detected using Quant-it GR Dye. The values of migrated cells were expressed as RFUs.

5.2.3 Cathepsin K Activity

In order for us to understand the effect of different substrates on Cathepsin K and macrophages behavior, different treatment groups with known effects on CTSK were included in this study:

Mϕ: Untreated naïve macrophages.

M1: Classically activated macrophages, treated with IFN-γ at 20 ng/ml and LPS at 100 ng/ml.

M2: Alternatively activated macrophages, treated with IL-4 at 20 ng/ml.

Collagen I: 1 mg/ml.

Chondroitin Sulfate: Chondroitin sulfate at 0.1 mg/ml + Collagen I at 1 mg/ml.

Dermatan Sulfate: Dermatan sulfate at 0.1 mg/ml + Collagen I at 1 mg/ml.

E64: E64 at 10 µM + Collagen I at 1 mg/ml.

Following 48 hours of treatment, BMDMs were lysed using 200 µl of lysis buffer followed by incubation on ice for 10 mins (BioVision, K141). The lysate was then centrifuged at 14,000 x g for 5 mins at 4 °C. 50 µl of the collected supernatants will be placed in a black 96-well plate and 50 µl of reaction buffer is added along with 2 µl of Cathepsin K fluorescent substrate Ac-LR-AFC (200 µM final concentration). The plate was then incubated at 37 °C for 1 hour. Negative controls were included using 2 µl CK inhibitor. Samples absorbance was measured using a plate reader with a 400-nm excitation filter and 505-nm emission filter.

5.2.4 Nitric Oxide Quantification and Arginase Activity Assay

After 48 hours of treatment, cell culture supernatants were collected to measure the Nitrite concentration was using Griess reagent. 150 µl of the cell culture supernatants were mixed with 10 µl of 1% sulfanilamide and 10 µl of 0.1% N-(1-naphthyl) ethylenediamine dihydrochloride (NED) solution and incubated for 30 min at room temperature.

Arginase activity was measured using macrophage cell lysate. Briefly, macrophages were lysed with 200 µl of 0.001% Triton x-100 with 1 × protease inhibitor cocktail on a rocker. The cell lysate was centrifuged at 14,000x g. Then 40 µl of cell lysate was added to 10 µl of 5x activation buffer including $MnCl_2$. Arginine hydrolysis was conducted by incubating the cell lysate at 37 °C for 2 hours. The reaction was then stopped with the addition of 200 µl of acid mixture. The urea concentration was measured at 540 nm with a microplate reader. One unit of arginase activity is defined as the amount of enzyme that catalyzes the formation of 1 mM of urea/min.

5.2.5 Cell Sorting for CD86 and CD206

After 48 hours of treatment, cells were treated with Accutase for 15 mins on ice repeated twice to ensure removal of all cells. Surface Staining of the collected cells was performed according to the following: Cells were washed once with plain PBS to remove all the protein in the samples and stained with Zombie Aqua (Live/dead stain) with 100 µl per 5 x 10^6 cells for 30 minutes at 4° C. After that cells were washed again with staining buffer (1% BSA and 0.1% Sodium Azide) and centrifuged at 400 g for 10 mins at 4 °C. Fifty µl of FC block was added to each tube and incubated at RT for 20 min in the dark. Fluorophore-conjugated primary antibodies for CD86 and CD206 were added to cells and incubated for 20 mins at 4 °C. Following the application of antibodies, the cells were washed with staining buffer and fixed using 200 µl of 2% PFA for 20 mins at 4 °C. After fixation, cells were washed and stored in PBS in the dark at 4 °C until used. Single color compensation controls were used for signal spill-over compensation.

5.2.6 In-vivo Immunohistochemistry

Constructs of tooth root filled with three lyophilized and sterilized scaffolds: Rat tail type I collagen, Porcine UBM, and Porcine DP-ECM were implanted subcutaneously in wild-type mice with an intact immune component for 2 weeks to characterize the infiltrating macrophage's response to the scaffolds. Upon retrieval of samples, the constructs were placed in a cold 10% Formalin for 24 hours. After that, samples were treated with 0.32 M of EDTA for 3 to 4 weeks. Radiographs were taken to determine decalcification of dentin. Following processing and embedding of samples, 7-µm sections were taken and were stained for H&E staining.

To detect and compare the presence of macrophages, M1 and M2 markers in the retrieved samples, sections of 7-µm thickness were stained for: F4/80 (Abcam, ab6640), iNOS (Abcam, Ab3523) and Arg-1 (Abcam, Ab91279) according to the following protocol: Sections were deparaffinized in Xylene and rehydrated in a series of alcohol changes. Once hydrated, samples were inspected for auto-fluorescence and treated with Sudan Black B 1.5% in 70% ethanol or Cupric Sulfate and Ammonium acetate 50mM if needed. Heat-induced antigen retrieval was performed using Sodium Citrate buffer pH: 6 at 98°C for 20 mins or Enzyme induced antigen retrieval was performed with Proteinase K. Primary antibodies were applied in the following ratios (F4/80 at 1:20, iNOS at 1:100, Arg-1 at 1:200) and incubated overnight at 4°C followed by washes and application of fluorophore-conjugated secondary antibody Goat anti-Rat and Goat anti-Rabbit (Alexa flour 488) at 1:500.

A total of 4 openings were used for quantification of positive cells using Cell Profiler. Numbers of cells expressing iNOS and Arg-1 were normalized to F4/80 and the normalized values were used to present M1/M2 ratio.

5.3 RESULTS

5.3.1 Nitric Oxide Production and Arginase Activity

After 7 days of treatment with 10% L929 medium, mature macrophages showed spread cell bodies and attached to the culture substrates. The cells were then stained for CD11b and F4/80 as markers for macrophages. Results show cells that are double positive for both markers to be the majority of cells, with a positivity percentage of 95-98%.

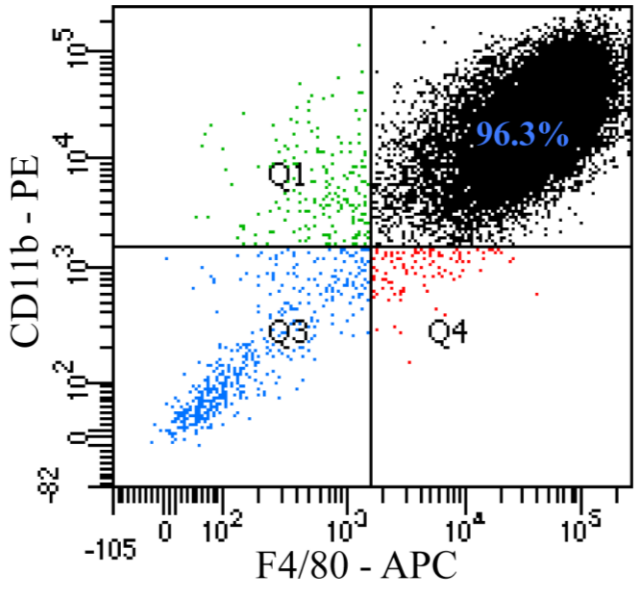

Figure 26. Flow cytometry performed on bone marrow cells after 7 days of differentiation for CD11b and F4/80 as markers for macrophages.

After differentiation, macrophages were treated with different cytokines to allow for a classic and alternative activation of cells as positive controls for nitric oxide and arginase quantification assays. Macrophages were also treated with 1 mg/ml of UBM, 1 mg/ml of DP-ECM and 10% pepsin as a control for endotoxins. Forty-eight hours after treatments, NO was

quantified from the supernatants with M1 groups showing highest levels of NO production, approximately 74 µM and UBM of about 13 µM. Untreated macrophages along with IL-4 treated, DP-ECM and pepsin group did not show any increase in the levels of nitric oxide production.

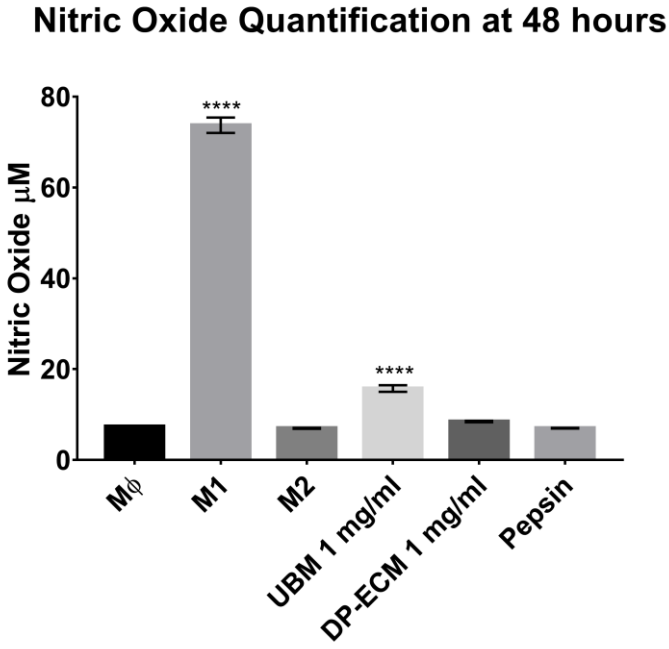

Figure 27. Quantification of Nitric Oxide production after treatment with UBM, DP-ECM and Control Pepsin. M1 was used as a positive control while Mϕ was used as a baseline level. Error bars are mean ± SEM (n=3) ****p≤0.0001

Following NO quantification, the same groups were used for cell lysis, protein extraction and arginase quantification as a marker for alternative activation. Arginase activity was highly increased when macrophages received treatment of 20 ng/ml of IL-4, while the untreated and the classically activated macrophages showing no change in the levels of arginase activity. The DP-ECM showed an increase in arginase activity when compared to the UBM and pepsin control group. Overall, the DP-ECM didn't induce the production of any levels of NO and allowed for an up-regulation in arginase activity in-vitro.

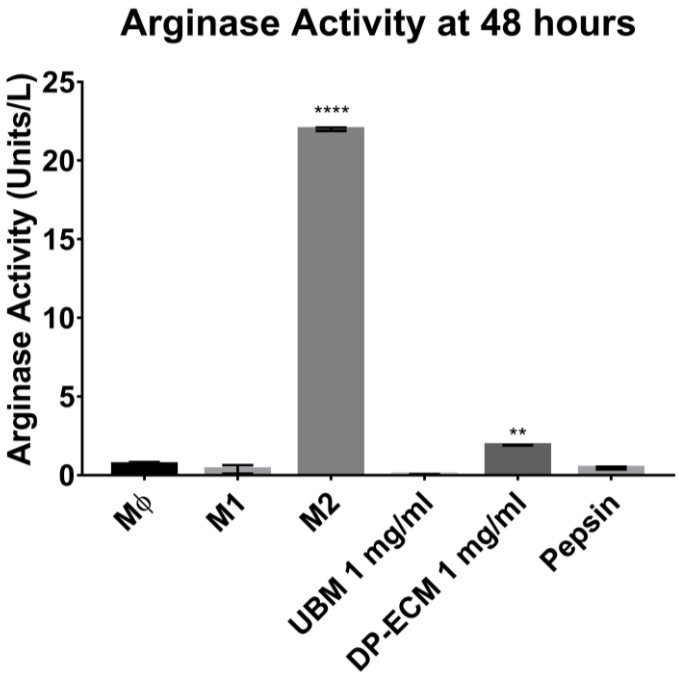

Figure 28. Quantification of Arginase Activity after treatment with UBM, DP-ECM and Control Pepsin. M2 was used as a positive control while Mϕ was used as a baseline level. Error bars are mean ± SEM (n=3) ** $p \leq 0.01$ **** $p \leq 0.0001$

5.3.2 Chemotaxis and Fizz-1 Expression

To investigate the chemotactic ability of the ECM based scaffolds to the host immune component, BMDMs were generated and seeded into Boyden chamber with DP-ECM 1 mg/ml, UBM 1 mg/ml, 10% FBS, 10% pepsin and 50 ng/ml of CCL2 as treatment and controls added to the lower chamber. At the end of the migration period, the positive control groups, CCL2, and 10% FBS showed an increase in the number of cells reflected as RFU of the DNA of migrated cells. Pepsin control and 0% FBS control show no increase in relative fluorescence units. The DP-ECM and UBM groups displayed an increase in the number of cells similar to the levels seen when 10% FBS was used as a chemoattractant.

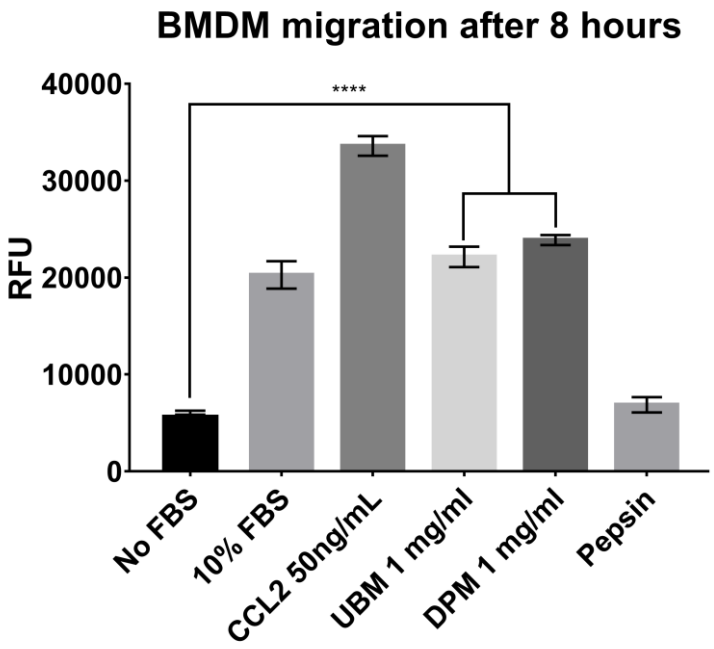

Figure 29. Migration of BMDM after treatment with UBM, DP-ECM and Control Pepsin. FBS and CCL2 were used as a positive control while No FBS was used to detect passive migration. Error bars are mean ± SEM (n=4) ****$p \leq 0.0001$

To determine the phenotype of macrophages following treatment with DP-ECM and UBM degradation products, immunofluorescent staining for F4/80, iNOS and Fizz-1 were performed 48 hours after treatment. Cells from all the groups were positive for pan-macrophage marker F4/80 as shown (Fig. 30). Macrophages treated with LPS/IFNγ were classically activated showing positivity for iNOS. On the other hand, macrophages treated with IL-4 were positive for Fizz-1, a marker for alternative activation in mice macrophages. Similar to IL-4 treated cells, the UBM and DP-ECM treated macrophage showed expression of Fizz-1 and minor positivity for iNOS even in IL-4 treated groups. Pepsin control shows no changes when compared to the untreated macrophages group.

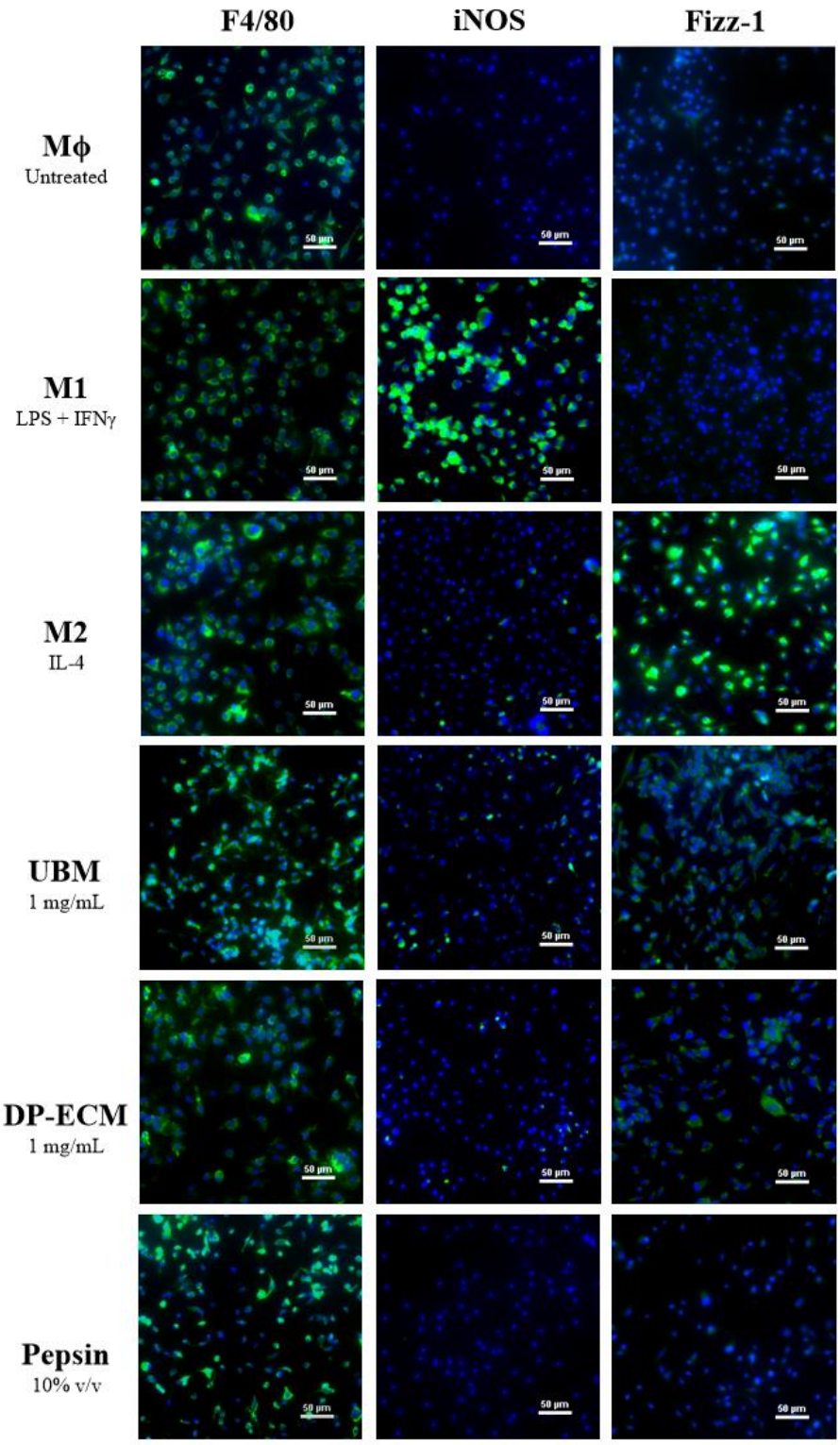

Figure 30. Immunofluorescent staining of F4/80, iNOS, and Fizz1-1. M1 and M2 groups were used as positive controls for iNOS and Fizz-1 respectively. Scale bars = 50 μm

5.3.3 In-vivo analysis of iNOS and Arg-1 Expression

After 2 weeks of implantation in immune-competent mice. The samples were processed for H&E alone with IF staining for mouse F4/80, iNOS, and Arg-1. Samples containing lyophilized collagen showed an infiltration of cells expressing F4/80 and iNOS. Following the inflammatory cells infiltration, the same samples showed Arg-1 positive cells distal to the inflammatory cells zone. The UBM powder showed infiltration of cells positive for F4/80, iNOS, and Arg-1 without a specific pattern of distribution. The DP-ECM was added as lyophilized minced tissue to the canal and shows infiltration of F4/80, iNOS, and Arg-1 positive cells. Compared to collagen alone, the UBM and the DP-ECM showed a statistically significant difference in the ratio of M1/M2.

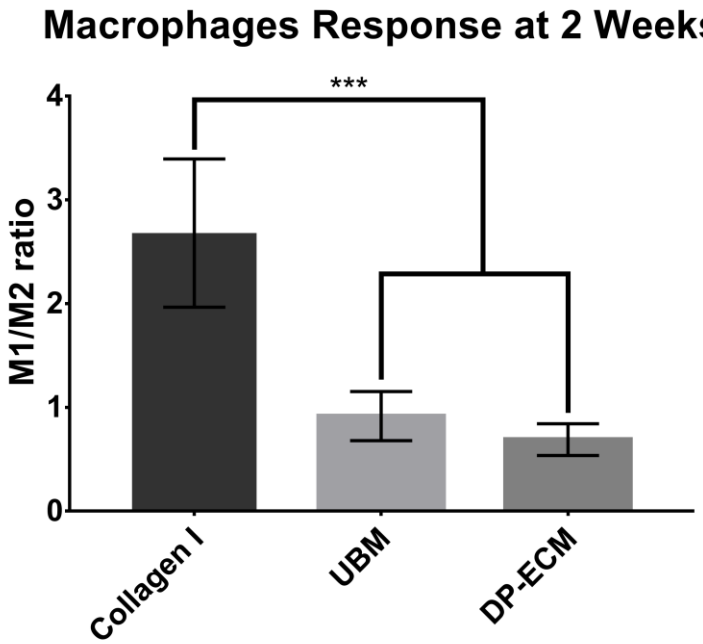

Figure 31. M1/M2 ratio derived from the numbers of iNOS/Arg-1 positive cells, constructs retrieved at 2 weeks contained lyophilized Collagen, UBM, and DP-ECM. Error bars are mean ± SEM (n=4) *** $p \leq 0.001$

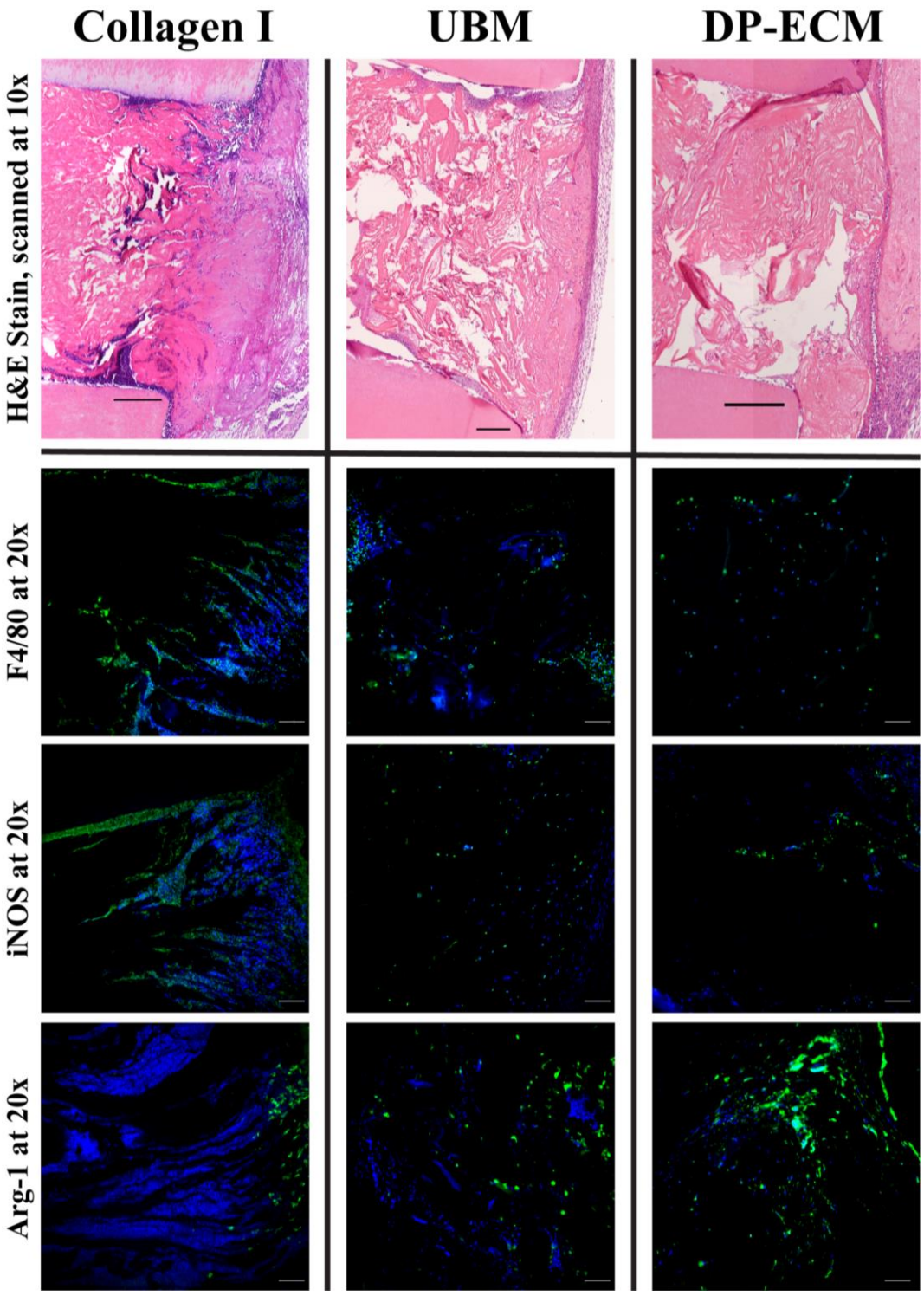

Figure 32. Collagen, UBM, and DP-ECM after 2 weeks of implantation, scanned and stained for H&E along with IF staining of F4/80, iNOS, and Arg-1. H&E (Scale bar = 250μm) IF (Scale bar = 100μm).

5.3.4 Effect of Scaffolds Composition on Host response and Expression of Mannose Receptor CD 206

5.3.4.1 Cathepsin K activity

To determine the effect of matrix composition on collagen degradation intracellularly, Cathepsin K activity assay was conducted. It shows that there is no increase in CTSK activity when comparing collagen treated macrophages and the untreated ones. When E64 was added the activity was significantly reduced. A similar trend in CTSK activity reduction is also seen when Dermatan Sulfate was added to collagen. On the other hand, CTSK activity was up-regulated when Chondroitin Sulfate was added to the collagen along with a notable increase in the activity of LPS/IFNγ treated macrophages.

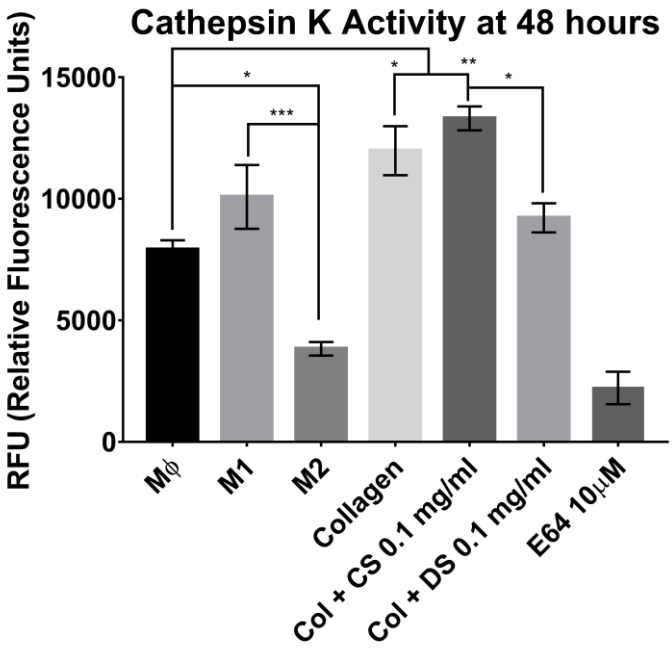

Figure 33. Quantification of Cathepsin K activity was performed on 48 hours post-treatment on cell lysate. Error bars are mean ± SEM (n=4) * $p \leq 0.05$ ** $p \leq 0.01$ *** $p \leq 0.001$

5.3.4.2 Nitric Oxide Production and Arginase Activity

After 48 hours of treatment, nitric oxide was measured from tissue culture supernatants. It showed an increase in classically activated macrophages with collagen, E64, chondroitin sulfate and dermatan sulfate showing minimal levels of NO. While the NO production levels are still similar to the levels produced by untreated macrophages, chondroitin sulfate shows the highest level of NO production in the treatment groups.

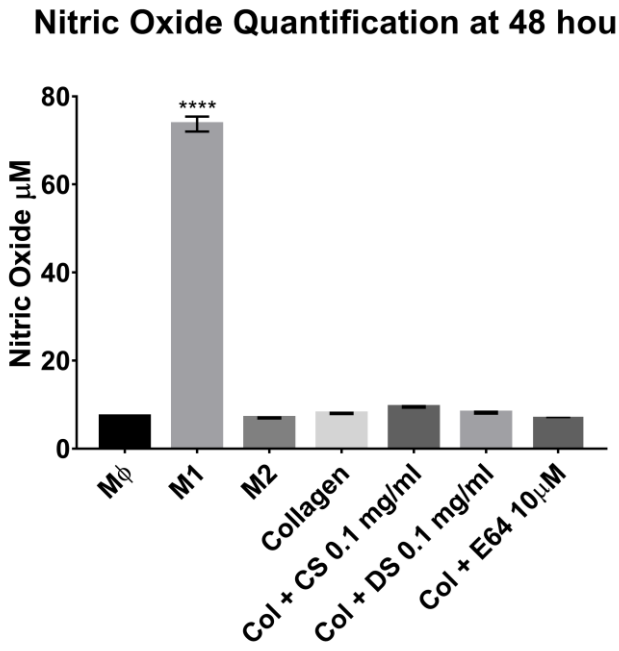

Figure 34. Quantification of Nitric Oxide production after 48 hours post-treatment. M1 was used as a positive control while Mϕ was used as a baseline level. Error bars are mean ± SEM (n=4) **** $p \leq 0.0001$

Following NO quantification, the same groups were used for cell lysis, protein extraction and arginase quantification as a marker for alternative activation. Arginase activity was highest when macrophages received treatment of 20 ng/ml of IL-4, while the untreated and the classically activated macrophages show no change in the levels of arginase activity. Collagen treated group did not show an increase in arginase activity when compared to the untreated

control group. When E64 and dermatan sulfate were added to collagen the arginase activity was up-regulated. Chondroitin sulfate adopted a response similar to collagen alone.

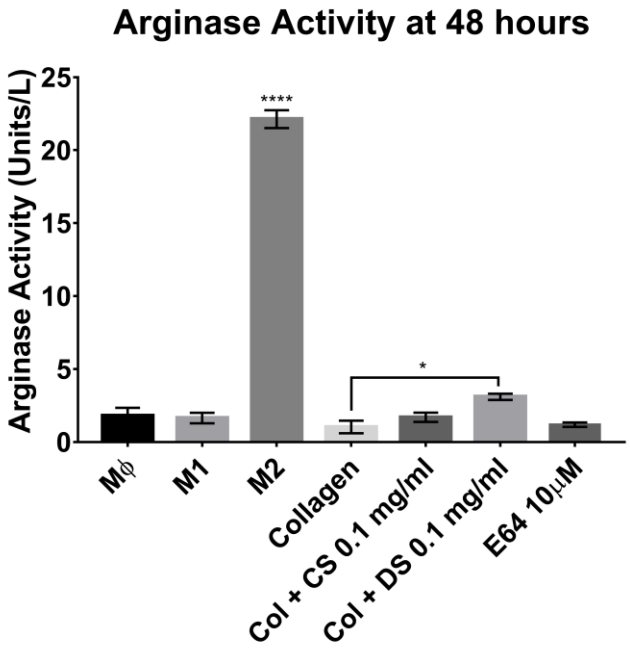

Figure 35. Quantification of Arginase Activity 48 hours after treatment. M2 was used as a positive control while Mϕ was used as a baseline level. Error bars are mean ± SEM (n=4) * $p \leq 0.05$ **** $p \leq 0.0001$

5.3.4.3 Expression of CD206

After the immune-labeling of treated macrophages with CD86-FITC and CD206-PerCP Cy5.5. The cells were sorted using flow cytometry to measure the events positive for CD86 or CD206 or both. When compared to the untreated group, M1 macrophages showed a shift and an increase in CD86 events while M2 macrophages were shifting to an increase in CD206 expression. Collagen group along with chondroitin sulfate group showed an increase in the expression of CD86 compared to the control. Dermatan sulfate showed a 5% decrease in CD86 positive evens and E64 groups showed no changes when compared to untreated macrophages. Lastly, collagen and

chondroitin sulfate groups show a decrease in cells expressing CD206 only, while dermatan sulfate and E64 retained its numbers in comparison to control.

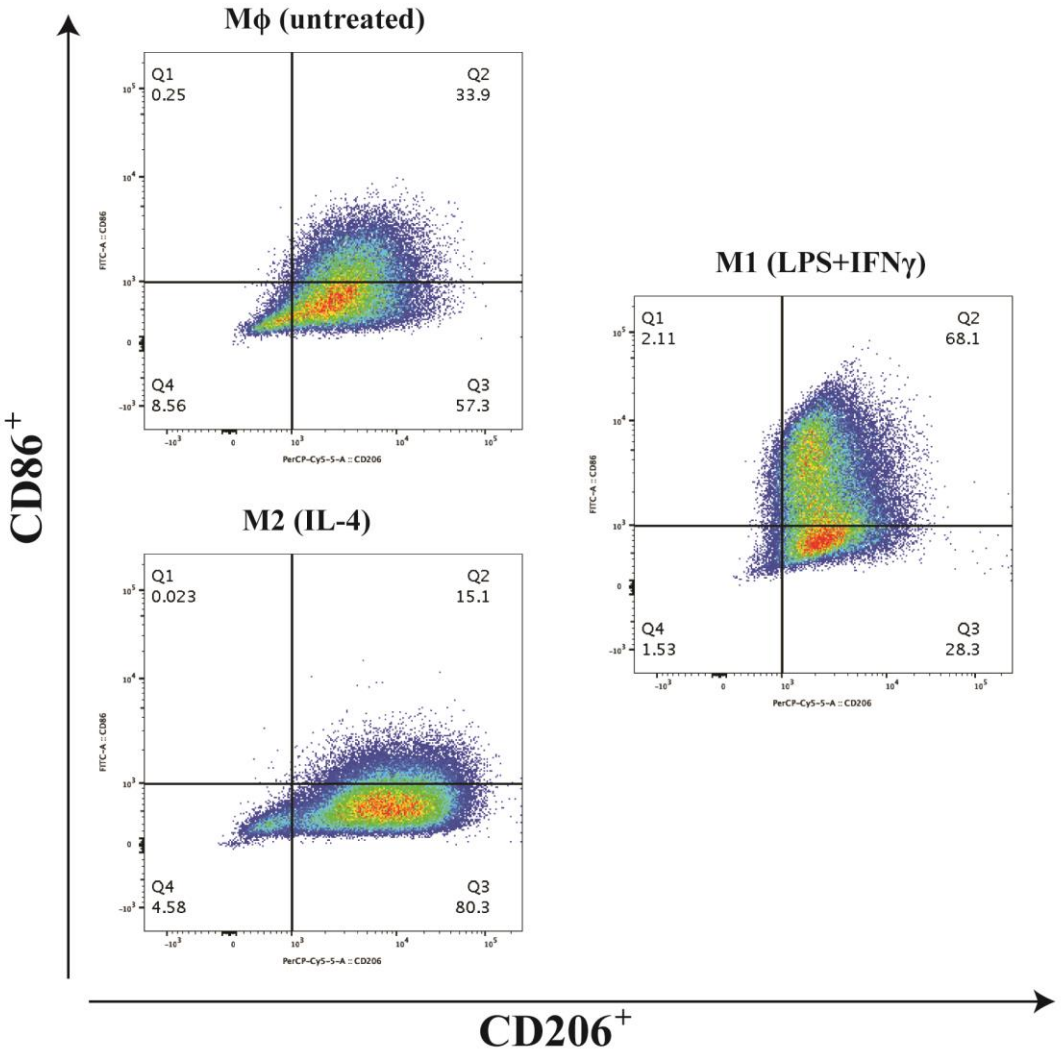

Population	Mφ (untreated)	M1 (LPS+IFNγ)	M2 (IL-4)
Total CD86+	34.15%	70.21%	15.12%
Total CD206+	91.2%	96.4%	95.4%
Only CD86+	0.25%	2.11%	0.02%
Only CD 206+	57.3%	28.3%	80.3%

Figure 36. Cell sorting for CD86 and CD206 positive cells. Mϕ, M1, and M2 were included as controls.

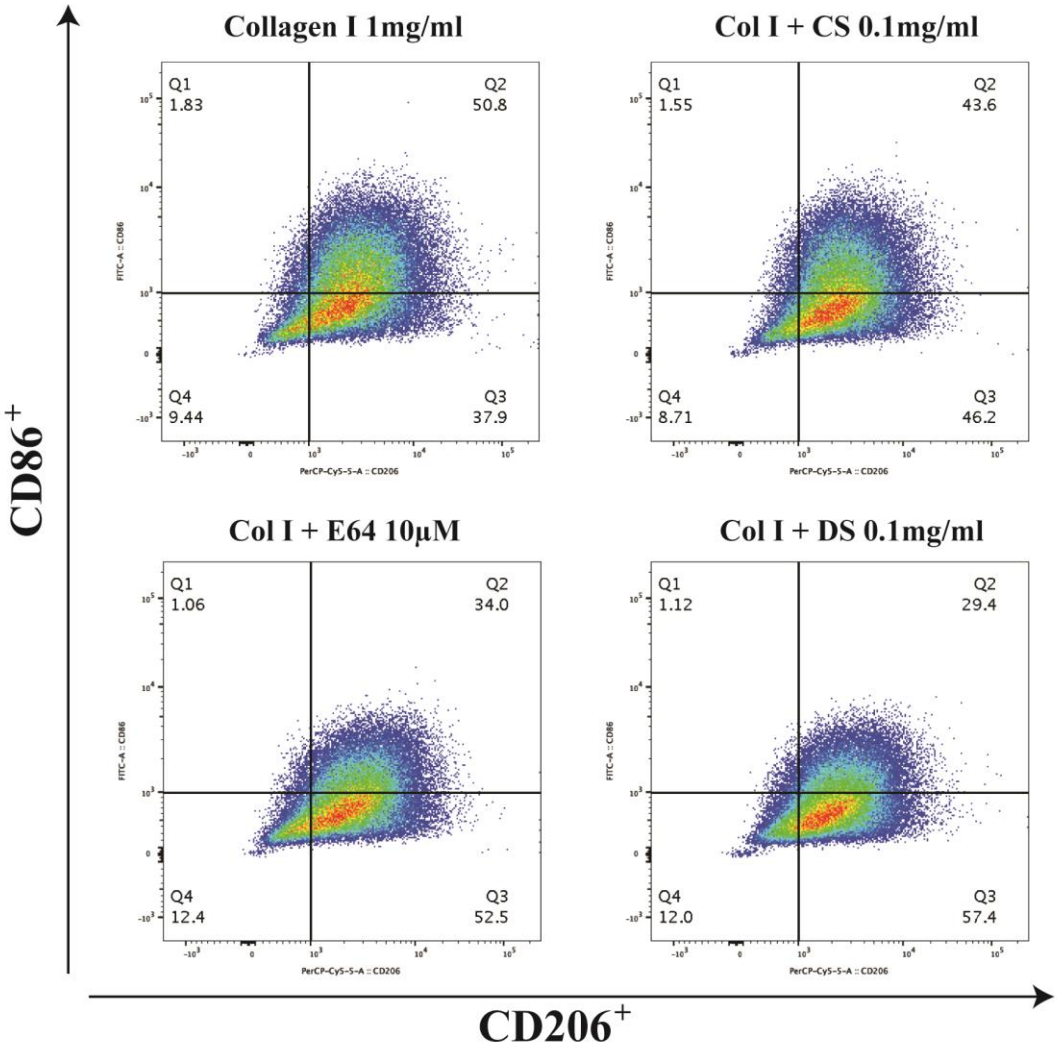

Population	Collagen I 1mg/ml	Col I + CS 0.1mg/ml	Col I + DS 0.1mg/ml	Col I + E64 10µM
Total CD86+	52.63%	45.15%	30.52%	35.06%
Total CD206+	88.7%	89.8%	86.8%	86.5%
Only CD86+	1.83%	1.55%	1.12%	1.06%
Only CD 206+	37.9%	46.2%	57.4%	52.5%

Figure 37. Cell sorting for CD86 and CD206 positive cells. Collagen alone, Collagen with Chondroitin Sulfate, Collagen with Dermatan Sulfate and Collagen with E64 were included.

5.4 DISCUSSION

In this work, bone marrow-derived cells were isolated and differentiated to macrophages expressing F4/80 and CD11b after 7 days of treatment. The goal of this work is to understand the host response to the exogenous stimulation of pepsin-digested ECM scaffolds. Previous studies have shown that the degradation products of the ECM can help in the recruitment of different cells along with the modulation of these cells behavior (Dziki et al. 2017). Herein we show the ability of the DP-ECM and the UBM to recruit macrophages in a trans-well migration assay when compared to reduced FBS control and pepsin.

Since the literature has emphasized on the ability of the ECM to elect an immune response characterized by the presence of M2 like macrophages around the implants in-vivo (Meng et al. 2015; Sicari et al. 2014). The next step was to investigate the phenotype of the recruited macrophages. For that propose, the amount of produced nitric oxide as a marker for inflammation was quantified 48 hours post stimulation. The same cells were used for the quantification of arginase activity as an anti-inflammatory marker for healing and repair. While the UBM shows a statistically significant difference the DP-ECM showed no difference in NO production when compared with the untreated macrophages. It is of note that published studies using similar methods showed no increase in NO production with UBM, this could possibly be attributed to the seeding numbers, incubation times and the differences between mice and rats derived macrophages (Meng et al. 2015). Based on the levels of chemotaxis, NO production and arginase activity, the ECM shows that it can elect a response and exert an effect on these cells, which might not be an absolute activation of M1 or M2 response.

To further investigate this response, BMDMs treated with ECM digest for 48 hours were stained for F4/80, iNOS, and Fizz-1. Recent studies have shown the ability of ECM based

scaffolds, including UBM and SIS, to upregulate and express Fizz-1 as an anti-inflammatory marker (Huleihel et al. 2017b). Interestingly, bone marrow-derived macrophages showed expression of Fizz-1 when treated with DP-ECM at 1 mg/ml for 48 hours. Similarly, the UBM treated macrophages were positive for Fizz-1 with some cells being positive for iNOS. While the expression Fizz-1 is not as pronounced as the one seen in the IL-4, the ECM degradation products appear to affect the BMDMs behavior by the expression of basal activities that could potentially modify the behavior in-vivo.

Currently, the literature shows the presence of M2 like macrophages around successfully remodeled ECM-based implant (Badylak et al. 2008; Valentin et al. 2009). In some studies, the ECM was used as a coating for mesh implants and showed better results when compared to mesh only (Wolf et al. 2014). To mimic this effect, lyophilized UBM powder, lyophilized minced DP-ECM and lyophilized Collagen gel as a control were subcutaneously implanted in mice within the canal of root segments for 14 days. The goal is to characterize the infiltrating cells for pan-macrophage marker along with M1/M2 markers. In this study, when compared to collagen, the UBM and the DP-ECM showed a statistically significant difference in the ratio of M1/M2. These findings further highlight the role of ECM scaffolds in modulating the host response which showed more M2 macrophages compared to collagen alone. The degradation products and the matrix release profile were shown to contain matrix vesicles that were capable of inducing Fizz-1 expression on BMDMs in-vitro (Huleihel et al. 2017a; Huleihel et al. 2016). The added complexity in the chemical components of the ECM appears to be advantageous over a single protein matrix. The modulation of the host response is a concern in the field of regenerative endodontics as most of the pulp extirpation cases were due to an inflammation (Zanini et al. 2017). The ability of ECM scaffolds to modulate the host response and the possession of

antibacterial activity, not shown here for DP-ECM, are favorable in the regeneration of the root canal system where bacteria and inflammation can cause rejection of the scaffold. Overall, the DP-ECM was able to recruit macrophages and modulate their response at 2 weeks similar to the UBM.

The results above show that collagen alone is not capable of modulating the host response yet its degradation is essential for remodeling (Huleihel et al. 2017b; Madsen et al. 2013). To enhance and hinder the degradation of collagen intracellularly, chondroitin sulfate and dermatan sulfate were added respectively. Studies have shown that cathepsin K activity, one of the main collagenolytic cathepsins, can be improved with the addition of chondroitin sulfate or dampened with the addition of dermatan sulfate (Aguda et al. 2014; Li et al. 2002). The goal is to understand the effect of collagen degradation rate on host response. For this purpose, cathepsin K activity was characterized and showed an increase in M1 (LPS/IFNγ), collagen and collagen with chondroitin sulfate treated macrophages. On the other hand, the activity was downregulated with M2 (IL-4), dermatan sulfate and the pan-cathepsin inhibitor E64. It appears that the activity of cathepsin K can be upregulated or down-regulated based on the activation status of macrophages as studies have shown the presence of cathepsin K in inflammatory macrophages (Platt et al. 2007).

To investigate the effect from an immune response point of view, nitric oxide and arginase activity were quantified from BMDMs 48 hours post-treatment. Macrophages did not show any statistically significant differences in NO production when compared to naïve untreated macrophages. Arginase activity showed an increase when treated with collagen + dermatan sulfate when compared to collagen alone. Of note, the increase due to treatment with collagen and dermatan sulfate was not significant when compared to the untreated macrophages.

For further investigation, flow cytometry analysis was done on two main markers: CD86 as an inflammatory marker and CD206 as an anti-inflammatory marker. These two markers were used in the literature of ECM for the discrimination of M1/M2 macrophages in-vitro and in-vivo (Brown et al. 2012b; Brown et al. 2009; Valentin et al. 2009). The results above show an increase of 18% and 11% in the number of CD86 positive cells for collagen and chondroitin sulfate respectively when compared to the untreated. The same groups have also shown a decrease in cells expressing CD206 only, 20% reduction with collagen and 11% reduction with the addition of chondroitin sulfate. On the contrary, the addition of dermatan sulfate to collagen showed a decrease in CD86 positive cells and maintained similar levels of CD206 expression when compared to control. Pan inhibition of cathepsins activity using E64 showed a 5% reduction in CD206 expressing cells without effects on CD86 expressing cells.

The results at hand highlight the complexity that the ECM offer and shows the importance of the manipulation of organic matrices. Studies using the brain ECM, known to contain glycosaminoglycans, showed an increase in the production of NO when compared to UBM (Dziki et al. 2017; Meng et al. 2015). The same study showed an increase in NO production in UBM when digested with hyaluronidase (Meng et al. 2015). Along with proper decellularization and characterization, these findings demonstrate the importance of the ECM chemical composition and the possibility to modify an ECM for the appropriate intended application.

6.0 CONCLUSIONS

The decellularized pulp extracellular matrix derived from porcine was characterized after decellularization and used in a pilot to investigate the ECM potential in an orthotopic implantation. The early results showed regeneration and remodeling to a pulp like tissue in the canals compared to collagen control. Furthermore, the DP-ECM when digested showed an ability to affect dental pulp and periodontal ligaments cells migration along with the expression of a vascular gene after 3 weeks of treatment. The in-vivo ectopic model demonstrated the potency of a cell-based approach over the use of the ECM scaffold alone. The total population of cells isolated from the dental pulp was capable of survival, enmeshment and remodeling of the ECM with the expression of CD31, Beta 3-tubulin and DSPP as markers for pulp tissue. In addition, the DP-ECM was also capable of electing a macrophage response similar to the UBM in-vivo and shows no increase in NO production in-vitro. ECM based scaffolds offer a variety of chemical components, some of which might affect its performance due to the presence or the lack of some components. The use of collagen, in this case, was intended as a baseline to build up a more complex matrix, where the addition of specific chondroitins showed an influence on the response of bone marrow-derived macrophages. Altogether, this work shows the feasibility of using ECM derived scaffolds for the regeneration of the dental pulp as these scaffolds possess favorable properties including but not limited to: chemotaxis, differentiation, and modulation of the host response all of which are required for the regeneration of a functional dental pulp.

[CHAPTER 2 APPENDIX]

A- PicoGreen Assay protocol

Tissue samples were dried by speed vacuum, weighed and mixed with 300µl of cell lysis buffer (50mM Tris pH 7.5; 100mM EDTA; 0.5% SDS in water) and 3µl of proteinase K for water bath overnight digestion at 55 ºC with agitation. Samples were then mixed and spun for 1 min in 100µl of protein precipitation solution (7.5M NH4 C2H3O2 in water). The supernatants were transferred to a new tube with 300µl of 100% 2-propanol then mixed and spun again for 2 min. Samples were washed with 300µl of 70% ethanol twice and left to dry overnight then re-suspended in 200µl of nanopure water for DNA quantification (n=15) by Quant-iT™ PicoGreen® dsDNA assay kit according to manufacturer's instructions. Native pulp tissue was subjected to the same digestion protocol as a control. The DP-ECM was considered successfully decellularized when the total DNA content was less than 50ng/mg of dry tissue weight.

B- Dental pulp cells and periodontal ligament cells isolation

To investigate the biological activity of the DP-ECM and UBM, human dental pulp cells and PDL cells were isolated and cultured according to the following: Healthy adult third molars were obtained from the University of Pittsburgh, School of Dental Medicine, after routine extraction. Dental pulp was exposed and removed with a barbed broach. The pulp was minced and then digested in an enzyme cocktail containing 3 mg/ml collagenase and 4 mg/ml dispase for 1 to 1.5 hr at 37°C. The total population of human dental pulp cells (DPCs) was plated and expanded in a maintenance medium (M.M) containing Alpha Minimum Essential Media (αMEM; Gibco,

Grand Island, NY, USA), with 10% fetal bovine serum (FBS; Atlanta Biologicals, Flowery Branch, GA, USA), and 1% penicillin/streptomycin (P/S; Gibco). Cells were used at P3 for proliferation, trans-well migration, wound healing, gene expression experiments, and in-vivo implantation experiment.

The PDL was scraped from the middle third of the root and then digested in an enzyme cocktail containing 3 mg/ml collagenase and 4 mg/ml dispase for 1 to 1.5 hr at 37°C. The total population of Periodontal Ligaments Cells (PDLCs) was plated and expanded in a maintenance medium (M.M) containing Alpha Minimum Essential Media (αMEM; Gibco, Grand Island, NY, USA), with 10% fetal bovine serum (FBS; Atlanta Biologicals, Flowery Branch, GA, USA), and 1% penicillin/streptomycin (P/S; Gibco). Cells were used at P3 for wound healing, gene expression, and in-vivo implantation experiments.

Similar to a previously published protocol (Freytes et al. 2008) DP-ECM and UBM were lyophilized and digested in Pepsin 1 mg/ml, 0.01N HCl at the concentration of 10 mg on a stirrer for 72 hours, neutralized using 0.1N NaOH and diluted to desired concentration using maintenance medium.

C- Post sacrifice (µCT), histology and immunohistochemistry.

Jaw explants (10% formalin-fixed for 3 days) were µCT scanned in PBS media at 30mm resolution, integration time of 299 ms, 55 keV, 142 mA with a cone beam and continuous rotation (VivaCT 40; Scanco) After µCT, teeth were hemi-sectioned into mesial (crown and root) and distal portions by diamond disc (102x0.3mm) on precision saw (Isomet-Buehler). Each root/bone explant was resin embedded (Osteo-bed bone embedding kit, Polysciences, Inc-USA) separately for maximum penetration. Resin-embedded samples were sectioned into 5µm sections

(Leica RM2255 with tungsten carbide blade C.L. Sturkey Inc.) that were collected on sticky tape (Tesa Film-Germany), deacrylated and stained for 1) Goldner's trichrome histology and 2) immunostaining for two antibodies that demonstrated reactivity against canine but not swine tissues (Appendix figure 3): CD31 (Labome bs-0468R, rabbit anti-human, conc. 1:50 with citrate antigen retrieval) and DSP (Larry Fisher LF151 rabbit anti-human, conc. 1:100, without antigen retrieval). Immunohistochemistry was performed by the Expose Mouse and Rabbit HRP kit (Abcam) according to manufacturer's instructions.

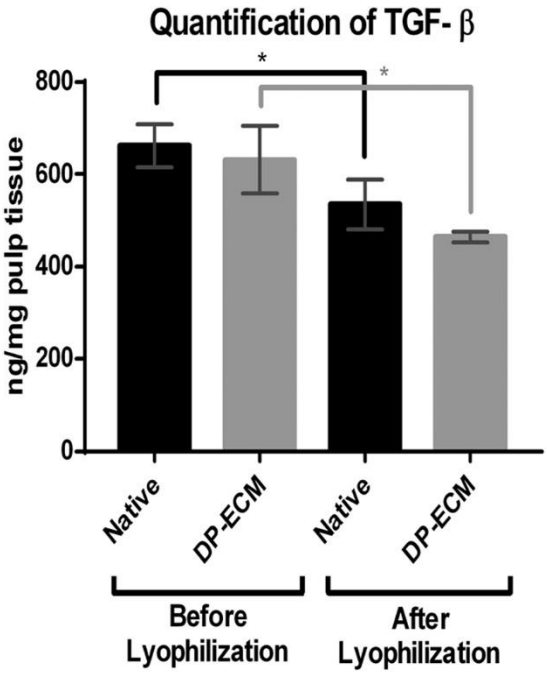

Appendix Figure 1. Histogram showing the contribution of the lyophilization process to the reduction of growth factors (tested on TGF-β) in both the native and DP-ECM matrices. This piece of data indicates that the lyophilization process may have had the greatest contribution to the reduction of growth factors rather than Ethylene oxide sterilization. n=3; *$p<0.05$.

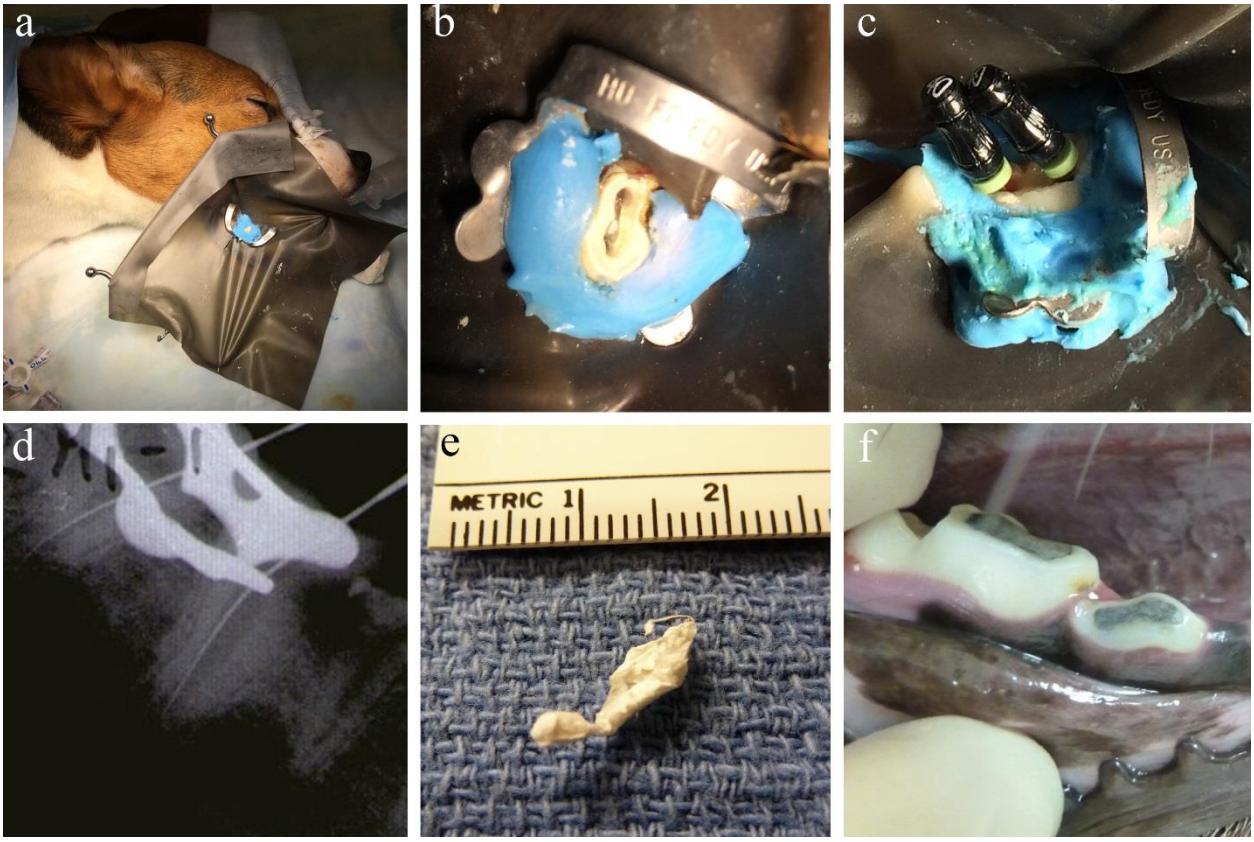

Appendix Figure 2. Canine surgery. a: Beagle under GA with tooth isolated by rubber dam and rubber-base impression material. b: Pulp chamber and root canals access. c: Mesial and Distal canals preparation by K-files. d: Guiding x-ray during surgery. e: Lyophilized DP-ECM to be inserted into the root canals. f: final restoration with glass ionomer filling material.

Procedure details: Under general anesthesia, the mandibular first molars and 4th premolars were isolated by rubbed dam supported by a rubber dam clamp. Teeth were scrubbed with Betadine and further isolation was maximized by silicone rubber-based impression material sealing around the placed clamp (App. fig. 2a). The dental pulp of each tooth was accessed by a #4 round carbide bur mounted on a high-speed dental handpiece. For each tooth, the apex was determined using stainless steel K type files guided by x-rays (NOMAD Pro™ – Handheld X-ray-USA on Ergonom.X self-developing dental film S.R.L-Italy) (App. fig. 2c&d). The canals where prepared and the pulp tissue extirpated with NiTi rotary Protaper NEXT files (Dentsply/Tulsa dental). The apex was opened to size 0.54mm by removing 1mm from a size 50/0.4-taper Profile NiTi rotary instrument (Dentsply/Tulsa dental). The canal was irrigated with a 0.5% NaOCl pH7 solution (Dankins' irrigation) followed by 17% EDTA solution (EndoCleanse, Roydent) to clean the canals from all debris. The canals were dried by sterile paper points and apical bleeding was induced by passing a sterile size 15 K file into the periapical tissue before material implantation.

Two teeth received lyophilized EtO-sterilized swine DP-ECM (App. fig. 2e) (in 4 root canals), 100mg of tissue in each canal inserted by hand pluggers, while 3 teeth (6 root canals) received collagen scaffold (Preparation described below) and 3 teeth (6 root canals) were left empty (blood clot alone) as controls. All pulp chambers were then sealed by MTA material (Dentsply, USA) at the canals orifice followed by a glass ionomer filling material (Ketac Silver-3M ESPE) within the pulp chamber (App. fig. 2f). The dogs were subjected to a 3-day analgesic (Meloxicam 0.2mg/Kg SID) and antibiotic (Amoxicillin 20mg/Kg BID) regimen according to the Division of Laboratory Animal Resources guidelines. Dogs were housed individually with enrichment methods. Animals stayed healthy and active until sacrifice at 8 weeks.

Preparation of collagen scaffolds as a control for in-vivo experimentation. Rat tail collagen and neutralizing solutions (Advanced Biomatrix Inc., San Diego, CA, USA) were chilled and kept on ice during scaffold preparation procedure. Both solutions were mixed in 9:1 ratio then transferred to sterile vials and incubated at 37°C for 4h for cross-linking. The formed gel was then lyophilized for 24h then sterilized in EtO. The collagen resulting sponge was stored in a vacuum desiccator at 4°C until used in animal surgery. The animal study conformed to the ARRIVE guidelines.

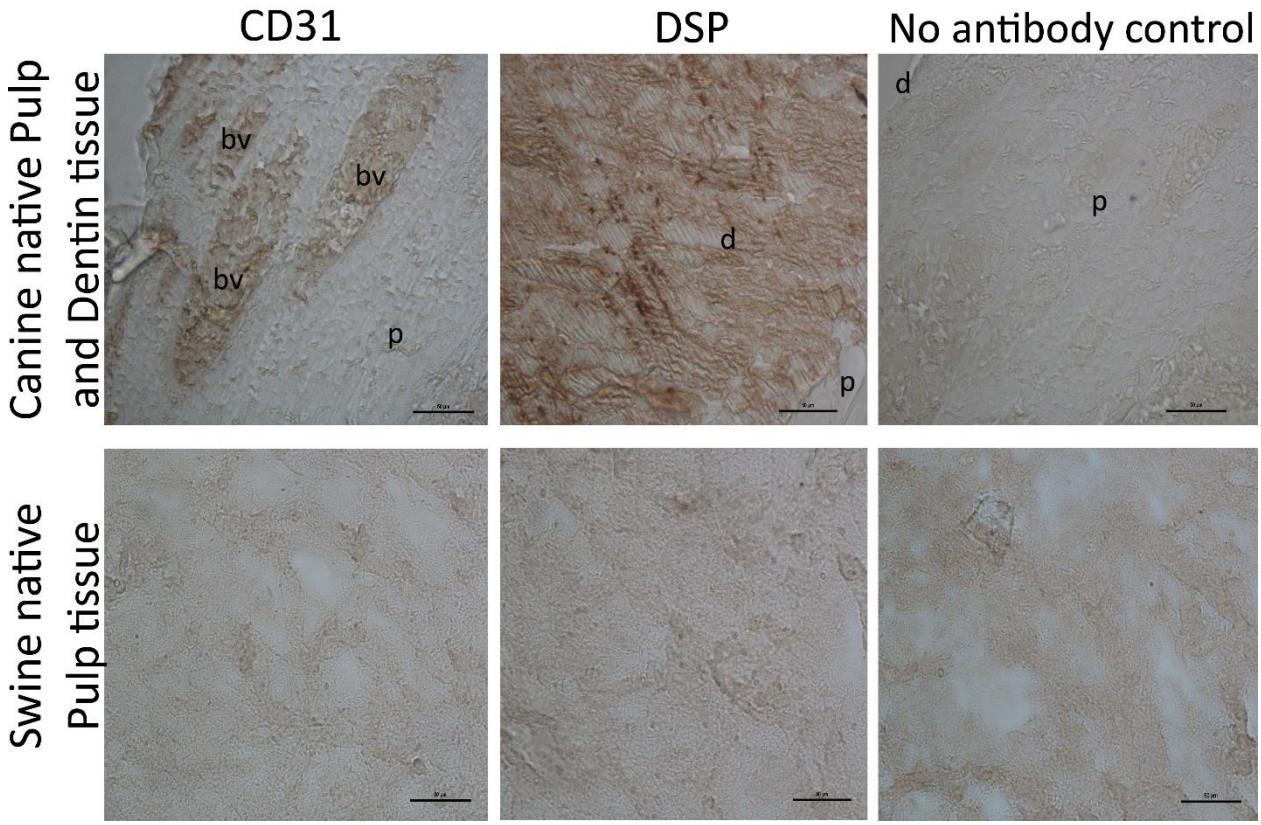

Appendix Figure 3. IHC controls. Canine and swine native pulp tissues stained with CD31 antibody (Labome bs-0468R, rabbit anti-human, conc. 1:50 with citrate antigen retrieval), DSPP (Larry Fisher LF151 rabbit anti-human, conc. 1:100, without antigen retrieval) and antibody negative controls. This experiment shows that the antibodies used to demonstrate the regenerative effects of swine DP-ECM are positive against tissues of canine origin only; confirming that the formed tissues within the root canals are of canine origin and not a part of the implanted swine ECM. bv: blood vessels; p: pulp; d: dentin.

BIBLIOGRAPHY

Agrawal V, Johnson SA, Reing J, Zhang L, Tottey S, Wang G, Hirschi KK, Braunhut S, Gudas LJ, Badylak SF. 2010. Epimorphic regeneration approach to tissue replacement in adult mammals. Proc Natl Acad Sci U S A. 107(8):3351-3355.

Agrawal V, Tottey S, Johnson SA, Freund JM, Siu BF, Badylak SF. 2011. Recruitment of progenitor cells by an extracellular matrix cryptic peptide in a mouse model of digit amputation. Tissue Eng Part A. 17(19-20):2435-2443.

Aguda AH, Panwar P, Du X, Nguyen NT, Brayer GD, Bromme D. 2014. Structural basis of collagen fiber degradation by cathepsin k. Proc Natl Acad Sci U S A. 111(49):17474-17479.

Alqahtani Q, Zaky SH, Patil A, Beniash E, Ray H, Sfeir C. 2018. Decellularized swine dental pulp tissue for regenerative root canal therapy. J Dent Res.22034518785124.

Arnold L, Henry A, Poron F, Baba-Amer Y, van Rooijen N, Plonquet A, Gherardi RK, Chazaud B. 2007. Inflammatory monocytes recruited after skeletal muscle injury switch into antiinflammatory macrophages to support myogenesis. J Exp Med. 204(5):1057-1069.

Aurora A, Roe JL, Corona BT, Walters TJ. 2015. An acellular biologic scaffold does not regenerate appreciable de novo muscle tissue in rat models of volumetric muscle loss injury. Biomaterials. 67:393-407.

Badylak SF. 2002. The extracellular matrix as a scaffold for tissue reconstruction. Semin Cell Dev Biol. 13(5):377-383.

Badylak SF. 2004. Xenogeneic extracellular matrix as a scaffold for tissue reconstruction. Transpl Immunol. 12(3-4):367-377.

Badylak SF, Hoppo T, Nieponice A, Gilbert TW, Davison JM, Jobe BA. 2011a. Esophageal preservation in five male patients after endoscopic inner-layer circumferential resection in the setting of superficial cancer: A regenerative medicine approach with a biologic scaffold. Tissue Eng Part A. 17(11-12):1643-1650.

Badylak SF, Taylor D, Uygun K. 2011b. Whole-organ tissue engineering: Decellularization and recellularization of three-dimensional matrix scaffolds. Annu Rev Biomed Eng. 13:27-53.

Badylak SF, Valentin JE, Ravindra AK, McCabe GP, Stewart-Akers AM. 2008. Macrophage phenotype as a determinant of biologic scaffold remodeling. Tissue Eng Part A. 14(11):1835-1842.

Balic A, Thesleff I. 2015. Tissue interactions regulating tooth development and renewal. Curr Top Dev Biol. 115:157-186.

Barnes CP, Sell SA, Boland ED, Simpson DG, Bowlin GL. 2007. Nanofiber technology: Designing the next generation of tissue engineering scaffolds. Adv Drug Deliv Rev. 59(14):1413-1433.

Beniash E, Deshpande AS, Fang PA, Lieb NS, Zhang X, Sfeir CS. 2011. Possible role of dmp1 in dentin mineralization. J Struct Biol. 174(1):100-106.
Bissell MJ, Aggeler J. 1987. Dynamic reciprocity: How do extracellular matrix and hormones direct gene expression? Prog Clin Biol Res. 249:251-262.
Bohl KS, Shon J, Rutherford B, Mooney DJ. 1998. Role of synthetic extracellular matrix in development of engineered dental pulp. J Biomater Sci Polym Ed. 9(7):749-764.
Bondesen BA, Mills ST, Pavlath GK. 2006. The cox-2 pathway regulates growth of atrophied muscle via multiple mechanisms. Am J Physiol Cell Physiol. 290(6):C1651-1659.
Boruch AV, Nieponice A, Qureshi IR, Gilbert TW, Badylak SF. 2010. Constructive remodeling of biologic scaffolds is dependent on early exposure to physiologic bladder filling in a canine partial cystectomy model. J Surg Res. 161(2):217-225.
Boudreau N, Myers C, Bissell MJ. 1995. From laminin to lamin: Regulation of tissue-specific gene expression by the ecm. Trends Cell Biol. 5(1):1-4.
Boyle M, Chun C, Strojny C, Narayanan R, Bartholomew A, Sundivakkam P, Alapati S. 2014. Chronic inflammation and angiogenic signaling axis impairs differentiation of dental-pulp stem cells. PLoS One. 9(11):e113419.
Brennan EP, Reing J, Chew D, Myers-Irvin JM, Young EJ, Badylak SF. 2006. Antibacterial activity within degradation products of biological scaffolds composed of extracellular matrix. Tissue Eng. 12(10):2949-2955.
Brennan EP, Tang XH, Stewart-Akers AM, Gudas LJ, Badylak SF. 2008. Chemoattractant activity of degradation products of fetal and adult skin extracellular matrix for keratinocyte progenitor cells. J Tissue Eng Regen Med. 2(8):491-498.
Brizzi MF, Tarone G, Defilippi P. 2012. Extracellular matrix, integrins, and growth factors as tailors of the stem cell niche. Curr Opin Cell Biol. 24(5):645-651.
Brown BN, Barnes CA, Kasick RT, Michel R, Gilbert TW, Beer-Stolz D, Castner DG, Ratner BD, Badylak SF. 2010. Surface characterization of extracellular matrix scaffolds. Biomaterials. 31(3):428-437.
Brown BN, Chung WL, Almarza AJ, Pavlick MD, Reppas SN, Ochs MW, Russell AJ, Badylak SF. 2012a. Inductive, scaffold-based, regenerative medicine approach to reconstruction of the temporomandibular joint disk. J Oral Maxillofac Surg. 70(11):2656-2668.
Brown BN, Freund JM, Han L, Rubin JP, Reing JE, Jeffries EM, Wolf MT, Tottey S, Barnes CA, Ratner BD et al. 2011. Comparison of three methods for the derivation of a biologic scaffold composed of adipose tissue extracellular matrix. Tissue Eng Part C Methods. 17(4):411-421.
Brown BN, Londono R, Tottey S, Zhang L, Kukla KA, Wolf MT, Daly KA, Reing JE, Badylak SF. 2012b. Macrophage phenotype as a predictor of constructive remodeling following the implantation of biologically derived surgical mesh materials. Acta Biomater. 8(3):978-987.
Brown BN, Valentin JE, Stewart-Akers AM, McCabe GP, Badylak SF. 2009. Macrophage phenotype and remodeling outcomes in response to biologic scaffolds with and without a cellular component. Biomaterials. 30(8):1482-1491.
Camacho-Alonso F, Torralba-Ruiz MR, Garcia-Carrillo N, Lacal-Lujan J, Martinez-Diaz F, Sanchez-Siles M. 2018. Effects of topical applications of porcine acellular urinary bladder matrix and centella asiatica extract on oral wound healing in a rat model. Clin Oral Investig.

Cao Y, Song M, Kim E, Shon W, Chugal N, Bogen G, Lin L, Kim RH, Park NH, Kang MK. 2015. Pulp-dentin regeneration: Current state and future prospects. J Dent Res. 94(11):1544-1551.

Carey LE, Dearth CL, Johnson SA, Londono R, Medberry CJ, Daly KA, Badylak SF. 2014. In vivo degradation of 14c-labeled porcine dermis biologic scaffold. Biomaterials. 35(29):8297-8304.

Caton J, Bostanci N, Remboutsika E, De Bari C, Mitsiadis TA. 2011. Future dentistry: Cell therapy meets tooth and periodontal repair and regeneration. J Cell Mol Med. 15(5):1054-1065.

Cawston TE, Young DA. 2010. Proteinases involved in matrix turnover during cartilage and bone breakdown. Cell Tissue Res. 339(1):221-235.

Chen G, Chen J, Yang B, Li L, Luo X, Zhang X, Feng L, Jiang Z, Yu M, Guo W et al. 2015. Combination of aligned plga/gelatin electrospun sheets, native dental pulp extracellular matrix and treated dentin matrix as substrates for tooth root regeneration. Biomaterials. 52:56-70.

Chen SE, Jin B, Li YP. 2007. Tnf-alpha regulates myogenesis and muscle regeneration by activating p38 mapk. Am J Physiol Cell Physiol. 292(5):C1660-1671.

Collins RA, Grounds MD. 2001. The role of tumor necrosis factor-alpha (tnf-alpha) in skeletal muscle regeneration. Studies in tnf-alpha(-/-) and tnf-alpha(-/-)/lt-alpha(-/-) mice. J Histochem Cytochem. 49(8):989-1001.

Costa AG, Cusano NE, Silva BC, Cremers S, Bilezikian JP. 2011. Cathepsin k: Its skeletal actions and role as a therapeutic target in osteoporosis. Nat Rev Rheumatol. 7(8):447-456.

Couve E, Osorio R, Schmachtenberg O. 2014. Reactionary dentinogenesis and neuroimmune response in dental caries. J Dent Res. 93(8):788-793.

Crapo PM, Gilbert TW, Badylak SF. 2011. An overview of tissue and whole organ decellularization processes. Biomaterials. 32(12):3233-3243.

Crapo PM, Medberry CJ, Reing JE, Tottey S, van der Merwe Y, Jones KE, Badylak SF. 2012. Biologic scaffolds composed of central nervous system extracellular matrix. Biomaterials. 33(13):3539-3547.

Crapo PM, Tottey S, Slivka PF, Badylak SF. 2014. Effects of biologic scaffolds on human stem cells and implications for cns tissue engineering. Tissue Eng Part A. 20(1-2):313-323.

Daly KA, Liu S, Agrawal V, Brown BN, Johnson SA, Medberry CJ, Badylak SF. 2012. Damage associated molecular patterns within xenogeneic biologic scaffolds and their effects on host remodeling. Biomaterials. 33(1):91-101.

Davis GE. 2010. Matricryptic sites control tissue injury responses in the cardiovascular system: Relationships to pattern recognition receptor regulated events. J Mol Cell Cardiol. 48(3):454-460.

Davis GE, Bayless KJ, Davis MJ, Meininger GA. 2000. Regulation of tissue injury responses by the exposure of matricryptic sites within extracellular matrix molecules. Am J Pathol. 156(5):1489-1498.

Diogenes A, Ruparel NB. 2017. Regenerative endodontic procedures: Clinical outcomes. Dent Clin North Am. 61(1):111-125.

Dissanayaka WL, Zhu L, Hargreaves KM, Jin L, Zhang C. 2014. Scaffold-free prevascularized microtissue spheroids for pulp regeneration. J Dent Res. 93(12):1296-1303.

Dziki JL, Giglio RM, Sicari BM, Wang DS, Gandhi RM, Londono R, Dearth CL, Badylak SF. 2018. The effect of mechanical loading upon extracellular matrix bioscaffold-mediated skeletal muscle remodeling. Tissue Eng Part A. 24(1-2):34-46.

Dziki JL, Wang DS, Pineda C, Sicari BM, Rausch T, Badylak SF. 2017. Solubilized extracellular matrix bioscaffolds derived from diverse source tissues differentially influence macrophage phenotype. J Biomed Mater Res A. 105(1):138-147.

Engler AJ, Sen S, Sweeney HL, Discher DE. 2006. Matrix elasticity directs stem cell lineage specification. Cell. 126(4):677-689.

Farges JC, Alliot-Licht B, Renard E, Ducret M, Gaudin A, Smith AJ, Cooper PR. 2015. Dental pulp defence and repair mechanisms in dental caries. Mediators Inflamm. 2015:230251.

Fonovic M, Turk B. 2014. Cysteine cathepsins and extracellular matrix degradation. Biochim Biophys Acta. 1840(8):2560-2570.

Freytes DO, Martin J, Velankar SS, Lee AS, Badylak SF. 2008. Preparation and rheological characterization of a gel form of the porcine urinary bladder matrix. Biomaterials. 29(11):1630-1637.

Friedman S, Mor C. 2004. The success of endodontic therapy--healing and functionality. J Calif Dent Assoc. 32(6):493-503.

Galler KM. 2016. Clinical procedures for revitalization: Current knowledge and considerations. Int Endod J. 49(10):926-936.

Galler KM, Aulisa L, Regan KR, D'Souza RN, Hartgerink JD. 2010. Self-assembling multidomain peptide hydrogels: Designed susceptibility to enzymatic cleavage allows enhanced cell migration and spreading. J Am Chem Soc. 132(9):3217-3223.

Galler KM, D'Souza RN, Federlin M, Cavender AC, Hartgerink JD, Hecker S, Schmalz G. 2011. Dentin conditioning codetermines cell fate in regenerative endodontics. J Endod. 37(11):1536-1541.

Galler KM, Eidt A, Schmalz G. 2014. Cell-free approaches for dental pulp tissue engineering. J Endod. 40(4 Suppl):S41-45.

Gao Z, Flaitz CM, Mackenzie IC. 1996. Expression of keratinocyte growth factor in periapical lesions. J Dent Res. 75(9):1658-1663.

Gaudin A, Renard E, Hill M, Bouchet-Delbos L, Bienvenu-Louvet G, Farges JC, Cuturi MC, Alliot-Licht B. 2015. Phenotypic analysis of immunocompetent cells in healthy human dental pulp. J Endod. 41(5):621-627.

Ghuman H, Gerwig M, Nicholls FJ, Liu JR, Donnelly J, Badylak SF, Modo M. 2017. Long-term retention of ecm hydrogel after implantation into a sub-acute stroke cavity reduces lesion volume. Acta Biomater. 63:50-63.

Ghuman H, Massensini AR, Donnelly J, Kim SM, Medberry CJ, Badylak SF, Modo M. 2016. Ecm hydrogel for the treatment of stroke: Characterization of the host cell infiltrate. Biomaterials. 91:166-181.

Gilbert TW. 2012. Strategies for tissue and organ decellularization. J Cell Biochem. 113(7):2217-2222.

Gilbert TW, Freund JM, Badylak SF. 2009. Quantification of DNA in biologic scaffold materials. J Surg Res. 152(1):135-139.

Gilbert TW, Sellaro TL, Badylak SF. 2006. Decellularization of tissues and organs. Biomaterials. 27(19):3675-3683.

Gilbert TW, Stewart-Akers AM, Badylak SF. 2007a. A quantitative method for evaluating the degradation of biologic scaffold materials. Biomaterials. 28(2):147-150.

Gilbert TW, Stewart-Akers AM, Simmons-Byrd A, Badylak SF. 2007b. Degradation and remodeling of small intestinal submucosa in canine achilles tendon repair. J Bone Joint Surg Am. 89(3):621-630.
Gordon S. 2003. Alternative activation of macrophages. Nat Rev Immunol. 3(1):23-35.
Gordon S, Martinez FO. 2010. Alternative activation of macrophages: Mechanism and functions. Immunity. 32(5):593-604.
Gordon S, Taylor PR. 2005. Monocyte and macrophage heterogeneity. Nat Rev Immunol. 5(12):953-964.
Gowen M, Lazner F, Dodds R, Kapadia R, Feild J, Tavaria M, Bertoncello I, Drake F, Zavarselk S, Tellis I et al. 1999. Cathepsin k knockout mice develop osteopetrosis due to a deficit in matrix degradation but not demineralization. J Bone Miner Res. 14(10):1654-1663.
Gronthos S, Brahim J, Li W, Fisher LW, Cherman N, Boyde A, DenBesten P, Robey PG, Shi S. 2002. Stem cell properties of human dental pulp stem cells. J Dent Res. 81(8):531-535.
Gronthos S, Mankani M, Brahim J, Robey PG, Shi S. 2000. Postnatal human dental pulp stem cells (dpscs) in vitro and in vivo. Proc Natl Acad Sci U S A. 97(25):13625-13630.
Hahn CL, Liewehr FR. 2007. Innate immune responses of the dental pulp to caries. J Endod. 33(6):643-651.
Hern DL, Hubbell JA. 1998. Incorporation of adhesion peptides into nonadhesive hydrogels useful for tissue resurfacing. J Biomed Mater Res. 39(2):266-276.
Hoganson DM, O'Doherty EM, Owens GE, Harilal DO, Goldman SM, Bowley CM, Neville CM, Kronengold RT, Vacanti JP. 2010. The retention of extracellular matrix proteins and angiogenic and mitogenic cytokines in a decellularized porcine dermis. Biomaterials. 31(26):6730-6737.
Hoshiba T, Chen G, Endo C, Maruyama H, Wakui M, Nemoto E, Kawazoe N, Tanaka M. 2016. Decellularized extracellular matrix as an in vitro model to study the comprehensive roles of the ecm in stem cell differentiation. Stem Cells Int. 2016:6397820.
Hsiong SX, Huebsch N, Fischbach C, Kong HJ, Mooney DJ. 2008. Integrin-adhesion ligand bond formation of preosteoblasts and stem cells in three-dimensional rgd presenting matrices. Biomacromolecules. 9(7):1843-1851.
Hu L, Gao Z, Xu J, Zhu Z, Fan Z, Zhang C, Wang J, Wang S. 2017. Decellularized swine dental pulp as a bioscaffold for pulp regeneration. Biomed Res Int. 2017:9342714.
Huang CC, Narayanan R, Warshawsky N, Ravindran S. 2018. Dual ecm biomimetic scaffolds for dental pulp regenerative applications. Front Physiol. 9:495.
Huang GT, Yamaza T, Shea LD, Djouad F, Kuhn NZ, Tuan RS, Shi S. 2010. Stem/progenitor cell-mediated de novo regeneration of dental pulp with newly deposited continuous layer of dentin in an in vivo model. Tissue Eng Part A. 16(2):605-615.
Huang S, Zhang Y, Tang L, Deng Z, Lu W, Feng F, Xu X, Jin Y. 2009. Functional bilayered skin substitute constructed by tissue-engineered extracellular matrix and microsphere-incorporated gelatin hydrogel for wound repair. Tissue Eng Part A. 15(9):2617-2624.
Huang WC, Sala-Newby GB, Susana A, Johnson JL, Newby AC. 2012. Classical macrophage activation up-regulates several matrix metalloproteinases through mitogen activated protein kinases and nuclear factor-kappab. PLoS One. 7(8):e42507.
Huleihel L, Bartolacci JG, Dziki JL, Vorobyov T, Arnold B, Scarritt ME, Pineda Molina C, LoPresti ST, Brown BN, Naranjo JD et al. 2017a. Matrix-bound nanovesicles recapitulate extracellular matrix effects on macrophage phenotype. Tissue Eng Part A. 23(21-22):1283-1294.

Huleihel L, Dziki JL, Bartolacci JG, Rausch T, Scarritt ME, Cramer MC, Vorobyov T, LoPresti ST, Swineheart IT, White LJ et al. 2017b. Macrophage phenotype in response to ecm bioscaffolds. Semin Immunol. 29:2-13.

Huleihel L, Hussey GS, Naranjo JD, Zhang L, Dziki JL, Turner NJ, Stolz DB, Badylak SF. 2016. Matrix-bound nanovesicles within ecm bioscaffolds. Sci Adv. 2(6):e1600502.

Hynes RO, Naba A. 2012. Overview of the matrisome--an inventory of extracellular matrix constituents and functions. Cold Spring Harb Perspect Biol. 4(1):a004903.

Ingber D. 1991. Extracellular matrix and cell shape: Potential control points for inhibition of angiogenesis. J Cell Biochem. 47(3):236-241.

Islam B, Khan SN, Khan AU. 2007. Dental caries: From infection to prevention. Med Sci Monit. 13(11):RA196-203.

Jablonska-Trypuc A, Matejczyk M, Rosochacki S. 2016. Matrix metalloproteinases (mmps), the main extracellular matrix (ecm) enzymes in collagen degradation, as a target for anticancer drugs. J Enzyme Inhib Med Chem. 31(sup1):177-183.

Kawashima N, Okiji T. 2016. Odontoblasts: Specialized hard-tissue-forming cells in the dentin-pulp complex. Congenit Anom (Kyoto). 56(4):144-153.

Kazanis I, ffrench-Constant C. 2011. Extracellular matrix and the neural stem cell niche. Dev Neurobiol. 71(11):1006-1017.

Keane TJ, Londono R, Carey RM, Carruthers CA, Reing JE, Dearth CL, D'Amore A, Medberry CJ, Badylak SF. 2013. Preparation and characterization of a biologic scaffold from esophageal mucosa. Biomaterials. 34(28):6729-6737.

Kim GH, Park YD, Lee SY, El-Fiqi A, Kim JJ, Lee EJ, Kim HW, Kim EC. 2015a. Odontogenic stimulation of human dental pulp cells with bioactive nanocomposite fiber. J Biomater Appl. 29(6):854-866.

Kim JY, Xin X, Moioli EK, Chung J, Lee CH, Chen M, Fu SY, Koch PD, Mao JJ. 2010. Regeneration of dental-pulp-like tissue by chemotaxis-induced cell homing. Tissue Eng Part A. 16(10):3023-3031.

Kim S, Shin SJ, Song Y, Kim E. 2015b. In vivo experiments with dental pulp stem cells for pulp-dentin complex regeneration. Mediators Inflamm. 2015:409347.

Kitamoto S, Sukhova GK, Sun J, Yang M, Libby P, Love V, Duramad P, Sun C, Zhang Y, Yang X et al. 2007. Cathepsin l deficiency reduces diet-induced atherosclerosis in low-density lipoprotein receptor-knockout mice. Circulation. 115(15):2065-2075.

Kojima K, Inamoto K, Nagamatsu K, Hara A, Nakata K, Morita I, Nakagaki H, Nakamura H. 2004. Success rate of endodontic treatment of teeth with vital and nonvital pulps. A meta-analysis. Oral Surg Oral Med Oral Pathol Oral Radiol Endod. 97(1):95-99.

Kumbar SG, James R, Nukavarapu SP, Laurencin CT. 2008. Electrospun nanofiber scaffolds: Engineering soft tissues. Biomed Mater. 3(3):034002.

Langer R, Vacanti JP. 1993. Tissue engineering. Science. 260(5110):920-926.

LeBaron RG, Athanasiou KA. 2000. Extracellular matrix cell adhesion peptides: Functional applications in orthopedic materials. Tissue Eng. 6(2):85-103.

Lee SY, Kim SY, Park SH, Kim JJ, Jang JH, Kim EC. 2012. Effects of recombinant dentin sialoprotein in dental pulp cells. J Dent Res. 91(4):407-412.

Lee TH, Kim WT, Ryu CJ, Jang YJ. 2015. Optimization of treatment with recombinant fgf-2 for proliferation and differentiation of human dental stem cells, mesenchymal stem cells, and osteoblasts. Biochem Cell Biol. 93(4):298-305.

Li Z, Hou WS, Escalante-Torres CR, Gelb BD, Bromme D. 2002. Collagenase activity of cathepsin k depends on complex formation with chondroitin sulfate. J Biol Chem. 277(32):28669-28676.

Li Z, Yasuda Y, Li W, Bogyo M, Katz N, Gordon RE, Fields GB, Bromme D. 2004. Regulation of collagenase activities of human cathepsins by glycosaminoglycans. J Biol Chem. 279(7):5470-5479.

Londono R, Dziki JL, Haljasmaa E, Turner NJ, Leifer CA, Badylak SF. 2017. The effect of cell debris within biologic scaffolds upon the macrophage response. J Biomed Mater Res A. 105(8):2109-2118.

Lu P, Takai K, Weaver VM, Werb Z. 2011. Extracellular matrix degradation and remodeling in development and disease. Cold Spring Harb Perspect Biol. 3(12).

Lutgens E, Lutgens SP, Faber BC, Heeneman S, Gijbels MM, de Winther MP, Frederik P, van der Made I, Daugherty A, Sijbers AM et al. 2006. Disruption of the cathepsin k gene reduces atherosclerosis progression and induces plaque fibrosis but accelerates macrophage foam cell formation. Circulation. 113(1):98-107.

Madsen DH, Ingvarsen S, Jurgensen HJ, Melander MC, Kjoller L, Moyer A, Honore C, Madsen CA, Garred P, Burgdorf S et al. 2011. The non-phagocytic route of collagen uptake: A distinct degradation pathway. J Biol Chem. 286(30):26996-27010.

Madsen DH, Leonard D, Masedunskas A, Moyer A, Jurgensen HJ, Peters DE, Amornphimoltham P, Selvaraj A, Yamada SS, Brenner DA et al. 2013. M2-like macrophages are responsible for collagen degradation through a mannose receptor-mediated pathway. J Cell Biol. 202(6):951-966.

Mantovani A, Sica A, Sozzani S, Allavena P, Vecchi A, Locati M. 2004. The chemokine system in diverse forms of macrophage activation and polarization. Trends Immunol. 25(12):677-686.

Maquart FX, Bellon G, Pasco S, Monboisse JC. 2005. Matrikines in the regulation of extracellular matrix degradation. Biochimie. 87(3-4):353-360.

Martin FE. 2003. Carious pulpitis: Microbiological and histopathological considerations. Aust Endod J. 29(3):134-137.

Massensini AR, Ghuman H, Saldin LT, Medberry CJ, Keane TJ, Nicholls FJ, Velankar SS, Badylak SF, Modo M. 2015. Concentration-dependent rheological properties of ecm hydrogel for intracerebral delivery to a stroke cavity. Acta Biomater. 27:116-130.

Matuska AM, McFetridge PS. 2015. The effect of terminal sterilization on structural and biophysical properties of a decellularized collagen-based scaffold; implications for stem cell adhesion. J Biomed Mater Res B Appl Biomater. 103(2):397-406.

Mauro A. 1961. Satellite cell of skeletal muscle fibers. J Biophys Biochem Cytol. 9:493-495.

Medberry CJ, Crapo PM, Siu BF, Carruthers CA, Wolf MT, Nagarkar SP, Agrawal V, Jones KE, Kelly J, Johnson SA et al. 2013. Hydrogels derived from central nervous system extracellular matrix. Biomaterials. 34(4):1033-1040.

Meng FW, Slivka PF, Dearth CL, Badylak SF. 2015. Solubilized extracellular matrix from brain and urinary bladder elicits distinct functional and phenotypic responses in macrophages. Biomaterials. 46:131-140.

Mrozik K, Gronthos S, Shi S, Bartold PM. 2017. A method to isolate, purify, and characterize human periodontal ligament stem cells. Methods Mol Biol. 1537:413-427.

Muir AR, Kanji AH, Allbrook D. 1965. The structure of the satellite cells in skeletal muscle. J Anat. 99(Pt 3):435-444.

Mullane EM, Dong Z, Sedgley CM, Hu JC, Botero TM, Holland GR, Nor JE. 2008. Effects of vegf and fgf2 on the revascularization of severed human dental pulps. J Dent Res. 87(12):1144-1148.

Na S, Zhang H, Huang F, Wang W, Ding Y, Li D, Jin Y. 2016. Regeneration of dental pulp/dentine complex with a three-dimensional and scaffold-free stem-cell sheet-derived pellet. J Tissue Eng Regen Med. 10(3):261-270.

Nakashima M, Akamine A. 2005. The application of tissue engineering to regeneration of pulp and dentin in endodontics. J Endod. 31(10):711-718.

Newby AC. 2008. Metalloproteinase expression in monocytes and macrophages and its relationship to atherosclerotic plaque instability. Arterioscler Thromb Vasc Biol. 28(12):2108-2114.

Paduano F, Marrelli M, Alom N, Amer M, White LJ, Shakesheff KM, Tatullo M. 2017. Decellularized bone extracellular matrix and human dental pulp stem cells as a construct for bone regeneration. J Biomater Sci Polym Ed. 28(8):730-748.

Platt MO, Ankeny RF, Shi GP, Weiss D, Vega JD, Taylor WR, Jo H. 2007. Expression of cathepsin k is regulated by shear stress in cultured endothelial cells and is increased in endothelium in human atherosclerosis. Am J Physiol Heart Circ Physiol. 292(3):H1479-1486.

Ramchandran R, Dhanabal M, Volk R, Waterman MJ, Segal M, Lu H, Knebelmann B, Sukhatme VP. 1999. Antiangiogenic activity of restin, nc10 domain of human collagen xv: Comparison to endostatin. Biochem Biophys Res Commun. 255(3):735-739.

Ravindran S, George A. 2015. Biomimetic extracellular matrix mediated somatic stem cell differentiation: Applications in dental pulp tissue regeneration. Front Physiol. 6:118.

Reddy VY, Zhang QY, Weiss SJ. 1995. Pericellular mobilization of the tissue-destructive cysteine proteinases, cathepsins b, l, and s, by human monocyte-derived macrophages. Proc Natl Acad Sci U S A. 92(9):3849-3853.

Reeh ES, Messer HH, Douglas WH. 1989. Reduction in tooth stiffness as a result of endodontic and restorative procedures. J Endod. 15(11):512-516.

Reilly GC, Engler AJ. 2010. Intrinsic extracellular matrix properties regulate stem cell differentiation. J Biomech. 43(1):55-62.

Reing JE, Brown BN, Daly KA, Freund JM, Gilbert TW, Hsiong SX, Huber A, Kullas KE, Tottey S, Wolf MT et al. 2010. The effects of processing methods upon mechanical and biologic properties of porcine dermal extracellular matrix scaffolds. Biomaterials. 31(33):8626-8633.

Reing JE, Zhang L, Myers-Irvin J, Cordero KE, Freytes DO, Heber-Katz E, Bedelbaeva K, McIntosh D, Dewilde A, Braunhut SJ et al. 2009. Degradation products of extracellular matrix affect cell migration and proliferation. Tissue Eng Part A. 15(3):605-614.

Rombouts C, Giraud T, Jeanneau C, About I. 2017. Pulp vascularization during tooth development, regeneration, and therapy. J Dent Res. 96(2):137-144.

Ruddle CJ. 2002. Broken instrument removal. The endodontic challenge. Dent Today. 21(7):70-72, 74, 76 passim.

Ruparel NB, de Almeida JF, Henry MA, Diogenes A. 2013. Characterization of a stem cell of apical papilla cell line: Effect of passage on cellular phenotype. J Endod. 39(3):357-363.

Sacchetti B, Funari A, Michienzi S, Di Cesare S, Piersanti S, Saggio I, Tagliafico E, Ferrari S, Robey PG, Riminucci M et al. 2007. Self-renewing osteoprogenitors in bone marrow sinusoids can organize a hematopoietic microenvironment. Cell. 131(2):324-336.

Sackett SD, Tremmel DM, Ma F, Feeney AK, Maguire RM, Brown ME, Zhou Y, Li X, O'Brien C, Li L et al. 2018. Extracellular matrix scaffold and hydrogel derived from decellularized and delipidized human pancreas. Sci Rep. 8(1):10452.

Salehrabi R, Rotstein I. 2004. Endodontic treatment outcomes in a large patient population in the USA: An epidemiological study. J Endod. 30(12):846-850.

Sawkins MJ, Bowen W, Dhadda P, Markides H, Sidney LE, Taylor AJ, Rose FR, Badylak SF, Shakesheff KM, White LJ. 2013. Hydrogels derived from demineralized and decellularized bone extracellular matrix. Acta Biomater. 9(8):7865-7873.

Seif-Naraghi SB, Singelyn JM, Salvatore MA, Osborn KG, Wang JJ, Sampat U, Kwan OL, Strachan GM, Wong J, Schup-Magoffin PJ et al. 2013. Safety and efficacy of an injectable extracellular matrix hydrogel for treating myocardial infarction. Sci Transl Med. 5(173):173ra125.

Sellaro TL, Ravindra AK, Stolz DB, Badylak SF. 2007. Maintenance of hepatic sinusoidal endothelial cell phenotype in vitro using organ-specific extracellular matrix scaffolds. Tissue Eng. 13(9):2301-2310.

Seo BM, Miura M, Gronthos S, Bartold PM, Batouli S, Brahim J, Young M, Robey PG, Wang CY, Shi S. 2004. Investigation of multipotent postnatal stem cells from human periodontal ligament. Lancet. 364(9429):149-155.

Sharpe PT. 2016. Dental mesenchymal stem cells. Development. 143(13):2273-2280.

Shi C, Chen W, Chen B, Shan T, Jia W, Hou X, Li L, Ye G, Dai J. 2017. Bladder regeneration in a canine model using a bladder acellular matrix loaded with a collagen-binding bfgf. Biomater Sci. 5(12):2427-2436.

Sicari BM, Dziki JL, Siu BF, Medberry CJ, Dearth CL, Badylak SF. 2014. The promotion of a constructive macrophage phenotype by solubilized extracellular matrix. Biomaterials. 35(30):8605-8612.

Simon S, Smith AJ. 2014. Regenerative endodontics. Br Dent J. 216(6):E13.

Siqueira JF, Jr. 2001. Aetiology of root canal treatment failure: Why well-treated teeth can fail. Int Endod J. 34(1):1-10.

Song JS, Takimoto K, Jeon M, Vadakekalam J, Ruparel NB, Diogenes A. 2017. Decellularized human dental pulp as a scaffold for regenerative endodontics. J Dent Res. 96(6):640-646.

St Pierre BA, Tidball JG. 1994. Differential response of macrophage subpopulations to soleus muscle reloading after rat hindlimb suspension. J Appl Physiol (1985). 77(1):290-297.

Sun Y, Li W, Lu Z, Chen R, Ling J, Ran Q, Jilka RL, Chen XD. 2011. Rescuing replication and osteogenesis of aged mesenchymal stem cells by exposure to a young extracellular matrix. FASEB J. 25(5):1474-1485.

Suzuki T, Lee CH, Chen M, Zhao W, Fu SY, Qi JJ, Chotkowski G, Eisig SB, Wong A, Mao JJ. 2011. Induced migration of dental pulp stem cells for in vivo pulp regeneration. J Dent Res. 90(8):1013-1018.

Swinehart IT, Badylak SF. 2016. Extracellular matrix bioscaffolds in tissue remodeling and morphogenesis. Dev Dyn. 245(3):351-360.

Swirski FK, Nahrendorf M, Etzrodt M, Wildgruber M, Cortez-Retamozo V, Panizzi P, Figueiredo JL, Kohler RH, Chudnovskiy A, Waterman P et al. 2009. Identification of splenic reservoir monocytes and their deployment to inflammatory sites. Science. 325(5940):612-616.

Syed-Picard FN, Ray HL, Jr., Kumta PN, Sfeir C. 2014. Scaffoldless tissue-engineered dental pulp cell constructs for endodontic therapy. J Dent Res. 93(3):250-255.

Takewaki M, Kajiya M, Takeda K, Sasaki S, Motoike S, Komatsu N, Matsuda S, Ouhara K, Mizuno N, Fujita T et al. 2017. Msc/ecm cellular complexes induce periodontal tissue regeneration. J Dent Res. 96(9):984-991.

Tassone E, Valacca C, Mignatti P. 2015. Membrane-type 1 matrix metalloproteinase downregulates fibroblast growth factor-2 binding to the cell surface and intracellular signaling. J Cell Physiol. 230(2):366-377.

Tatullo M, Marrelli M, Shakesheff KM, White LJ. 2015. Dental pulp stem cells: Function, isolation and applications in regenerative medicine. J Tissue Eng Regen Med. 9(11):1205-1216.

Teixeira CF, Zamuner SR, Zuliani JP, Fernandes CM, Cruz-Hofling MA, Fernandes I, Chaves F, Gutierrez JM. 2003. Neutrophils do not contribute to local tissue damage, but play a key role in skeletal muscle regeneration, in mice injected with bothrops asper snake venom. Muscle Nerve. 28(4):449-459.

Thoden van Velzen SK. 2005. [root canal treatment. Quality and result]. Ned Tijdschr Tandheelkd. 112(11):411-415.

Tidball JG. 2005. Inflammatory processes in muscle injury and repair. Am J Physiol Regul Integr Comp Physiol. 288(2):R345-353.

Tidball JG, Villalta SA. 2010. Regulatory interactions between muscle and the immune system during muscle regeneration. Am J Physiol Regul Integr Comp Physiol. 298(5):R1173-1187.

Tidball JG, Wehling-Henricks M. 2007. Macrophages promote muscle membrane repair and muscle fibre growth and regeneration during modified muscle loading in mice in vivo. J Physiol. 578(Pt 1):327-336.

Turk V, Stoka V, Vasiljeva O, Renko M, Sun T, Turk B, Turk D. 2012. Cysteine cathepsins: From structure, function and regulation to new frontiers. Biochim Biophys Acta. 1824(1):68-88.

Turner NJ, Badylak JS, Weber DJ, Badylak SF. 2012. Biologic scaffold remodeling in a dog model of complex musculoskeletal injury. J Surg Res. 176(2):490-502.

Turner NJ, Yates AJ, Jr., Weber DJ, Qureshi IR, Stolz DB, Gilbert TW, Badylak SF. 2010. Xenogeneic extracellular matrix as an inductive scaffold for regeneration of a functioning musculotendinous junction. Tissue Eng Part A. 16(11):3309-3317.

Valentin JE, Stewart-Akers AM, Gilbert TW, Badylak SF. 2009. Macrophage participation in the degradation and remodeling of extracellular matrix scaffolds. Tissue Eng Part A. 15(7):1687-1694.

van der Rest M, Garrone R. 1991. Collagen family of proteins. FASEB J. 5(13):2814-2823.

Varlan C, Dimitriu B, Varlan V, Bodnar D, Suciu I. 2009. Current opinions concerning the restoration of endodontically treated teeth: Basic principles. J Med Life. 2(2):165-172.

Vidal G, Blanchi T, Mieszawska AJ, Calabrese R, Rossi C, Vigneron P, Duval JL, Kaplan DL, Egles C. 2013. Enhanced cellular adhesion on titanium by silk functionalized with titanium binding and rgd peptides. Acta Biomater. 9(1):4935-4943.

Villalta SA, Nguyen HX, Deng B, Gotoh T, Tidball JG. 2009. Shifts in macrophage phenotypes and macrophage competition for arginine metabolism affect the severity of muscle pathology in muscular dystrophy. Hum Mol Genet. 18(3):482-496.

Vlodavsky I, Goldshmidt O, Zcharia E, Atzmon R, Rangini-Guatta Z, Elkin M, Peretz T, Friedmann Y. 2002. Mammalian heparanase: Involvement in cancer metastasis, angiogenesis and normal development. Semin Cancer Biol. 12(2):121-129.

Vo TN, Kasper FK, Mikos AG. 2012. Strategies for controlled delivery of growth factors and cells for bone regeneration. Adv Drug Deliv Rev. 64(12):1292-1309.
Votteler M, Kluger PJ, Walles H, Schenke-Layland K. 2010. Stem cell microenvironments--unveiling the secret of how stem cell fate is defined. Macromol Biosci. 10(11):1302-1315.
Wang J, Feng JQ. 2017. Signaling pathways critical for tooth root formation. J Dent Res. 96(11):1221-1228.
Wang Y, Papagerakis S, Faulk D, Badylak SF, Zhao Y, Ge L, Qin M, Papagerakis P. 2018. Extracellular matrix membrane induces cementoblastic/osteogenic properties of human periodontal ligament stem cells. Front Physiol. 9:942.
Wang Y, Zhao Y, Jia W, Yang J, Ge L. 2013. Preliminary study on dental pulp stem cell-mediated pulp regeneration in canine immature permanent teeth. J Endod. 39(2):195-201.
Wang Y, Zhu X, Zhang C. 2015. Pulp revascularization on permanent teeth with open apices in a middle-aged patient. J Endod. 41(9):1571-1575.
Wen X, Yi LZ, Liu F, Wei JH, Xue Y. 2016. The role of cathepsin k in oral and maxillofacial disorders. Oral Dis. 22(2):109-115.
Werb Z. 1997. Ecm and cell surface proteolysis: Regulating cellular ecology. Cell. 91(4):439-442.
Wilson S, Hashamiyan S, Clarke L, Saftig P, Mort J, Dejica VM, Bromme D. 2009. Glycosaminoglycan-mediated loss of cathepsin k collagenolytic activity in mps i contributes to osteoclast and growth plate abnormalities. Am J Pathol. 175(5):2053-2062.
Winter W, Karl M. 2012. Dehydration-induced shrinkage of dentin as a potential cause of vertical root fractures. J Mech Behav Biomed Mater. 14:1-6.
Witte L, Fuks Z, Haimovitz-Friedman A, Vlodavsky I, Goodman DS, Eldor A. 1989. Effects of irradiation on the release of growth factors from cultured bovine, porcine, and human endothelial cells. Cancer Res. 49(18):5066-5072.
Wolf MT, Carruthers CA, Dearth CL, Crapo PM, Huber A, Burnsed OA, Londono R, Johnson SA, Daly KA, Stahl EC et al. 2014. Polypropylene surgical mesh coated with extracellular matrix mitigates the host foreign body response. J Biomed Mater Res A. 102(1):234-246.
Wolf MT, Daly KA, Reing JE, Badylak SF. 2012. Biologic scaffold composed of skeletal muscle extracellular matrix. Biomaterials. 33(10):2916-2925.
Wolf MT, Dearth CL, Sonnenberg SB, Loboa EG, Badylak SF. 2015. Naturally derived and synthetic scaffolds for skeletal muscle reconstruction. Adv Drug Deliv Rev. 84:208-221.
Wu Y, Wang J, Shi Y, Pu H, Leak RK, Liou AK, Badylak SF, Liu Z, Zhang J, Chen J et al. 2016. Implantation of brain-derived extracellular matrix enhances neurological recovery after traumatic brain injury. Cell Transplant.
Wynn TA, Barron L. 2010. Macrophages: Master regulators of inflammation and fibrosis. Semin Liver Dis. 30(3):245-257.
Yadlapati M, Biguetti C, Cavalla F, Nieves F, Bessey C, Bohluli P, Garlet GP, Letra A, Fakhouri WD, Silva RM. 2017. Characterization of a vascular endothelial growth factor-loaded bioresorbable delivery system for pulp regeneration. J Endod. 43(1):77-83.
Zaky SH, Cancedda R. 2009. Engineering craniofacial structures: Facing the challenge. J Dent Res. 88(12):1077-1091.
Zanini M, Meyer E, Simon S. 2017. Pulp inflammation diagnosis from clinical to inflammatory mediators: A systematic review. J Endod. 43(7):1033-1051.

Zantop T, Gilbert TW, Yoder MC, Badylak SF. 2006. Extracellular matrix scaffolds are repopulated by bone marrow-derived cells in a mouse model of achilles tendon reconstruction. J Orthop Res. 24(6):1299-1309.

Zavasnik-Bergant T, Turk B. 2007. Cysteine proteases: Destruction ability versus immunomodulation capacity in immune cells. Biol Chem. 388(11):1141-1149.

Zhu M, Kohan E, Bradley J, Hedrick M, Benhaim P, Zuk P. 2009. The effect of age on osteogenic, adipogenic and proliferative potential of female adipose-derived stem cells. J Tissue Eng Regen Med. 3(4):290-301.

Zhu WH, Pan J, Yong W, Zhao XY, Wang SM. 2008. Endodontic treatment with mta of a mandibular first premolar with open apex: Case report. Oral Surg Oral Med Oral Pathol Oral Radiol Endod. 106(1):e73-75.

Zizka R, Sedy J. 2017. Paradigm shift from stem cells to cell-free regenerative endodontic procedures: A critical review. Stem Cells Dev. 26(3):147-153.